UTHealth™ | Medical School

The University of Texas
Health Science Center at Houston

2015 SUMMER RESEARCH PROGRAM

STUDENT ABSTRACTS

This page left blank

Contents

Preface…… 5

Acknowledgements …… 7

Lab Research Ownership ……. 9

Index

List of Medical Students ……... 11
List of Undergraduate Students …….. 12
List of International Medical Students …… 13
Abstracts – Medical Students …… 14
Abstracts – Undergraduates ……. 118
Abstracts – International Medical Students ……..…….. 163

This page left blank

Preface

The University of Texas Medical School at Houston (UTMSH) Summer Research Program provides intensive, hands-on laboratory research training for MS-1 medical students and undergraduate college students under the direct supervision of experienced faculty researchers and educators. These faculty members' enthusiasm for scientific discovery and commitment to teaching is vital for a successful training program. It is these dedicated scientists who organize the research projects to be conducted by the students.

The trainee's role in the laboratory is to participate to the fullest extent of her/his ability in the research project being performed. This involves carrying out the technical aspects of experimental analysis, interpreting data and summarizing results. The results are presented as an abstract and are written in the trainees' own words that convey an impressive degree of understanding of the complex projects in which they were involved.

To date, more than 1,900 medical, college, and international medical students have gained research experience through the UTMSH Summer Research Program. Past trainees have advanced to pursue research careers in the biomedical sciences, as well as gain an appreciation of the relationship between basic and clinical research and clinical practice.

UTMSH student research training is supported by a grant from the National Institute of Diabetes and Digestive and Kidney Diseases (NIDDK) and/or by financial support from the Dean and the departments and faculty of the medical school and School of Dentistry.

Biomedical science education remains a vital and integral part of our nation's interests. The UTMSH Summer Research Program, and the dedication of our faculty and administration exemplify the institution's commitment to training and educating the future leaders in our biomedical scientific communities.

Gary C. Rosenfeld, Ph.D.
Director, Summer Research Program
Associate Dean for Educational Programs

This page left blank

Acknowledgements

This publication marks the completion of the twenty-sixth year of The University of Texas Medical School at Houston's (UTMSH) Summer Research Program. The longevity and success of the program are rooted in the overwhelming support received from the deans, faculty, staff and students of the medical school.

Indicative of this support is the administrative assistance and financial support for the Program's college and medical students provided by UTMSH. Sincere appreciation is expressed to Dean Giuseppe Colasurdo M.D. and Patricia M. Butler, M.D., Vice Dean, Office of Educational Programs who continue to ensure the yearly success of the Summer Research Program.

Major financial assistance for medical students has also been provided through a short term research grant by the National Institute of Diabetes and Digestive and Kidney Diseases (NIDDK; 5 T32 DK007676).

Negotiated cooperative agreements with several international medical schools have been set up to offer tailored research programs at UTMSH for selected foreign medical students who interact fully with the other students in the Summer Research Program.

The success of the Summer Research Program depends primarily on the faculty who volunteer to mentor the trainees. These dedicated educators organize and guide the research projects that includes for each student data analysis, preparation of an abstract and public presentation of results. Our sincere appreciation to all faculty mentors.

This page left blank

Lab Research Ownership

Publication and/or Disclosure

Each student participating in this program is required to read, agree to, and sign this disclosure form. The original signed copy is on file in the Summer Research Program office; the student and their faculty mentors are each furnished with a copy.

"In reference to the laboratory research you will perform this coming summer through The University of Texas Medical School at Houston's Summer Research Program, you are required to comply with the standard restrictions regarding participation in the Summer Research Program:

"All of your laboratory research is *CONFIDENTIAL* and although your abstract will be available through our website, you cannot independently disclose or publish any research findings or data in any form (including at meetings or conferences) without the express prior written approval of The University of Texas Medical School at Houston. If you wish to submit your abstract to any third party, you must first contact your faculty mentor no less than three (3) weeks prior to any deadlines in order to obtain the necessary written approvals.

"Because your research was generated from ideas and funds that originated with your faculty mentor and The University of Texas Medical School at Houston, ownership of any data generated by you during the Summer Research Program belongs to The University of Texas Medical School at Houston or the Principle Investigator (PI)."

This page left blank

UTHealth | Medical School
The University of Texas
Health Science Center at Houston

Medical Students

Last Name	First Name	Page #
Abdelaziz	Abed	15
Ahn	Stephanie	16
Aria	Alexander	17
Beach	Richard	18
Benoist	Logan	19
Bowers	Kyle	20
Caldwell	Kelly	21
Carroll	Melanie	22
Carter	Dalton	23
Covey	Sarah	25
Dean	Riley	26
Deleija	Juan	28
Diffley	Michael	29
Ding	Karen	30
Dooley	Matthew	32
Dursteler	Amy	33
Eguia	Arturo	34
Emelogu	Ikenna	35
Engelhardt	Margaret	36
Freemyer	Benjamin	37
Gants	Shavonia	38
Gibson	Anthony	40
Gonzalez	Adam	42
Grable	Cullen	43
Gu	Joshua	44
Ha	Lina	45
Henchcliffe	Blake	46
Hildebrandt	Aubrey	47
Ho	Kim-Trang	48
Howard	Ericka	49
Huang	Neal	50
Hurley	Matthew	52
Hurling	Jermaine	53
Huynh	Jonathan	55
Igbinoba	Randy	56
Jenner	Zachary	57
Johnson	Margaret	59
Jones	Neal	60
Karim	Tahseen	61
Karnes	Paden	62

Last Name	First Name	Page #
Lahiri	Sharmistha	64
Liu	Victor	66
Lopez	Carmen	67
Martin	Clay	69
McMenemy	Madison	70
Minifee	Chris	72
Minzenmayer	Andrew	73
Mitchell	Nicholas	74
Mitchell	Thomas	75
Nguyen	Justin	76
Patel	Sagar	77
Peery	Travis	78
Poi	Tyler	79
Price	James	81
Riojas	Justin	83
Rivas	Orlyn	85
Rivera	Marvin	86
Rosales Santillan	Monica	87
Royalty	Samantha	88
Sadd	Corey	90
Schiffer	Walter	91
Schrock	Nicole	92
Schroeder	Andrew	94
Sharp	Bruce	95
Shaw	Jacob	97
Tewari	Ankita	99
Valilis	Evangelia	101
van Brummen	Alexandra	102
Villegas	Natacha	104
Wang	Margaret	105
Warren	Benjamin	106
Webb	Ashley	107
Wheeler	Austin	109
Wu	Joanna	110
Xiao	Albert	111
Yanney	Rayce	112
Yao	Chen	114
Yazdani	Laila	115
Zuniga	Joshua	117

Undergraduate Students

Last Name	First Name	Page #
Alexander	Alex	119
Awano	Ebore	120
Barahona	Kelvin	121
Borden	Kylie	122
Chen (Wu)	Alissa	123
Costantini	Matteo	124
Devakottai	Sundar	126
Dinh	Nhi	127
Do	Megan	128
Estrada	Darlene	129
Folkerts	Madeline	130
Gadot	Ron	131
Haeberle	Heather	132
Hanif	Sarah	133
Hayes	Jane	134
Hsiao	Thomas	135
Jeong	Suhyun	136
Kissoon	Kimberley	137
Landis	Henry	138
Ling	Han	139

Last Name	First Name	Page #
Ozguc	Fatma	140
Patlan	Mario	141
Pernik	Mark	142
Rae	Meredith	143
Raina	Abe	144
Rivera	Angel	145
Rodriguez	Efrain	147
Rogers	John	148
Schnupp	Trevor	149
Schwab	Cara	150
Sheena	Brittney	151
Tseng	Luke	152
Tucker	Sara	153
Westerman	Kimberly	154
Won	Michelle	155
Yang	Grace	156
Yin	Caroliina	157
Youn	Sean	159
Zhou	Allen	161

UTHealth | Medical School
The University of Texas
Health Science Center at Houston

International Medical Students

Last Name	First Name	Page #
Chen	Yongyan	164
Hayashi	Atsushi	165
Higashi	Saki	167
Jiang	Hongyue	169
Li	Guilin	171
Lin	Wei Ting	172
Saijo	Saki	173
Sun	Le	174
Wang	Yiman	175
Xie	Yizhao	177
Xu	Yunze	178
Yamazaki	Ai	179
Zhao	Zhicong	180

UTHealth™ | Medical School

The University of Texas
Health Science Center at Houston

Medical Students

ABSTRACT

Comparing Osteocalcin in Older Trauma Patients who Suffered Fractures Based on Type 2 Diabetes Status

Abed Abdelaziz *The University of Texas at Houston Medical School* *Class of 2018*

Sponsored by: Catherine Ambrose, PhD, Department of Orthopedic Surgery; Nahid Rianon, MD, DrPH, Department of Internal Medicine – Geriatric and Palliative Medicine

Supported by: National Institute of Diabetes and Digestive and Kidney Diseases, 2T35DK007676-22

Key Words: Diabetes, Fracture Risk, Osteocalcin, Preventative Care

Patients with type 2 diabetes (T2D) are at an increased risk of fracture. There is currently no consistent indicator of this risk. Fractures in T2D patients with non-osteoporotic bone density levels have led to discussions about investigating markers of bone turnover, e.g., osteocalcin, as an indicator of the fracture risk in the diabetic population. Osteocalcin is an osteoblast-specific secreted protein that is a marker of bone turnover and formation. Previous studies have shown osteocalcin levels to be decreased in T2D patients compared to non-diabetics. The hypothesis was that mean total osteocalcin levels in the fracture patients with T2D would be significantly lower than those without diabetes. The project involved a cross-sectional study of Memorial Hermann trauma patients who were at least 50 years of age and suffered a femoral, acetabular, or vertebral fracture between March 2012 and May 2015. Patients were grouped into diabetic and non-diabetic groups based on a positive diabetes diagnosis in their medical records. A total of 48 patients were included in the study, 17 T2D and 31 non-diabetics. The total serum osteocalcin levels were assayed from stored serum samples taken upon admission for each patient. As the serum samples were obtained within eight hours of fracture occurrence, osteocalcin assays could be used to best estimate osteocalcin levels immediately pre-fracture. The mean osteocalcin level for the non-diabetic group was 11.69 ng/ml compared to 10.29 ng/ml in the T2D group ($p > 0.05$). Although not statistically significant, T2D status was inversely correlated with total osteocalcin level. The T2D patients in our study were 1.74 more likely to have had a low energy fracture compared to the patients without diabetes. The results are similar to previously reported trends of lower osteocalcin in T2D patients and may reflect on the decreased bone turnover in T2D patients. The lack of significance may be attributed to the small sample size. Further studies with larger sample sizes should be done relating osteocalcin levels to bone health in the diabetic population.

ABSTRACT

The Opioid-Sparing and Analgesic Effects of IV Acetaminophen in Craniotomy: A Prospective, Randomized, Placebo-controlled, Double-Blind Study

Stephanie Ahn *The University of Texas at Houston Medical School* *Class of 2018*

Sponsored by: Carin A. Hagberg, MD, Carlos Artime, MD, Department of Anesthesiology

Supported by: Carin A. Hagberg, MD, Carlos Artime, MD, Department of Anesthesiology; The University of Texas Health Science Center at Houston Medical School – Office of the Dean

Key Words: IV Acetaminophen, Craniotomy, Opiod, Analgesic

Background: Patients undergoing a craniotomy for tumor resections have reported many side effects from receiving opioids for pain. These side effects include post-operative nausea and vomiting (PONV), opioid-induced respiratory depression, and opioid dependence. As a result, IV acetaminophen is being explored to see if its use, in craniotomies, can reduce the requirements for narcotics and the risks associated with opioid use. There have been some clinical trials reporting its advantages in postoperative pain management such as, allowing for a quicker response during postoperative neurological assessment, greater satisfaction (pain treatment), less side effects, and greater pain control, versus those who only receive opioid analgesia.

Primary Aim: Establish the beneficial analgesic and opioid-sparing effects of IV acetaminophen in patients undergoing a craniotomy for intracranial tumor resection by determining the reduction of morphine use within 24 hours after surgery.

Methods: This study was randomized, double-blind, and placebo-controlled. It compared IV acetaminophen to a placebo. Eighty patients presenting for elective supratentorial craniotomy for resection of an intracranial mass were enrolled in this study. Randomized Group 1 received 1g doses of IV acetaminophen at certain time intervals while Group 2 received 100cc of IV normal saline (placebo) at the same time intervals. Pain was assessed using the visual analog scale (VAS) as the patient arrived to the Post Anesthesia Care Unit (PACU), or at extubation in the PACU. And again, at 1, 2, 4, 8, 12, 16, 20, and 24 hours pain assessments were recorded. Nausea was recorded using the numeric rating scale (NRS) at the same time intervals as the pain assessments.

Results: 80 patients were recruited for this study. We are currently preparing the data for analysis, and therefore we are unable to make any conclusions at this time.

ABSTRACT

Stem Cell Differentiation and Growth on Polyethylene Glycol 2D Scaffolds with Varying RGD Concentration

Alex Aria *The University of Texas at Houston Medical School* *Class of 2018*

Sponsored by: Laura Smith Callahan, PhD, Department of Neurosurgery and the Center for Stem Cell and Regenerative Medicine

Supported by: Laura Smith Callahan, PhD, Department of Neurosurgery and the Center for Stem Cell and Regenerative Medicine; The University of Texas Health Science Center at Houston Medical School – Office of the Dean

Key Words: Human neural stem cells, tissue engineering, scaffolds, protein gradient, differentiation

BACKGROUND: The ability to restore neurological lesions such as brain or spinal cord injuries is of major interest to the medical community. While engineered scaffolds have been shown to increase the viability of implanted stem cells, the incorporation of known extracellular matrix proteins and signaling molecules in these scaffolds may lead to further nervous system tissue regrowth and regeneration. Ile-Lys-Val-Ala-Val peptide (IKVAV), a fragment of laminin, is known to promote neuronal growth and differentiation. However, hiPSC derived NSCs do not initially attach to two-dimensional (2D) IKVAV gradients. This lack of initial cellular attachment to the IKVAV functionalized PEG scaffolds inhibits the use of the IKVAV peptide for human applications. Therefore, an optimal concentration of another peptide capable of promoting attachment must be found to study the effects of IKVAV in 2D on human cells. ARG-GLY-ASP (RGD) is a small protein fragment present in numerous proteins that promotes cellular attachment and will be examined to promote hiPSC derived NSC attachment in this study.

METHODS: Scaffolds with RGD were prepared using a syringe to push poly(ethylene) glycol (PEG) solution with RGD concentrations ranging from 0.07 mM to 2.52 mM into a custom mold. The sample was then photopolymerized and placed in culture media. Samples were seeded with hiPSC derived NSCs on top and time points were taken at days 1,7, and 14. To acquire images, samples were first treated with rabbit anti-mouse neuron-specific class III β-tubulin and then treated with fluorescently conjugated donkey anti-rabbit IgG antibodies. Cell nuclei were stained with DAPI. A fluorescence microscope was then used to take images.

RESULTS: Day 1,7 and 14 imaging samples showed similar cell attachment for all RGD concentrations. Only a concentration of 2.52 mM RGD maintained a high percentage of TUJ1 positive cells and a neurite length of greater than 20 μm.

DISCUSSION: It was determined that RGD concentration significantly affects neuron attachment and neural differentiation. The optimum concentration of RGD for hiPSC derived NSC attachment on functionalized PEG scaffolds is 2.52 mM. This will be incorporated in IKVAV gradients in future studies of hiPSC derived NSC in 2D.

ABSTRACT

Risk Factors for Anastomosis Leakage in Colonic Surgery

Richard Beach *The University of Texas at Houston Medical School* *Class of 2018*

Sponsored by: John Harvin, MD, Department of Surgery
Supported by: John Harvin, MD, Department of Surgery
Key Words: Trauma patients with comorbidities

Introduction: Risk factors for anastomotic leakage for destructive colon injuries repaired by a primary laparotomy or damage control laparotomy (DCL) have not been well established. Vasopressor use has been linked in previous papers but not much else has been consistently identified with anastomotic leakage incidence increase. The authors performed a retrospective study to identify which comorbidities correlated with an increase incidence of anastomotic leakage.
Methods: patients ages 16 and older between 2011 and 2015 with destructive colon injuries were identified at the institution. Patients were then divided into two groups: definitive laparotomies and DCL. The two groups were then divided by the presence or lack of anastomotic leakage.
Results: We identified 142 patients undergoing colon resection with 67 (47%) undergoing definitive laparotomies and 75 (53%) with DCL. There was a higher incidence of anastomotic leakage in DCL patients compared to primary repair (18% vs 8%). There was a significant different in base excess in both definitive and DCL patients. Vasopressor usage only had significance with the definitive group with 50% of the leaking patients on post op vasopressors. There were four deaths with all having DLC and anastomotic failure.
Conclusions: Anastomotic disruptions in destructive colonic injury repairs cause an increased length of stay in the hospital and sometimes death. As predicted vasopressor use did correlate with an increase incidence of anastomotic leakage. Base excess also showed an increased correlation with anastomotic leakage and should be considered when treating patients with destructive colon injuries.

ABSTRACT

Review of Communication after One Year Implementation of Post Anesthesia Care Unit (PACU) Checklist

Logan Benoist *The University of Texas at Houston Medical School* *Class of 2018*

Sponsored by: Maria Matuszczak, MD, Department of Anesthesiology
Supported by: Maria Matuszczak, MD, Department of Anesthesiology
Key Words: Checklist, handoff, communication, post anesthesia care unit (PACU)

Background: Ineffective communication between clinicians has been found to lead to an increase in medical errors and a decrease in patient satisfaction. Effective communication should occur during handoffs in the post anesthesia care unit (PACU) where hundreds of transfers occur daily. This high turnover of patients makes it important to implement a handoff tool that reduces the amount of missed communication. Checklists provide structure and ensure that all pertinent patient information is communicated. We developed and implemented a meaningful checklist to standardize this communication process last year, which resulted in a significant increase in handoff reliability. This year the study was replicated to measure the effectiveness of using checklists during handoffs after one year of implementation.
Methods: During the first week of the project, we observed handoffs and audited according to the checklist developed during the study last year (pre-education). After the data was reviewed, pediatric anesthesia care providers were reminded via email to use the checklist during handoffs in the pediatric post anesthesia care unit. During the following week, we observed and audited more handoffs according to the checklist (re-education).
Results: The reliability of handoffs went from 62% to 58% after the re-education email was sent to the anesthesia care providers. A total of 100 handoffs were observed over a three-week period distributed over two study phases: pre-education and re-education. There was variability among care providers giving each report. Some anesthesia providers consistently gave full reports and other consistently gave reports lacking a number of subjects included on the checklist. It was noticed that some parts of the checklist like medications given to the patient during the procedure, type of procedure, and patient age were reported frequently but other items including blood band and blood products were often omitted from the report.
Conclusion: While it appears vital patient information necessary for continued care is not reported to the nurse during the handoff to the PACU, the nurse from the operating room also gives a thorough report to the PACU nurse. However, a full report from the anesthesia care provider provides nurses with pertinent patient information in an organized manner and is important for standardized care of all patients. The results support how difficult it is to maintain implementation of new protocol. In order to achieve our goal of 100% adherence, more education and a strong emphasis on the details of the checklist to anesthesia providers is needed.

ABSTRACT

Investigating a PNKP Mutation of Unknown Significance

Kyle Bowers *The University of Texas at Houston Medical School* *Class of 2018*

Sponsored by: Gretchen K. Von Allmen, MD, Department of Pediatrics
Supported by: West Syndrome Foundation
Key Words: PNKP, Epilepsy, Database, Mutation

Introduction: Mutations in the PNKP gene have been discovered in patients with intractable epilepsy. Gene panel analysis of patients diagnosed with epilepsy has revealed five patients with the exact same PNKP mutation. From the identification of these mutations, we can better understand the phenotypic outcomes in these patients. Homozygous or compound heterozygous mutations in the PNKP gene are known to cause early infantile epileptic encephalopathy, progressive cerebellar atrophy, hypotonia, polyneuropathy, and ataxia, indicating that PNKP mutations either directly cause epileptic seizures or are part of a specific genetic burden that results in the epileptic phenotype.
Methods: A database was created consisting of pediatric epilepsy patients and their profiles detailing genetic testing and relevant clinical information. Patients with suspected genetic mutations have undergone whole exome sequencing or gene panel testing. Patients that were admitted to the pediatric epilepsy clinic between 2007 and the present date were included in this investigation.
Results: Each of the 5 patients has a missense mutation at the same location (c.416G>A), resulting in a substitution of a histidine for an arginine at the 139-codon. For each of the patients, the genetic report stated that this particular mutation was one of unknown significance, as opposed to pathogenic or benign. All 5 patients have epilepsy intractable to multiple anticonvulsant medications, with EEG findings of multifocal or generalized epileptiform discharges, age of seizure onset between birth and 13 years old, and all have developmental delay/cognitive impairment.
Conclusion: While it is unknown exactly what role the PNKP mutation plays in causing these patients' overall phenotypes, the fact that the same exact mutation appears five times in a sample size of 296 merits further investigation of this mutation and how it may contribute to the genetic burden of patients possessing it.

ABSTRACT

Pardon the Interruption: An Observational Study of OR Interruptions

Kelly M. Caldwell *The University of Texas at Houston Medical School* *Class of 2018*

Sponsored by: KuoJen Tsao, MD, Department of Pediatric Surgery
Supported by: KuoJen Tsao, MD, Department of Pediatric Surgery; The University of Texas Health Science Center at Houston Medical School – Office of the Dean
Key Words: Interruptions, Distractions, Patient Safety, Quality Care

Introduction: Teamwork and effective communication are principles of safe patient care, especially in surgery. Distractions in the operating room can impair and/or interrupt these hallmarks as well as increase surgeon stress and fatigue, potentially compromising patient safety. However, little is known about the type and frequency of distractions in operating rooms. We aimed to characterize interruptions in pediatric operating rooms in order to identify areas for intervention.

Methods: Over an eight week period, a prospective, direct observational study was performed by five trained observers in an academic children's hospital. Convenience sampling was performed across all pediatric surgical specialties. The number of phone calls, people entering, pages/text messages, equipment failures, and other events that interrupted workflow were recorded. Interruptions were further defined as essential or non-essential based on their contribution to patient care. Interruptions were analyzed in relation to surgical subspecialty and case duration.

Results: 208 operations were observed with a median (interquartile range) operating time of 40 (19-86) minutes. A total of 1,037 interruptions were recorded with a median of 2 (1-5) interruptions per case. People entering the operating room accounted for the highest proportion of interruptions (61%), where approximately one-third were non-essential (30.5%). Overall, 64% of all the interruptions were non-essential to patient care (Figure). In total, 63% of the operations had at least one non-essential interruption. Interruptions were more frequent as case length increased (median per case; <30 min = 1, 31-60 min = 2, 61-120 min = 4, >121 min = 14).

Conclusion: Non-essential interruptions are common in pediatric operating rooms. The impact of these distractions on patient safety remains unknown. Although no single interruption was observed to cause direct patient harm, patient safety in the operating room may be optimized through awareness, education, and limiting non-essential interruptions. Future interventions should target eliminating non-essential interruptions and minimizing essential ones through prevention and process improvement.

ABSTRACT

Chibby's Regulation of Canonical Wnt Signaling in *Xenopus laevis* Pronephros Development

Melanie Carroll *The University of Texas at Houston Medical School* *Class of 2018*

Sponsored by: Rachel K. Miller, PhD, Department of Pediatrics
Supported by: National Institute of Diabetes and Digestive and Kidney Diseases, 2T35DK007676-22
Key Words: Wnt, pronephros, polycystic kidney

Introduction: Furthering understanding of kidney development has implications for several human diseases, including cystic kidney diseases and cancers such as Wilms tumor. The Chibby gene encodes a nuclear protein that inhibits β-catenin in the canonical Wnt pathway, which has been shown to be involved in kidney development. Targeted knockdown of Chibby in the kidney has not been previously attempted. *Xenopus laevis* frogs provide an excellent model for kidney development due to their external embryo growth, established methods for gene expression regulation, and ease of visualization through immunofluorescence. We hypothesize that knockdown of Chibby will disrupt tubulogenesis in kidney development in *X. laevis* embryos.

Methods: Chibby morpholino (MO) was injected into the progenitor cell of the pronephros, the embryonic kidney, at the eight cell stage. MOs are antisense oligonucleotides that bind mRNA transcripts and block translation, resulting in effective knockdown of the gene of interest. A membrane targeted red fluorescent tracer (MEM-RFP) was coinjected with MO to verify accuracy of injection. Embryos were fixed at tadpole stage and stained using 3G8 and 4A6 antibodies, which stain the proximal tubule and distal tubule-collecting duct, respectively.

Results: Out of seven surviving MO-injected embryos, six had successful targeting to the pronephros. Three of these embryos showed decreased tubulogenesis on the injected side as compared to the uninjected side. Additionally, two embryos showed a possible duplicate axis, a known effect of overexpressing beta-catenin ventrally in the early embryo. Injecting the Chibby MO ventrally at the four cell stage gave duplicate axis formation in 36% of embryos (n=28) which is comparable to embryos injected with beta-catenin (40%, n=20) using the same method.

Conclusion: Chibby may affect development of *Xenopus* embryonic kidneys. Removing Chibby's inhibition of beta-catenin induces duplicate axis in the same manner as overexpressing beta-catenin. Further work is necessary to confirm knockdown of Chibby expression and fully characterize the Chibby knockdown phenotype.

ABSTRACT

Optimization of Method to Measure tPA-Mediated Thrombolysis In Vivo (Rabbit Stroke Model)

Dalton Emile Carter *The University of Texas at Houston Medical School* *Class of 2018*

Sponsored by: Melvin E. Klegerman, PhD, Department of Internal Medicine and Cardiology
Supported by: Melvin E. Klegerman, PhD, Department of Internal Medicine and Cardiology; David Volk, PhD, Department of Nanomedicine and Biomedical Engineering
Key Words: Ultrasound, Thrombolysis, tPA

Background:. Experimental animal models evaluating clot dissolution treatments have traditionally utilized similar methods to those used for hospital stroke patients. One way we can improve on this is to measure clot loss using ultrasound visualization. In order to do this, we must form thrombi that contain an effective contrast agent. In this case, a microparticle agent such as simethicone-coated cellulose (SonoRX), which is used for GI contrast imaging, offers a promising solution. This though was found no longer to be in production and we replaced it with microcrystalline cellulose (Sigma-Aldrich).

Methods: In 1.5ml eppendorf tubes, clots were formed from: whole rabbit blood (100 µl) 1 M $CaCl_2$ (25 µl) + 0.02 M PBS, pH 7.4 (50 µl) and human thrombin (25 µl; 2.5 units) with the volume of PBS representing the maximum concentration of contrast to be used later. The clots were allowed to consolidate at 37°C for 2-18 hours. Using clots made by this method, we determined the optimal tPA concentration for our experiment. The concentrations tested were 60 µg/ml, 80 µg/ml and 100 µg/ml, prepared in porcine plasma as a source of plasminogen. From these we added 500 µl to each tube with three replicates for each time point (30/60/90 min.) We compared the reproducibility of data using mean zero time point masses and mass loss specific to each clot. Once completing this step, we measured the echogenicity of 7.5 mg/ml cellulose suspension dilutions of 50x, 100x, 200x, 400x and 800x. Once cellulose echogenicity was established, we produced clots integrated with cellulose in amounts of 10 µl, 20 µl, 30 µl stock suspension and compared for dissolution properties to untreated clots. B-mode ultrasound imaging was performed with a Philips HDI 5000 ultrasound system using an L12-5 linear array probe. Microcrystalline cellulose-doped clots in 1.5 ml Eppendorf tubes were imaged in an anechoic chamber consisting of a gel standoff pad (with rectangular cutout) on a RhoCee rubber pad. Images were recorded on MO optical disks at 30-60-90 min intervals in replicates of 3 with individual zero time point images taken of all 9 clots prior to tPA dissolution. These images were analyzed using the software, Image Pro Plus Version 4.5 to determine MGSV. For comparison of MGSV reduction with clot mass loss data, the percent reduction of both parameters was used.

Results: We have shown that 200 µl rabbit blood clots in Eppendorf tubes were suitable for this in vitro study. Of the tPA concentrations tested, 100 µg/ml in porcine plasma demonstrated the

highest clot dissolution rates. Microcrystalline cellulose was shown to be appreciably echogenic at a concentration of 150 µg/ml, establishing a minimum level of clot doping; 30 µl (1.12 mg/ml) addition of cellulose to our clots demonstrated acceptable echogenicity with no effect on tPA dissolution rate. Upon imaging, we are able to visualize and measure our clots' MGSV over time. Percent reduction of clot MGSV and mass correlated well.

Conclusion: Clot mass loss regressions exhibit significantly elevated y-intercepts, suggesting higher dissolution rates prior to 30 minutes. However, this does not seem to be the case in the MGSV regressions. The relatively low 30-minute point for the % reduction plot, supports this hypothesis. Further experiments measuring clot mass loss within the first 30 minutes will test the hypothesis. Contingent on funding, a rabbit thrombotic stroke model can now be developed.

ABSTRACT

Do All Intestinal Malrotations Require a Ladd Procedure? Prophylactic vs Post-Symptomatic Outcomes

Sarah E. B. Covey *The University of Texas at Houston Medical School* *Class of 2018*

Sponsored by: KuoJen Tsao, MD, Department of Pediatric Surgery
Supported by: KuoJen Tsao, MD, Department of Pediatric Surgery
Key Words: Ladd's Procedure, Volvulus, Malrotation

Introduction: Intestinal malrotation can lead to midgut volvulus resulting in sepsis, short bowel syndrome, and death. Treatment includes the Ladd procedure to correct intestinal malrotation for symptomatic patients. However, debate remains regarding the timing of the procedure for asymptomatic infants with known malrotation. We hypothesized that the benefits of prophylactic Ladd procedure outweigh the risks of post-symptomatic repair.
Methods: A retrospective chart review of pediatric patients undergoing the Ladd procedure was performed. Prophylactic Ladd procedures were identified as those that occurred prior to any malrotation-related symptoms (i.e. abdominal pain, distention, nausea, emesis, constipation, or feeding intolerance). Results were analyzed with Mann-Whitney U and chi-squared tests.
Results: From 2011-2014, 42 patients (prophylactic=19, post-symptomatic=23) underwent the Ladd procedure for intestinal malrotation. The median (interquartile range) age of patients was 9.6 (3.9-18) months and 18 (2.4-52) months for prophylactic and post-symptomatic patients, respectively (p=0.38). In patients who underwent post-symptomatic Ladd procedures, 9 (39%) were found to have volvulus and 1 (4.3%) had bowel necrosis at time of surgery. No prophylactic Ladd procedure patients required reoperation while 6 (26%) post-symptomatic patients required reoperation for gastrointestinal-related complications (p=0.02). Prophylactic versus post-symptomatic Ladd procedure patients required a median (interquartile range) of 5.0 (3.3-6.8) days vs 7.4 (5.0-11) days to tolerate full enteral feeds (p=0.11) and 8.0 (6.1-11) days vs 11 (7.5-32) days until discharge (p=0.09). There was one respiratory-related death in each group.
Conclusion: Although the post-symptomatic group represents sicker children, the postoperative complications appear to be higher. For infants with known malrotation, prophylactic operations may be beneficial and should be considered. A larger, prospective study comparing prophylactic Ladd procedures to observation is needed to demonstrate its comparative effectiveness and generalizability.

ABSTRACT

Assessing Burden of Care in the Cleft Lip and Palate Patient: Factors Influencing Success and Failure of Nasoalveolar Molding

Riley A. Dean *The University of Texas at Houston Medical School* *Class of 2018*

Sponsored by: Matthew Greives, MD, Department of Pediatric Plastic Surgery

Supported by: Matthew Greives, MD, Department of Pediatric Plastic Surgery; The University of Texas Health Science Center at Houston Medical School – Office of the Dean

Key Words: nasoalveolar molding, cleft lip, cleft plate

Cleft lips and palates are some of the most commonly occurring congenital deformities worldwide. Nasoalveolar molding (NAM) is a pre-surgical therapy for patients born with complete cleft lip and/or palates. NAM therapy utilizes custom oral splints to reshape the alveolar process and nose in patients with complete cleft deformities, leading to improved post-operative outcomes. While the benefits of NAM therapy are numerous, the burden of the labor-intensive treatment may leave certain patient populations at risk for therapy failure. We hypothesize that the number of patients reporting notable difficulty when trying to complete NAM will be higher than the value predicted using existing clinical research. In addition, we predict that patients from families with less education, lower socioeconomic status, less access to supportive resources, or those that live farther away will be less likely to complete NAM therapy protocol.

An IRB-approved 30-question survey was developed and administered at the University of Texas at Houston Cleft-Craniofacial Clinic to investigate patient experiences with NAM therapy. Several known complications were addressed to assess their rate of occurrence, and free response sections were included to understand how problems were presented, managed, or resolved. Demographic information such as ethnicity, age, and monthly family income of primary caregivers was also collected to identify potential barriers to care for patients and their families. Responses were collected and analyzed using SurveyMonkey software.

A total of 48 responses were received and included in the analysis. Of the patients interviewed, 7 (15%) failed to complete the NAM therapy protocol. Patient-reported outcomes mentioned several reasons for treatment failure: 1) obstructive sleep apnea, 2) airway obstruction concurrent with other birth defects, 3) lack of home support while primary caregiver was at work, 4) persistent gagging on the device, 5) acute dermatitis from tape or glue used, and 6) Loss of NAM appliance. While the small data set did not allow us to observe statistical significance, several trends are evident between failed and successful patient subgroups. Prevalence of bilateral cleft lips was higher in failed NAM group than in the completed group (43% vs. 22%). A larger percentage of failed NAM patient caregivers were less than the 26 years of age (71% vs. 46%). Failed NAM patients more frequently reported skin reactions to tape or

glue used, ulcerations in the mouth, and breathing difficulties (86% vs. 59%, 71% vs. 17%, and 43% vs. 10%, respectively). No other patient demographic metrics varied significantly between patient subgroups.

NAM therapy is a useful technique for reducing pre-surgical breadth of a cleft deformity, allowing for superior aesthetic results. It was discovered that some patients are not able to complete the therapeutic regimen. Certain risk factors have been suggested by our study, but more data is needed to elucidate true prevalence of NAM failure and to establish evidence-based guidelines to identify future patients at risk.

ABSTRACT

Effects of Ultrasound on Monocyte Migration using a Transwell Model

Juan Deleija-Lujano *The University of Texas at Houston Medical School* *Class of 2018*

Sponsored by: Melvin E. Klegerman, PhD, Department of Internal Medicine
Supported by: Melvin E. Klegerman, PhD, Department of Internal Medicine
Key Words: Monocyte, ultrasound, HUVEC, transwell

Progressing atherosclerosis disease is a process marked by accumulation of lipids and inflammatory cells that become unstable and may even disrupt, producing ischemia or infarction in the vessels and organs distal to the site of rupture. The role of stem cells to help mitigate and alleviate the progression of atherosclerosis disease has been well documented in the literature. Of special importance are CD34+ hematopoietic stem cells, a small population of monocytes in peripheral blood which play an important role in tissue regeneration by cell differentiation. Previously, our lab has demonstrated the use of bifunctional echogenic liposomes as a viable delivery method for CD34+ cells. We have also demonstrated the role of ultrasound in increasing migration of all monocyte populations using transwell inserts as an *in vitro* model. However, the mechanism by which this cell extravasation takes place is still unknown, making it difficult to assess the importance of ultrasound directed therapy *in vivo* studies. In this study, a model for *in vitro* monocyte migration was developed in order to interrogate the mechanism, and consequently produce evidence contributing to the effectiveness of echogenic liposomes for stem cell delivery to reduce atheroma progression. The model was developed using a transwell plate on which human umbilical vein endothelial cells were grown to confluence. After demonstrating confluence, monocytes were isolated from a buffy coat preparation, stained with Oregon Green, and pipetted into transwell inserts plated with confluent endothelial monolayers. The fluorescence of the plates was measured before and after ultrasound exposure in an anechoic chamber. A standard curve was used to demonstrate the sensitivity of the instrument to the stained monocytes, providing a r^2 value of 0.9968 along a decreasing concentration. Assuming all cells went through the insert and did not get caught between the endothelial cells, initial studies demonstrated an increase in cell migration, but not significant when compared to controls (54.04% ± 3.25%, 53.44 ± 4.12%, p = 0.83) at 1 hour post experiment. At 18 hours, however, there was an increase in cell migration for the ultrasound group compared to controls, however still not significant (28.11% ± 14.2%, 9.94 ± 6.21%, p = 0.07). The preliminary data of this experiment have provided evidence to support the results produced earlier by this lab. Further experiments are required to isolate the cells in each group and identify subpopulations, particularly CD34+, under the influence of TNFα, as well as interrogating the mechanism of cell extravasation through the endothelial monolayer.

ABSTRACT

Good Catches and Near Misses: The Hidden Benefit of Surgical Safety Checklists

Michael Diffley *The University of Texas at Houston Medical School* *Class of 2018*

Sponsored by: KuoJen Tsao, MD, Department of Pediatric Surgery

Supported by: KuoJen Tsao, MD, Department of Pediatric Surgery; The University of Texas at Houston Medical School—Office of The Dean

Key Words: Good Catches, Near Misses, Checklist

Introduction: The effectiveness of surgical safety checklists (SSCs) in reducing post-operative morbidity and mortality is difficult to measure when these outcomes are rare, as in pediatric surgery. However, SSCs may have additional benefits. Good catches and near misses are defined as events which can lead to patient harm but are prevented from occurring. We hypothesized that SSCs increase good catches and near misses.

Methods: A direct observational study from May-July 2015 was conducted. During the performance of the 19-point, pre-incision phase of the SSC, five trained observers documented checklist adherence and good catch or near miss events. The events were organized into five categories by a patient safety expert: communication failures, medication issues, equipment issues, process issues, and safety issues. Regression analysis was used to evaluate the association between events and the performance of the checklist (adherence to all checkpoints), surgical specialty and case duration. Inter-rater reliability (kappa) was determined for checklist adherence.

Results: Among 212 cases from 9 pediatric surgical subspecialties, SSCs resulted in detection of at least one event in 37 (17%) cases. The most common events were related to process issues (32.4%); the least common events were due to equipment issues (2.7%, Figure). Median (range) pre-incision checkpoints completion was 18 (7-19). Pediatric cardiovascular surgery cases had the highest event rate of 33%: one good catch or near miss for every 3 cases. Kappa for the pre-incision checklist was 0.70 (95%CI 0.63-0.88). On regression analysis, there were no significant associations between the number of events per checklist and checklist adherence, surgical specialty, or case duration. The median number of events did not vary with case length (<30 min = 1, 31-60 min = 1, 61-120 min = 1, >121 min = 1).

Conclusion: Surgical safety checklists, when performed with high fidelity, can detect good catches and near misses. Evaluation of SSCs often focuses only on morbidity and mortality, while good catches and near misses are not reported. Identification and categorization of these events should be routinely measured since they provide targets for focused quality improvement which may lead to reduced errors and adverse events.

ABSTRACT

Glucose 6-phosphate Levels Correlate with Mechanistic Target Of Rapamycin Complex 1 Activity and mTOR/HK-2 Interaction in Human Heart Muscle

Karen Ding *The University of Texas at Houston Medical School* *Class of 2018*

Sponsored by: Heinrich Taegtmeyer, MD, DPhil, Department of Internal Medicine
Supported by: National Institute of Diabetes and Digestive and Kidney Diseases, 2T35DK007676-22
Key Words: mTORC1, glucose 6-phosphate, HK-2, heart muscle

Background: In the heart, metabolism is a key driver of ATP production for contraction and also a rich source of signals for the regulation of protein turnover. An example is glucose 6-phosphate (G6P). Classically regarded as an intermediary metabolite, G6P is also a key metabolic signal. Increased G6P is required for activation of the mechanistic Target Of Rapamycin Complex 1 (mTORC1) in hearts subjected to high workload or insulin treatment. Furthermore, *in vitro* studies have shown that the underlying mechanism of G6P-mediated mTORC1 activation is the loss of physical interaction between mTOR and the enzyme hexokinase II (HK-2). Previous work in the lab has shown that G6P levels in failing human hearts decrease after mechanical unloading, and this correlates with decreased activation of the mTORC1 signaling pathway. I strived to elucidate the details behind this phenomenon.
Hypothesis: mTORC1 activation in the failing human heart is due to HK-2 unbinding from mTORC1 in the presence of high G6P levels.
Methods: Human heart samples from left ventricle free wall of patients undergoing heart-lung transplant from primary pulmonary hypertension were used as non-failing controls and obtained from The Methodist Hospital Houston. For the failing group, human heart samples from left ventricle apex of patients with end stage heart failure undergoing left ventricular assist device (LVAD) implantation were used and obtained from the Texas Heart Institute human biobank. The following inclusion criteria was applied for sample selection of the failing group: non-ischemic cardiomyopathy, LVAD implantation in 2006 or later, and paraffin embedded formalin fixed slides from biopsy samples available for study. G6P levels were measured by spectrophotometric enzymatic analysis using G6PDH coupled to NADPH production with extinction at 340 nm. Proteins were extracted from frozen tissue, and western blotting was performed for insulin signaling pathway proteins, mTORC1, and its downstream targets.
Results: G6P levels were significantly higher in failing versus non-failing heart muscle of non-diabetic patients. In non-failing heart muscle, diabetics have higher G6P levels. Western blotting revealed greater mTOR phosphorylation in failing heart muscle compared with non-failing heart muscle. Importantly, phosphorylation of upstream proteins of the insulin signaling pathway were not different in the two groups, suggesting mTORC1 activation in the failing

group occurs via a non-canonical pathway. Furthermore, there was a positive correlation between G6P levels and mTOR phosphorylation in heart muscle.

Conclusions and current work: Taken together, these results suggest that mTORC1 activation in the failing human heart is due to HK-2 unbinding from mTOR rather than activation through the insulin signaling pathway. This provides further evidence that in the human heart, metabolic remodeling triggers structural remodeling.

Currently, the lab is performing proximity ligation assays in paraffin embedded formalin fixed tissue slides to confirm mTOR/HK-2 interaction correlates with G6P levels and mTORC1 activity. Also, our collaborators at The Methodist Hospital are recruiting more patients into the study to obtain more non-failing human heart samples to increase the power of our study.

ABSTRACT

The Antibody Response to Epstein-Barr Pproteins BFRF3 and BRRF2 is Increased in Multiple Sclerosis

Matthew M. Dooley *The University of Texas at Houston Medical School* *Class of 2018*

Sponsored by: John W. Lindsey, M.D, Department of Neurology
Supported by: FCMSC Inserra Family Research Scholarship
Key Words: Multiple Sclerosis, Epstein-Barr virus, Antibodies

Background: Infection with Epstien-Barr Virus (EBV) has long been associated with the development of multiple sclerosis (MS). Recent studies into more explicit portions of the virus's proteome have demonstrated that MS patients possess an increased antibody response to specific EBV antigens. EBV proteins Epstein-Barr nuclear antigen-1 (EBNA-1), viral capsid antigen (VCA), and early antigen (EA) have been explored, but have failed to show a statistically significant increase in their elicited antibody response. We intend to identify additional EBV antigens that do exhibit an increased antibody response, and investigate these resultant antibodies for their potential cross-reactivity with healthy brain tissue. Such a finding could suggest a possible autoimmune route of disease progression in MS.
Hypothesis: Specific EBV antigens elicit an increased antibody response in MS patients. These antibodies contribute to disease progression via autoimmune cross-reactivity with healthy brain tissue.
Methods: 5 EBV proteins (gH, MCP, BLRF3, BFRF3, BRRF2) were expressed in E. Coli. After isolation via centrifugation, effective recovery of the target protein was verified with western blots and coomassie staining. Quantitative ELISAs with 80 paired plasma samples were then used to evaluate the relative antigenicity of each protein versus their bacterial control. The proteins that demonstrated a statistically significant elevation in their elicited antibody response were then further investigated. Affigel 10 agarose beads coupled to these antigens were use to isolate their respective specific antibody via column chromatography. These antibodies were then used to immunoprecipitate cross-reactive brain tissue. The bound brain proteins were identified via mass spectrometry.
Results: BFRF3 ($p<.007$) and BRRF2 ($p<.006$) were shown to elicit significantly higher antibody responses in MS over controls. Of note, Anti-BFRF3 antibodies showed affinity for several septin proteins (in decreasing order of concentration: 9, 5, 7, 8, 11, 6, 4, 3). Anti-BRRF2 antibodies showed affinity for desmoplakin.
Conclusions: Both BFRF3 and BRRF2 are significantly more antigenic in MS patients than controls, and their elicited specific antibodies demonstrate an ability to cross-react with normal brain proteins. This autoimmunity may contribute the disease progression of MS via disruption of the normal function of septin (BFRF3) and desmoplakin (BRRF2). While further investigation is warranted in the case of both of these proteins, desmoplakin's role in tight junctions is congruent with the hypothesis that a disrupted blood brain barrier is critical in the development of multiple sclerosis.

ABSTRACT

High-fat Meals, Postprandial Endothelial Dysfunction, and Antidiabetic Medications in Prediabetic Patients

Amy Dursteler *The University of Texas at Houston Medical School* *Class of 2018*

Sponsored by: Absalon Gutierrez, MD, Department of Internal Medicine, Division of Endocrinology, Diabetes, and Metabolism; Heinrich Taegtmeyer, MD, DPhil, Department of Internal Medicine, Division of Cardiovascular Medicine

Supported by: National Institute of Diabetes and Digestive and Kidney Diseases, 2T35DK007676-22

Key Words: Prediabetes, type 2 diabetes, endothelial dysfunction, cardiovascular disease

Intensive glycemic control may not be the optimal strategy for reducing cardiovascular events in adults with type 2 diabetes mellitus (T2DM). However, some of the newer antidiabetic medications may prevent endothelial dysfunction and delay atherosclerosis. Endothelium – the inner lining of blood vessels – controls vasoconstriction and vasodilatation. An imbalance of these actions – known as "endothelial dysfunction" – increases the risk of atherosclerosis and cardiovascular disease in individuals with prediabetes and T2DM, especially in the postprandial state. Exenatide, a glucagon-like peptide 1 (GLP-1) agonist, decreases postprandial endothelial dysfunction in individuals with impaired glucose tolerance (a type of prediabetes). Saxagliptin and pioglitazone - a dipeptidyl peptidase-IV (DPP-IV) inhibitor and a PPAR-γ agonist, respectively - may produce similar effects, but this hypothesis has never been tested effectively. This randomized, crossover, placebo-controlled, double-blinded prospective trial tests the efficacy of exenatide, saxagliptin, and pioglitazone in reducing postprandial endothelial dysfunction and postprandial lipid levels in obese adults with prediabetes. Each subject is studied 4 times in day-long outpatient visits, each representing one of the 4 study arms (placebo, exenatide, saxagliptin, and pioglitazone). The study medication is given prior to a high-fat standardized meal. Peak forearm blood flow (FBF) – a method of quantifying endothelial function - is measured at baseline and at 3 and 6 hours after the meal. Other outcomes include plasma triglycerides and free fatty acid levels. The data show an increase in peak FBF from baseline to 6 hours in at least one of the study arms, whereas the other arms exhibited either no change or a decrease in FBF. This suggests that one of the medications is preserving endothelial function. This may be exenatide, based on prior observations. However, the identification of treatment arms will not be known until the end of the study, as per design. Data on triglycerides and free fatty acids are being analyzed and will be correlated with FBF data for all subjects at the time of study completion.

ABSTRACT

An Evaluation of eHealth Utilization in Pediatric Surgery – What is the Parent's Perspective?

Arturo Eguia *The University of Texas at Houston Medical School* *Class of 2018*

Sponsored by: Mary T. Austin, MD, MPH, Department of Pediatric Surgery

Supported by: Mary T. Austin, MD, MPH, Department of Pediatric Surgery; The University of Texas at Houston Medical School – Office of the Dean

Key Words: eHealth, Barriers, Pediatric Surgery

Introduction: eHealth is the use of digital information and online communication to improve a person's health or health care. Previous studies have shown that patients face many barriers when attempting to utilize e-Health including factors related to socioeconomic status, language, age, and education. We hypothesized that barriers exist that significantly impact a parent's ability to access and feel comfortable with using eHealth.

Methods: We performed a cross-sectional study which included 24 non-randomly selected parents of 21 pediatric surgical patients. After obtaining informed consent, semi-structured interviews were conducted in an outpatient clinic by one of two co-authors (AE and BF). The interviews were conducted in each participant's primary language (11 English and 10 Spanish) and participants were asked about access to eHealth, mechanism(s) of use and challenges faced in accessing and using eHealth. The interviews were recorded and transcribed, and the qualitative data were analyzed using thematic analysis. English-speaking participants (ESP) and Spanish-speaking participants (SSP) were compared.

Results: All participants, except one SSP, had access to the Internet at home. Compared to SSP, ESP were more likely to use the Internet to learn about their own (73% vs 38%) or their child's health (80% vs 50%). In both groups, parents who used eHealth were more likely to look up information regarding their child's health versus their own health. ESP tended to use computers and cell phones, whereas SSP were more likely to use only tablets or cell phones. Challenges to using eHealth for ESP included the vast amount of knowledge available, uncertainty of resource credibility and poor Internet connections. Among SSP, non-Spanish websites, inadequate access and lack of knowledge on how to use the Internet presented challenges to utilizing eHealth. In both groups, most participants viewed the potential for email communication with their child's physician as positive (85%).

Conclusion: While most parents report access to the Internet, both English-speaking and Spanish-speaking parents face challenges in utilizing eHealth. In this pilot project, we identified several key differences between ESP and SSP. We will use our results to inform content in developing a survey to identify and characterize comfort level and barriers that might hinder a parent's ability to navigate eHealth. This will lay the foundation for the development of a program that can facilitate patient and parent access to and comfort engaging in eHealth.

ABSTRACT

Can Hyperglucagonemia Cause Type I Diabetes?

Ikenna K. Emelogu *The University of Texas at Houston Medical School* *Class of 2018*

Sponsored by: Qingchun Tong, PhD, Center for Metabolic and Degenerative Diseases, Institute of Molecular Medicine

Supported by: National Institute of Diabetes and Digestive and Kidney Diseases, 2T35DK007676-22

Key Words: Hyperglucagonemia, type 1 diabetes, DREADD, Cre, CNO

Background: Type I diabetes (T1D) mellitus, the most common chronic endocrine disease among children, is a major problem in today's society. Also known as insulin-dependent diabetes mellitus, type I diabetes is an autoimmune disease that occurs due to the destruction of the beta cells of the pancreas which produce insulin. However, a recent study compared glucagon receptor knockout mice to wild-type mice after both groups were treated with streptozotocin (STZ), a toxin used in diabetes research to kill beta cells. The wild-type mice went on to develop type I diabetes, but the glucagon receptor knockout mice had no clinical manifestations of the disease, suggesting that insulin deficiency alone is not enough to cause T1D and that glucagon might have an important role to play. Most type I diabetes cases are associated with hyperglucagonemia. However, whether hyperglucagonemia is the primary reason for the development of T1D is unknown. The aim of this research project is, therefore, to examine whether hyperglucagonemia itself will be sufficient to cause chronic hyperglycemia and beta cell death leading to type I diabetes.
Methods: Cre-lox P recombination technology was used to produce transgenic mice that have selective expression of an artificial receptor known as DREADD (Designer Receptors Exclusively Activated by Designer Drugs) in the alpha cells of the pancreas. A novel system was generated in which DREADD was coupled with Gsα-coupled receptors knocked into the Rosa26 locus. The construct was designed in such a way that the expression of Gsα-coupled DREADD (as well as the genetic markers: luciferase and GFP) would depend on the presence of Cre. Glucagon-Cre mice were crossed with the DREADD mice, thereby localizing the expression of DREADD to alpha cells. Clozapine-N-oxide (CNO), which can activate DREADD albeit a biologically inert drug, was administered to the bigenic glucagon-Cre Rosa26-DREADD mice (0.5 mg/kg 2x daily for 1 week) to activate alpha cells in a chronic fashion.
Results: Genotyping for DREADD and Cre were confirmed by PCR. However, no signal was obtained from immunostaining of the mouse pancreas using anti-luciferase, pCREB (CREB is one typical downstream signaling molecule of Gsα), and anti-GFP antibodies. No significant differences in blood glucose levels were observed between experimental and control mice after a one-time injection of CNO in the former, both in normal and fasted states. Also, no significant differences in blood glucose levels were observed after one week of CNO administration (2x daily).
Conclusion: It appears that the current CNO and Gsα-DREADD system does not allow sufficient activation of alpha cells to effectively test our hypothesis. A similar but more rigorous system is needed to test our hypothesis, for example using Gq DREADD.

ABSTRACT

Gene Signatures Vital to Patient Survival in Ovarian Cancer

Margaret Engelhardt *The University of Texas at Houston Medical School* *Class of 2018*

Sponsored by: Anil K Sood, MD, M.D. Anderson Cancer Center Department of Gynecologic Oncology; David E Volk, PhD, Department of Nanomedicine and Biomedical Engineering
Supported by: David E Volk, PhD, Department of Nanomedicine and Biomedical Engineering
Key Words: Ovarian cancer, survival, TMEM62

Background: Ovarian cancer is the most lethal gynecologic malignancy in the United States and other developed countries. Despite displaying similar histology, patients with high grade serous ovarian carcinoma (HGSOC) often show significantly variable outcomes for reasons not well understood. To address this knowledge gap, the objectives of this study were (1) to identify genes that are differentially expressed in tumors derived from ovarian cancer patients with long-term (LT; >10 years) and short term (ST; <6 months) survival, (2) to determine the downstream effects and dominant pathways affected by genes of interest, and (3) to examine the therapeutic benefit of overexpressing or knocking down the target genes.
Methods: RNA sequencing (RNA-seq) was conducted on tumor samples from a discovery cohort of 12 LT survivors and 12 ST survivors. cDNA synthesis and quantitative real time-PCR (qPCR) were used to validate these preliminary results using RNA isolated from tumor samples from a separate patient cohort of 15 LT and 14 ST survivors. The human HGSOC line OCVA432 was treated with both a control plasmid and a plasmid expressing the protein of interest. qPCR and Western blot were used to evaluate protein expression after plasmid transfection.
Results: Eight genes highly expressed in ST survivors were identified in the initial RNA-seq analysis ($p<.00001$); of these, five had sufficient expression for potential knockdown – PCSK2, SCN2B, SULT1E1, PLXNB1, and RSPO1. Three genes were overexpressed in LT survivors ($p<.00001$); one had sufficient expression for future therapeutic benefit – TMEM62. Of these, TMEM62 (transmembrane protein 62) showed the most significant result in the validation cohort. Transfection of OVCA432 with the TMEM62 plasmid produced a substantial increase in TMEM62 mRNA over the control plasmid treatment ($p<0.0005$). An increase in TMEM62 protein was seen on Western blot after the TMEM62 plasmid transfection.
Conclusion: There are significant molecular differences between short-term and long-term survivors of ovarian cancer. These changes (e.g. TMEM62) may represent novel therapeutic opportunities. As the function of TMEM62 is unknown, further studies are necessary to illuminate its possible role as a tumor-suppressor gene. A gene expression array is currently ongoing to determine its downstream roles in cell physiology. Further cell viability, proliferation, and apoptosis assays will be performed to determine the effects of TMEM62 protein expression on these processes.

ABSTRACT

Treatment Outcomes in Pediatric Melanoma - Are There Benefits to Specialized Care?

Benjamin Freemyer *The University of Texas at Houston Medical School* *Class of 2018*

Sponsored by: Mary Austin, MD, MPH, Department of Pediatric Surgery
Supported by: Mary Austin, MD, MPH, Department of Pediatric Surgery
Key Words:

Purpose: To evaluate the impact of hospital specialization on treatment outcomes in pediatric melanoma.

Methods: After IRB approval, we retrospectively reviewed all patients < 18 years old diagnosed with cutaneous melanoma and evaluated in a comprehensive cancer center between 2000 and 2015. We compared overall survival (OS) and disease-free survival (DFS) between patients who underwent surgical treatment at a National Cancer Institute (NCI)-designated comprehensive cancer center (Group A, n=146) to those who underwent initial surgical treatment at a non-NCI hospital or outpatient surgery center (Group B, n=58). Demographic and clinical factors were compared using Fisher's exact test or Wilcoxon rank sums test as appropriate. Kaplan-Meier survival curves were compared using the log-rank test.

Results: The median age at diagnosis was 13.7 years (range 1.2-17.8 years). The 5-year OS from diagnosis and 5-year DFS was 94.3% (95%CI 89.7%, 96.9%) and 89.8% (95%CI 84.2%, 93.4%), respectively. Group A patients were more likely White, family history of skin cancer, thinner primaries, and earlier stage disease (all $p < 0.05$). Group B patients were more likely to receive adjuvant therapy (50% versus 32%, $p<0.05$). Group A had significantly better OS and DFS with a 5-year OS of 96.8% (95% CI 91.8%, 98.8%) and 5-year DFS of 94.4% (95% CI 88.5%, 97.3%) compared to 5-year OS of 87.5% (95% CI 74.2%, 94.2%) and 5-year DFS of 77.2% (95% CI 62.5%, 86.7%) in Group B (both $p<0.001$). The survival differences were most notable in Stage 3 and 4 patients (Figure 1). Other factors associated with a higher risk of death included Non-white race/ethnicity, primary tumor ulceration, lymphovascular invasion, Breslow thickness > 4mm, stage 3 or 4 disease, unknown primary, older age, and receipt of adjuvant therapy (all $p<0.05$).

Conclusion: Surgical treatment at a comprehensive cancer center may improve outcomes for pediatric melanoma especially for patients presenting with later stage disease.

ABSTRACT

Distress Tolerance in Trauma-Exposed, Acute-Care Psychiatric Inpatients: Associations with Substance Use and Posttraumatic Stress

Shavonia Gants *The University of Texas at Houston Medical School* *Class of 2018*

Sponsored by: Anka A. Vujanovic, PhD, Department of Psychiatry and Behavioral Sciences
Supported by: The Bernard Saltzberg Summer Research Fellowship
Key Words: distress tolerance, trauma, PTSD, substance use

Background: The highly prevalent co-occurrence of posttraumatic stress disorder (PTSD) and substance use is associated with poor treatment outcomes for both conditions. Distress tolerance, defined as the perceived or actual ability to experience negative emotional states, is a factor, targetable via cognitive-behavioral intervention, with demonstrated relevance to both PTSD and substance use. Better understanding associations among distress tolerance, PTSD symptomatology, and substance use behaviors have the potential to inform novel specialized psychotherapeutic interventions for individuals with both conditions. However, due to the multitude of self-report and behavioral indices of distress tolerance, studies often include certain measures to the exclusion of others, precluding our ability to generalize and synthesize findings across indices. Thus, it is important to include measures of perceived and actual (behavioral) distress tolerance in studies of PTSD and substance use to better understand this construct in the context of PTSD symptomatology and substance use.
Significance: First, no studies to date have concurrently examined perceived and actual distress tolerance in terms of both PTSD symptoms and substance. Second, no studies have examined such associations in an acute-care psychiatric inpatient population.
Hypothesis: It was hypothesized that both perceived and actual (behavioral) distress tolerance, measured via the Distress Tolerance Scale (DTS) and Breath Holding Task (BH), respectively, will be incrementally negatively (inversely) associated with (1) PTSD symptom severity, (2) nicotine dependence, (3) problematic alcohol use, and (4) problematic drug use. Covariates will include trauma exposure severity and number of psychiatric diagnoses.
Experimental Design: A total of 155 acute-care inpatient adults (66 women; *M*age = 33.83, *SD* = 11.19) participated in the current study. Approximately 43.9% identified as white/Caucasian, 38.1% as black/African American, 15.5% as Hispanic, 1.9% as Asian, and 0.6% as Native Hawaiian/Pacific Islander. Participants completed a series of self-report questionnaires, including the Life Events Checklist (LEC) to assess trauma exposure, PTSD Checklist for DSM-5 (PCL-5) to assess PTSD symptom severity, DTS to assess perceived emotional distress tolerance via self-report; BH to assess actual physical distress tolerance; and the Addiction Severity Index (ASI) and Fagerstrom Test for Nicotine Dependence (FTND) to assess substance use and nicotine dependence, respectively. Electronic Medical Records Review provided information regarding psychiatric diagnoses and demographic characteristics.
Results/Data: A series of four hierarchical linear regression analyses was conducted. At step one of each of the models, the covariates of number of psychiatric diagnoses and trauma

exposure severity (LEC: number of trauma exposures) were entered. At step two of each of the models, two indices of distress tolerance (BH and DTS) were entered as predictors. Criterion variables included: (1) PTSD symptom severity (PCL-5 Total Score), (2) nicotine dependence (FTND Total Score), (3) past-month alcohol problems (ASI: number of days), and (4) past-month drug problems (ASI: number of days).

With regard to PTSD symptomatology, the overall model accounted for 35.7% of variance ($p < .01$). At step one, trauma exposure severity was significantly associated with PTSD symptom severity ($t = 5.09$, $\beta = .44$, $p < .001$); step two accounted for 14.2% of unique variance, with DTS as the only significant predictor ($t = 4.82$, $\beta = .39$, $p < .001$). The model relevant to nicotine dependence was not significant; none of the variables in the model was significantly associated with nicotine dependence (p's > .05). With regard to past-month alcohol problems, the overall model accounted for 11.9% of variance ($p < .05$). At step one, number of psychiatric diagnoses was significantly associated with past-month alcohol problems ($t = 2.04$, $\beta = .22$, $p < .05$). At step two, DTS was a significant predictor ($t = 2.21$, $\beta = .23$, $p < .05$); the overall step was not significant ($p = .07$). With regard to past-month drug problems, the overall model accounted for 10.4% of variance ($p < .05$). At step one, number of psychiatric diagnoses was significantly associated with past-month drug problems ($t = 2.99$, $\beta = .28$, $p < .01$). Step two was not significant.

Conclusions: Higher levels of distress tolerance were associated with PTSD symptoms as well as past-month alcohol and drug problems. This is contrary to past work wherein distress tolerance was negatively (inversely) associated with PTSD symptoms and substance use. These findings might indicate that distress in-tolerance or over-tolerance are both potential risk factors for PTSD and substance use. Further replication and extension of these findings is necessary in acute-care psychiatric populations. In this sample, contrary to past work, distress tolerance was not significantly associated with nicotine dependence. Interestingly, only perceived (self-reported) tolerance of negative emotional states, as opposed to actual tolerance of uncomfortable physical sensations (BH), was significantly associated with the outcomes of interest. Taken together, the results indicate that distress tolerance is a significant factor to consider with regard to both PTSD symptomatology and substance use in trauma-exposed populations; and one that may usefully inform treatment development efforts. Results also supported the well-established association between psychiatric disorders and substance use problems.

ABSTRACT

Secondary Cleft Nasal Reconstruction Using Resorbable Plates: Complications and Indications

Anthony P. Gibson *The University of Texas at Houston Medical School* *Class of 2018*

Sponsored by: Matthew R. Greives, MD, Department of Pediatric Plastic Surgery
Supported by: The University of Texas at Houston Medical School – Office of Educational Programs
Key Words: Resorbable plate, secondary nasal reconstruction, cleft lip

Abnormal cartilage in cleft nose patients does not provide adequate nasal support and leads to subsequent nasal deformity. Pediatric cleft patients have a limited amount of cartilage that can be harvested to provide additional support. Cranial vault surgery utilizes resorbable plates to successfully reinforce structurally weak areas, similar to cartilage graft supports in nasal surgery. Therefore, we sought to demonstrate the utility and complication profile of absorbable plates compared to conventional cartilage grafts in secondary cleft nasal reconstruction.
An IRB approved (HSC-MS-12-0408) retrospective chart review was conducted of patients who underwent secondary nasal reconstruction from January 1, 2000 till May 1, 2015 at Children's Memorial Hermann Hospital. Retrieved data included age at surgery, type of surgery, type of cleft, whether a cartilage or absorbable graft was utilized, and any possible complications. All absorbable plate outcomes were compared to the cartilage graft outcomes using a statistical Fisher's exact test (α=0.05). Photographs from the UT Physicians Department of Pediatric Surgery Cleft Center were also analyzed. Selected patients had their facial photos analyzed from preoperatively and post operatively views.

Secondary nasal reconstruction was performed in 197 patients. Out of the 197 patients, 27 patients lacked sufficient outcome/graft information and were excluded from the study. Of the remaining 170 patients (44.1% female, 55.9% male, avg. age - 8.5yrs), 39 utilized an absorbable plate, 42 used a cartilage graft, and 89 did not use a cartilage graft or absorbable plate. There was no difference between the absorbable plate group (43.6% female, 56.4% male) and the cartilage graft alone group (42.9% female, 57.1% male). Absorbable plates were used as a strut graft (28), alar graft (10), or tip graft (1). Types of clefts in the absorbable plate patients were unilateral/complete (23), unilateral/incomplete (4), bilateral/complete (7), and bilateral/incomplete (4). Surgical complications of absorbable plate patients vs. conventional cartilage graft patients were as follows: an infection rate of 2.6% vs. 4.8% (P=1), an extrusion rate of 10.3% vs. 7.1% (P=0.71), no malposition, a deformation rate of 0% vs. 2.4% (P=1), and no seroma/hematoma. Additional tertiary nasal revisions were 33.3% vs. 40.5% (P=0.65). Airway/breathing complications were a sleep apnea rate of 5.1% vs. 2.4% (P=0.61), and snoring rate of 2.6% vs. 0% (P=0.48). There was no significant difference found between the incidences

of complications of the secondary nasal reconstructions utilizing absorbable plates vs. traditional cartilage grafts.

The data shows that absorbable plates can be used as a safe alternative to cartilage grafts in secondary nasal reconstructions in the pediatric cleft population. The complication profile is similar to traditional cartilage grafting without the need for additional donor sites and potential morbidities.

ABSTRACT

Serum Brain-Derived Neurotrophic Factor as an Indication of Disease State in Parkinsonism and REM Sleep Behavior Disorder

Adam Gonzalez *The University of Texas at Houston Medical School* *Class of 2018*

Sponsored by: Keri C. Smith, PhD, Department of Pathology and Laboratory Medicine
Supported by: Keri C. Smith, PhD, Department of Pathology and Laboratory Medicine
Key Words: Parkinson's Disease, Brain-derived Neurotrophic Factor, REM Behavior Disorder, Multiple System Atrophy, Deep Brain Stimulation

Current literature indicates that brain-derived neurotrophic factor (BDNF) plays a role in the pathogenesis of synucleinopathies including prodromal REM sleep behavior disorder (RBD), Parkinson's disease (PD) and multiple system atrophy (MSA) due to its ability to support neuronal survival and synaptic plasticity in the brain. Evidence for local involvement of BDNF in the pathogenesis of movement disorders has been demonstrated in animal and cell culture models, but it is unknown if levels in peripheral blood are indicative of disease state.

Using serum samples collected as part of an ongoing longitudinal study, BDNF was measured via ELISA from patients with PD (N=34), MSA (N=17), RBD (N=12), and age-matched normal controls (N=20). BDNF levels were significantly increased in patients with PD ($p=0.0019$), MSA ($p=0.0031$), and RBD ($p=0.0161$) when compared to controls, suggesting that increased serum BDNF is associated with the development of movement disorders. Next, the relationship between BDNF and symptoms of PD was probed by comparing serum levels before and after deep-brain stimulation (DBS), an effective therapy that markedly improves motor function in patients with PD. PD patients who underwent DBS (N=6) for treatment of their symptoms exhibited a significant decrease in their BDNF values ($p=0.0079$), which correlated with a change in motor scores demonstrating improvements in symptoms (UPDRS-Total $p=0.0247$; UPDRS-Motor values $p=0.026$).

These results strongly suggest that peripheral concentrations of BDNF reflect the progression of Parkinson's disease and related disorders, as indicated by the link between clinical measurements of disease state and evident decreases in BDNF after DBS, when symptoms have been alleviated. This property suggests that BDNF might be a useful biomarker for monitoring neurodegenerative disease activity.

ABSTRACT

A Possible Role for Pulmonary Surfactant Protein A on the Modulation of Inflammation in the Maturing Gut

Cullen Grable *The University of Texas at Houston Medical School* *Class of 2018*

Sponsored by: Joseph L. Alcorn, PhD, Department of Pediatrics
Supported by: National Institute of Diabetes and Digestive and Kidney Diseases, 2T35DK007676-22
Key Words: Surfactant Protein A, Inflammation, NEC, prematurity

The second most common cause of mortality in premature infants, necrotizing enterocolitis (NEC), is a condition where the lower gastrointestinal tract becomes inflamed and undergoes necrosis. Unfortunately, outside of surgery, treatment options are limited. While the causes of NEC are multi-factorial, inflammation, the presence of lipopolysaccharide (LPS) and activation of toll-like receptor 4 (TLR4) play important roles. Surfactant protein-A (SP-A), which is under-expressed in premature infants, is produced by epithelial cells of the jejunal and colonic mucosa. SP-A has been shown to modulate inflammation, bind LPS and dampen the activity of TLR4, all of which are part of the pathogenesis of NEC. SP-A has been previously shown to reduce inflammation in a mouse model of NEC. We aim to characterize the physiological architectural differences and changes in the levels of inflammatory cytokines of the ileum and the colon of mice in the presence and absence of SP-A by comparing gut tissue of WT and SP-A knockout (KO) mice at 1, 2, 3, and 4 weeks of age. Intestinal and colonic levels of TLR4 protein were measured by Western blot, and levels of the pro-inflammatory cytokine IL1β were measured by ELISA. SP-A KO mice showed a greater than 2-fold increase in expression of TLR4 in the ileum relative to WT mice at 1, 2 and 3 weeks of age. The relative difference between WT and KO mice decreased to 1.8-fold by four weeks of age. In WT mice, ileal and colonic IL-1β levels increased 2.5-fold from week 1 to week 2, but were dramatically reduced by week 3. On the other hand, ileal and colonic IL-1β levels in SP-A KO mice were 2-fold lower than WT at week 1 of age and then increased 4-fold by week 3. These results suggest that SP-A may have a role modulating the inflammatory responses of the newborn intestine; SP-A seems to have a pro-inflammatory role in the early newborn mice and an anti-inflammatory role as mice age. SP-A may modulate the inflammatory environment of the gut at 2 to 3 weeks of age, exposing the gut to high levels of inflammation that ultimately lead to a healthy mature gut environment as development progresses. Thus, the relative lack of SP-A in premature infants may limit the development of the normal gut defenses and predispose them to NEC.

ABSTRACT

Correlating Prenatal Imaging Findings of Fetal Ventriculomegaly with the Need for Surgical Intervention at Birth

Joshua Gu *The University of Texas at Houston Medical School* *Class of 2018*

Sponsored by: David I. Sandberg, MD, Department of Pediatric Neurosurgery
Supported by: Department of Pediatric Surgery
Key Words: Fetal Hydrocephalus/Ventriculomegaly, Surgical Intervention

Introduction: Our objective was to determine which prenatal imaging measurements best predicts the need for cerebrospinal fluid (CSF) diversion at birth.

Methods: We retrospectively reviewed medical records of fetuses screened for hydrocephalus from January, 2011 to December, 2014. Prenatal measurements on ultrasound and/or MRI included head circumference (HC), biparietal diameter (BPD), and lateral ventricle (LV) width. Patients requiring CSF diversion within 12 weeks of birth were compared to those who did not using Wilcoxon Rank Sum Test. Receiver operating characteristic (ROC) analysis was used to evaluate threshold values.

Results: 50 of 1,303 screened patients had ventriculomegaly. 33 patients had open neural tube defects, 6 had aqueductal stenosis, and 11 had hydrocephalus of miscellaneous causes or unknown etiology. 31 patients required CSF diversion within 12 weeks after birth. Mean LV width (mm) during the entire pregnancy was greater for the surgery group than the non-surgery group (19.9 ± 4.8 vs. 14.1 ± 8.6; $p = 0.014$). Largest LV width between 28-32 weeks was also greater for the surgery group (26.8 ± 16.9 vs 17.4 ± 6.6 mm; $p = 0.047$). Neither BPD nor HC showed differences between the groups. A LV of 15mm predicted the need for a diversion procedure with a sensitivity of 0.91 and specificity of 0.43.

Conclusions: LV width is the prenatal imaging measurement that best predicts the need for postnatal CSF diversion. Awareness of this finding will facilitate accurate prenatal counseling when a fetus is diagnosed with ventriculomegaly.

ABSTRACT

Role of Gremlin on Insulin Secretion: A Link Between Chronic Pancreatitis and Diabetes

Lina Ha *The University of Texas at Houston Medical School* *Class of 2018*

Sponsored by: Tien C. Ko, MD, Yanna Cao, MD, Department of Surgery

Supported by: Tien C. Ko, MD, Yanna Cao, MD, Department of Surgery; The University of Texas at Houston Medical School – Office of the Dean

Key Words: Chronic pancreatitis, diabetes, Gremlin, BMP, Min6, insulin

INTRODUCTION: Chronic pancreatitis (CP) is a progressive inflammatory disorder marked in late stage by extensive fibrosis and endocrine insufficiency in the pancreas. The latter effect leads to secondary diabetes in 30-50% of CP patients and accounts for nearly 1% of total diabetes. Bone morphogenetic protein (BMP) signaling is anti-fibrogenic in the pancreas. Our group has recently demonstrated that Gremlin (Grem1), a natural BMP antagonist, is elevated in CP and plays a pro-fibrogenic role. We hypothesize that BMP signaling is suppressed by increased Grem1 in CP, resulting in decreased insulin secretion and development of CP-induced diabetes.

METHODS: Min6 cells, derived from mouse insulinoma, were used as an in vitro model for examining the effects of Grem1 and BMP2 on insulin secretion. The cells underwent four treatments: Vehicle control, BMP2 (50 ng/ml), Grem1 (500 ng/ml), and Grem1 (500 ng/ml) and BMP2 (50 ng/ml). The cells were pretreated with Grem1 for 30 min followed by BMP2 treatment, and harvested at 30 min, 60 min, and 24 hours for measurement of BMP2 signaling, insulin secretion, and cell growth, respectively. BMP2 signaling was detected by Western blot of phosphorylation(p) of Smad1/5/8. Insulin secretion from cell culture supernatant was determined by ELISA. Cell growth was determined by cell counting. Analysis of Variance (ANOVA) was used for comparison of multiple treatment groups. P value < 0.05 is considered significant.

RESULTS: Compared to Vehicle, Grem1 alone did not induce significant pSmad1/5/8. BMP2 alone induced 16-fold of pSmad1/5/8 ($p<0.05$), while Grem1 pretreatment suppressed BMP2-induced pSmad1/5/8 level to 1.5-fold. Vehicle, BMP2, Grem1, and Grem1 combined with BMP2 induced insulin secretion at 5.7, 5.3, 9.7 ($p<0.05$), and 10.0 ($p<0.05$) ng/ml, respectively. Cell counts of both alive and dead cells in all groups did not show any significant difference.

CONCLUSIONS: BMP2 signaling was suppressed by Grem1. Grem1 alone and in combination with BMP2 induced insulin secretion. These unexpected results do not support our original hypothesis; this instead suggests that Grem1 may have protective effects on pancreatic endocrine function at early stage of CP. These paradoxical effects of Grem1 on pancreatic fibrosis and endocrine function deserve further investigation.

ABSTRACT

Barriers to Participation in Preoperative Risk-reduction Programs Prior to Ventral Hernia Repair: An Assessment of Underserved Patients at A Safety-Net Hospital

Blake E. Henchcliffe *The University of Texas at Houston Medical School* *Class of 2018*

Sponsored by: Lillian S. Kao, MD, MS, FACS; Mike K. Liang MD, FACS, Department of Surgery

Supported by: Center for Clinical and Translational Sciences, National Institutes of Health Clinical and Translational Award UL1 TR000371 and KL2 TR000370, National Center for Advancing Translational

Key Words: Barriers, Preoperative Risk Reduction, Stakeholders, Ventral Hernia

Importance: Patients presenting with a ventral hernia often have modifiable risk factors. Preoperative risk reduction programs have been shown to be efficacious in behavior modification; however, generalizability of these outcomes to underserved patients may be hindered by unrecognized barriers.

Objective: The aim of this study is to identify patient-reported barriers to successful implementation of a preoperative risk reduction program at a safety-net hospital.

Design: This was a prospective exploratory qualitative study. The study was initiated concurrently with a new preoperative risk reduction program. One-on-one semi-structured interviews were conducted. Latent content analysis applying inductive coding methods was used to code and condense raw qualitative data.

Setting: A safety-net hospital

Participants: Patients seeking ventral hernia surgery

Main Outcome and Measure(s): Responses to semi-structured interviews

Results: The study population (n=43) was largely unemployed (77.1%) and uninsured (81.4%), minorities (88.3%). Patients self-identified as being overweight (76.7%), a smoker (18.6%), and diabetic (20.9%). Over half (51.2%) of respondents reported a barrier to participation in the preoperative program including lack of transportation (20.9%), lack of time (9.3%), distance from the program site (7.0%), and scheduling conflicts (7.0%). Administration of the survey correlated with an improved enrollment rate in the preoperative program (20.8% vs 66.7%, p=0.006).

Conclusions: Patients at a safety-net hospital report numerous barriers to participation in a preoperative risk reduction program despite significant potential benefits. Integrating patients as key stakeholders in the development of clinical programs and initiating interactions with open ended questions may stimulate self-reflection, patient interest, and adaptive changes that can improve enrollment and effectiveness.

ABSTRACT

What's Wrong with the Surgical Safety Checklist? Thinking Outside the Checkbox

Aubrey Hildebrandt *The University of Texas at Houston Medical School* *Class of 2018*

Sponsored by: KuoJen Tsao, MD, Department of Pediatric Surgery
Supported by: KuoJen Tsao, MD, Department of Pediatric Surgery
Key Words: Surgical safety checklist, patient safety, quality of care, perioperative care

Introduction: Three-phase (pre-induction, pre-incision, debriefing) surgical safety checklists (SSC) have been widely adopted as an effective tool for decreasing postoperative morbidity and mortality. However, checklist effectiveness has recently been questioned. We aimed to identify potential flaws in the execution of a local, stakeholder-derived SSC, which could lead to its ineffectiveness.
Methods: From May to July 2015, five trained observers directly observed the completion of 11 pre-induction, 19 pre-incision, and 9 debriefing checkpoints during the three-phase SSC for pediatric operations. All checkpoints were assessed for adherence (checking the box). Of the 19 pre-incision checkpoints, 10 were assessed for high fidelity performance (meaningful completion). These fidelity checkpoints represent complex measurable tasks relying on a high-level of team cohesion and communication for meaningful completion. Inter-rater reliability and chi-squared tests were performed; p-values <0.05 were considered significant.
Results: 212 pediatric operations were observed representing 35 surgeons and 9 surgical subspecialties. At least one phase of the SSC was conducted in 100% of cases. 174 pre-induction, 212 pre-incision, and 199 debrief checklists were evaluated with an average adherence to each checklist of 56%, 95%, and 76%, respectively. For the pre-incision phase, adherence to checkpoint completion ranged from 85-100% and averaged 95%, yet high fidelity performance ranged from 36-98% and averaged 75%. Three pre-incision checkpoints (induction concerns, anticipated case duration, and site marking) were performed most consistently with associated meaningful completion. However, 7 checkpoints were performed at a high frequency (range 85-99%) but had a significantly lower rate of fidelity (range 36-86%, $p<0.05$). Inter-rater reliability kappa values for pre-induction, pre-incision, and debriefing were 0.68, 0.70, and 0.89, respectively.
Conclusion: Although surgical safety checklists are routinely performed, meaningful execution of each and every step remains suboptimal. Monitoring of implementation fidelity can identify specific processes and checkpoints upon which to focus improvement efforts.

ABSTRACT

Assessing the Independence of Ski7-mediated mRNA Quality Control from Ltn1-mediated Protein Quality Control

Kim Ho *The University of Texas at Houston Medical School* *Class of 2018*

Sponsored by: Ambro van Hoof, PhD, Department of Microbiology and Molecular Genetics
Supported by: National Institute of Diabetes and Digestive and Kidney Diseases, 2T35DK007676-22
Key Words: mRNA quality control, protein quality control

Tight regulation of gene expression is a critical function in all three kingdoms of life. Different types of mRNA aberrancies are known to activate different mRNA surveillance pathways: mRNAs that contain rare codons or secondary structures that result in ribosomal stalling activate the no-go decay pathway, whereas transcripts that lack in-frame stop codons are targeted by the non-stop decay pathway. Aberrant gene expression is also modulated by proteasome-targeted nascent peptide degradation, facilitated by the E3 ubiquitin ligase Ltn1. Ski7 and Hbs1 are key factors in mRNA quality control that recognize ribosomes stalled on non-stop and no-go transcripts, respectively. Hbs1 is an active GTPase, and this allows Hbs1 to disassemble the ribosome. After disassembly, Ltn1 recognizes the complex of nascent peptide that is still bound to the 60S ribosomal subunit and target the peptide for degradation. We hypothesize that Ski7 is inactive as a GTPase and should be unable to disassemble the ribosome, and thus unable to trigger Ltn1-mediated protein quality control. We have tested whether Ski7 and Hbs1 act in different or overlapping pathways, and whether the Ski7 pathway also triggers Ltn1-mediated protein quality control. Three aberrant mRNAs were created and introduced into *Saccharomyces cerevisiae* strains that contained ski7Δ, hbs1Δ, ltn1Δ, ski7Δltn1Δ, ski7Δhbs1Δ, or hbs1Δltn1Δ. Aberrant protein accumulation for each of these strains was analyzed with Western blot. These aberrant transcripts were primarily targeted by the Ski7-mediated non-stop decay pathway, whereas Hbs1-mediated no-go decay played a minor role in degradation of these aberrant transcripts. Moreover, the Ski7 and Ltn1 double deletion strain accumulated more aberrant protein than either the Ski7 or Ltn1 single deletion strains, indicating that these two proteins act in independent pathways. These results suggest that ribosome disassembly is not critical for Ski7-mediated non-stop decay, and this is consistent with the finding that Ski7 is not an active GTPase.

ABSTRACT

Helios$^+$ Foxp3$^+$ Regulatory T Cell Subset in Healthy and HIV$^+$ Individuals

Ericka Howard *The University of Texas at Houston Medical School* *Class of 2018*

Sponsored by: Dat Q. Tran, MD, Department of Pediatrics
Key Words: Regulatory T Cells, Helios, HIV, Foxp3, TCR repertoire

Helios, a member of the ikaros transcription factor family, remains a controversial marker for distinguishing thymic versus peripheral derived Foxp3$^+$ regulatory T cells (Tregs). To add evidence to the reliability of Helios, we analyzed the differences between Helios$^+$ and Helios$^-$ Treg subsets in both healthy and HIV infected individuals. Flow cytometry was performed to analyze Foxp3 and Helios expression within CD4$^+$ T cells from cord blood, pediatric thymus and peripheral blood of healthy controls and HIV patients. Additional analyses of cytokine expression and T cell receptor (TCR) repertoire were performed. The mean percentages of Helios$^+$ Tregs were similar between pediatric thymus (94.2%, n=9) and cord blood (95.5%, n=12, p=0.114) but significantly greater than adult peripheral blood (71.5%, n=30, p< 0.0001). A negative correlation between age and percentage of Helios$^+$ Tregs was seen (R^2= 0.858, p< 0.0001) in which the percentage of Helios$^+$ Tregs decreased as age increased. The percentages of Helios$^+$ Tregs in the pediatric HIV and adult HIV patients compared to the healthy controls were decreased (79.2% pediatric controls vs. 67.9% pediatric HIV, p =0.006; 71.5% adult controls vs. 64.1 % adult HIV, p=0.005), indicating an increase in the portion of Helios$^-$ subset in the HIV patients. Similar to healthy controls, there was a direct correlation between the frequencies of Helios$^+$ and total Tregs within CD4$^+$ for HIV patients. However, the portion of Helios$^+$ within Tregs did not change with increasing percentages of Tregs for both healthy and HIV. The concentration of Foxp3 measured by geometric mean florescence intensity (gMFI) was consistently higher for the Helios$^+$ than the Helios$^-$ subsets in healthy and HIV. Increased cytokine production (IL2, IFNγ, IL17A) was significantly greater in Helios$^-$ subset for healthy and HIV (p<0.0001). There was no difference in the overall mean TCR Vβ usage amongst the Helios$^+$, Helios$^-$ and nonTreg subsets in controls and HIV. Similarly, utilizing the economic Gini skewing index, we saw no statistical difference in repertoire skewing amongst the subsets. In conclusion, Helios$^+$ Tregs represent a distinct subset manifested by higher concentration of Foxp3 and little cytokine expression. The portion of Helios$^+$ within Tregs decreased with age and in HIV infection. There was no apparent distinction in the TCR repertoire amongst the subsets. Overall, this data adds to the existing literatures supporting that Helios$^+$ Tregs are derived from the thymus and represent a stable subset of Tregs. More studies are needed to interrogate the role of these two subsets in diseases.

ABSTRACT

Bacterial Viability Parameters for the Early Molecular Detection of Sepsis

Neal Huang *The University of Texas at Houston Medical School* *Class of 2018*

Sponsored by: Heidi Kaplan, PhD, Depart of Molecular Microbiology and Genetics
Supported by: Center for Translational Injury Research (CeTIR); The University of Texas Medical School at Houston – Office of the Dean
Key Words: Sepsis, Molecular detection, Infection

INTRODUCTION: Sepsis is a very costly and dangerous condition that affects over 1 million Americans a year. It was the single most expensive condition to treat in 2011 at a total cost of $20.3 billion, and patients who entered into severe sepsis has a fatality rate of 28 to 50 percent. Treatment of sepsis is time sensitive endeavor that needs to be considered; for every hour that passes without treatment, sepsis patients have a decrease in chance of survival. The current gold standard for treating sepsis is obtaining a blood culture and gram stain from a patient showing signs of sepsis. This culture-dependent method is not appropriate for handling sepsis due to its delay in results and a prevalence of false negatives. The Kaplan lab has developed a culture-independent method, the EMD assay, utilizing qRT-PCR on the bacterial 16s ribosome for detecting sepsis in patients. The purpose of my research is to determine if the EMD assay can differentiate between whether or not DNA detected originated from live bacteria or dead bacteria. I hypothesized that live bacteria will be intact and their DNA will be found in the pellet of centrifuged blood while dead bacterial DNA will be present in the serum of centrifuged blood.

METHODS: E. coli was grown to a mid-logarithmic growth phase and harvested, and spiked into whole blood samples. The blood samples were then extracted with a MoBio (Carlsbad, CA) Bacteremia DNA Isolation Kit. After DNA was extracted and isolated a qRT-PCR was run on the samples and data was analyzed for bacteria quantity and detection efficiency. Pure E. coli DNA was also spiked into whole blood and EMD assay was performed on the samples.
E. coli was also grown to a mid-logarithmic phase and harvested at an OD600=0.500. These bacteria were put into different tubes and killed either by 80^{o}C heat or 70% Isopropanol. The bacteria were then plated and stained by propidium iodide and CYTO9 to determine viability.
E. coli was treated with cefeime while in either PBS or whole blood. The bacteria in PBS had its OD600 observed over night to determine speed of killing exerted by Cefepime. Blood spiked with E. coli and treated with cefepime is allowed to incubate over time to kill bacteria in a physiologically relevant way.

RESULTS: Pure live bacteria spiked into whole blood was found to have 93.5% (st dev. = 1.75%) of the bacterial DNA detected in the blood pellet.
Bacteria killed by heat and ethanol remained intact but was shown to be 100% killed under

observation by florescent microscopy, and 99.999% killed by bacterial plate count.

CONCLUSION: Further experiments need to be performed after EMD assay is fully optimized to determine where pure bacterial DNA and cefepime killed bacterial DNA localize. Live bacterial blood spikes suggest that live bacteria have their DNA intact and found mostly in the pellet.

ABSTRACT

Three Potential Methods for Prehospital Treatment of Abdominal Hemorrhage

Matthew J. Hurley *The University of Texas at Houston Medical School* *Class of 2018*

Sponsored by: John B. Holcomb, MD, Department of Surgery, CeTIR
Supported by: John B. Holcomb, MD, Department of Surgery, CeTIR
Key Words: Abdominal Hemorrhage; Foam; Balloon Aortic Occlusion; Junctional Tourniquet

Background: Uncontrolled intra-abdominal hemorrhage after injury is associated with increased mortality. Current treatment consists of rapid transport to a trauma center and emergent laparotomy. Three potential prehospital hemorrhage control interventions that could lead to improved outcomes are resuscitative endovascular balloon occlusion of the aorta (REBOA), self-expanding foam and the abdominal junctional tourniquet (AJT).
Hypothesis: The purpose of this retrospective study was to assess the number of patients who had intra-abdominal injury and received a laparotomy that could have potentially benefited from one of these three new interventions.
Methods: This retrospective study included patients who received an emergent trauma laparotomy between 1/1/2013 to 1/1/2015 at an urban Level 1 trauma center. We reviewed all the injuries found at laparotomy and based on the specific indications for each device determined if the patients would have been potentially helped or hurt by each of the three interventions. For instance, the AJT only controls bleeding from injuries below the aortic bifurcation (located below the umbilicus), while the foam is contraindicated in patients with large abdominal wall defects or diaphragm injuries. McNemar's test was used with Bonferonni correction for statistical analysis (α=0.017).
Results: 402 patients met the inclusion criteria. REBOA was potentially beneficial for 384, (96%) of patients, foam was potentially beneficial for 351, (87%), while the AJT was potentially beneficial for only 35, (9%). There was no significant difference between REBOA and foam ($p=0.022$), while there was a difference between REBOA or foam and AJT ($p<0.001$). There were 170 (42%) patients with penetrating injuries, while only 9 (5%) patients with penetrating injuries would have been potentially helped by the AJT. 33 patients had cutaneous wounds located in the right lower quadrant (RLQ), while 45 patients had cutaneous wounds located in the left lower quadrant (LLQ). Diaphragm injuries occurred in 58 (14%) of patients, with REBOA potentially of benefit in 55 of those patients, while foam would have potentially helped only 36.
Conclusion: REBOA and foam both would potentially benefit the largest number of patients, (≥ 87%) who had intra-abdominal injury and laparotomy. AJT was found to be helpful in only 9% of patients in need of prehospital intervention for hemorrhage. These results suggest that the AJT should not be used for prehospital hemorrhage control unless it is absolutely sure that all injuries causing hemorrhage are below the aortic bifurcation.

ABSTRACT

Determination of Xenon and Xenon-Loaded Echogenic Liposomes (Xe-ELIP) in Water and Blood

Jermaine Hurling *The University of Texas at Houston Medical School* *Class of 2019*

Sponsored by: Melvin E. Klegerman, PhD, Internal Medicine - Cardiovascular Medicine

Supported by: Melvin E. Klegerman, PhD, Internal Medicine - Cardiovascular Medicine, The University of Texas at Houston Medical School – Office of the Dean

Key Words: Xenon, xenon containing echogenic liposomes (Xe-ELIP), cerebral ischemia, neuroprotective

Background: Neuronal damage arising in cerebral ischemia (stroke) can be divided into two regions: a core area of irreversibly damaged tissues and a surrounding region of reversibly damaged tissues, the penumbra. If the penumbra is left untreated the core will expand into the penumbra through a series of cellular events worsening clinical outcomes for stroke patients. Neuroprotective agents look to slow the progression of tissue damage in stroke patients by opposing the core's expansion. Xenon's ability to antagonize NMDA receptor-mediated excitotoxicity following an ischemic attack and its ready diffusion into target tissues makes it an excellent neuroprotective candidate. Previous experiments have demonstrated an effective mechanism of xenon delivery to our target tissue by encapsulating xenon into echogenic liposomes (Xe-ELIP). Actual neuroprotective blood levels of xenon have only been estimated based on previous literature. The objective of this study is to develop a reliable assay to measure the amount of dissolved xenon released from Xe-ELIP in water and blood samples.

Methods: Gas chromatography-Mass Spectrometry (GC-MS) was used to quantify 5 µl aliquots of headspace gas in 2 mL vials containing 1 mL samples of either 200 µl of 10 mg/mL Xe-ELIP mixed with 800 µl of water or 25 µl of 10 mg/mL Xe-ELIP mixed with 975 µl of rabbit blood. In order to determine the local blood concentration of xenon in animals after Xe-ELIP administration, 6 mg/ 0.6 mL Xe-ELIP was infused into a rat at a rate of 1 mg per minute. Rat blood samples were drawn directly from a catheterized right carotid artery. After introduction of the samples, each vial was sealed, allowed to equilibrate to 37° C in a temperature-controlled sonicating water bath, followed by 20 minutes of sonication prior to sampling. For uniformity, headspace gas was sampled from the same vertical location in each vial. Concentrations were calculated from a gas dose-response curve and converted to percent xenon assuming complete equilibration with the headspace. Results were normalized using the published xenon water-gas partition coefficient.

Results: The mean corrected percent of xenon from Xe-ELIP released into water was 3.87 ± 0.56% (n = 8), corresponding to 19.3 ± 2.8 µl/mg lipid, which is consistent with previous independent Xe-ELIP measurements. The corresponding xenon content of Xe-ELIP in rabbit

blood was 23.38 ± 7.36 (SD, n = 8) µl/mg lipid. Rat blood xenon concentrations after IV administration of Xe-ELIP were 0.025% and 0.016%, corresponding to 10 and 6 µM, respectively.

Conclusion: Blood concentrations for the anesthetic dose of xenon have been established. Based on previous literature, the proposed concentration conferring xenon's neuroprotective properties is 20% of the anesthetic dose. The xenon content measured in the water and blood studies are approximately 1/10 of the projected value. Neuroprotective effects have been observed at this level. More work will need to be done to determine the full neuroprotective level of xenon.

ABSTRACT

Mild Traumatic Brain Injury Alters the Morphology of Medial Prefrontal Cortex Neurons: Implications in Impaired Fear Memory Extinction

Jonathan Huynh *The University of Texas at Houston Medical School* *Class of 2018*

Sponsored by: Pramod K. Dash, PhD, Department of Neurobiology and Anatomy

Supported by: Pramod K. Dash, PhD, Department of Neurobiology and Anatomy; The University of Texas at Houston Medical School – Office of the Dean

Key Words: Concussion, PTSD, fear memory, pyramidal neuron spines

Introduction: Fear memory extinction is a form of learning in which an animal learns that a conditioned stimulus no longer predicts the fearful stimulus. Impaired fear memory extinction has been implicated in anxiety disorders such as post-traumatic stress disorder (PTSD). It has been hypothesized that PTSD results from hypoactivity of the mPFC, which can no longer inhibit the amygdala. This can result in hyperarousal and recurrence of memory for the traumatic event. The prefrontal cortex, which accounts for one-third of the brain volume in humans, is vulnerable to mild TBI, and post-concussive symptoms can manifest in the absence of overt damage. This suggests that dysfunction of mPFC neurons can impair the ability of the mPFC to effectively inhibit the amygdala and suppress the expression of fear memory.

Hypothesis: I hypothesize that an alteration in the number of dendritic spines (information receiving protrusions) as a result of mTBI is a mechanism for impaired fear memory extinction.

Study design: Sprague-Dawley rats were subjected to either mild FPI (1.5 atm, n=5) or sham surgery (n=5) then tested 4 weeks later for their ability to extinguish a fearful contextual memory. Brains from these animals were then removed, and processed using a Rapid Golgi staining kit in order to visualize individual dendrites and spines. The number of dendritic spines on terminal branches of layer II/III pyramidal neurons within the mPFC were counted to determine apical and basal dendritic spine density.

Results: My preliminary analysis revealed a decrease in the density of both apical and basal dendritic spines in mild FPI rats as compared to sham controls, although these decreases did not achieve statistical significance. I am in the process of performing further analysis.

Conclusion: mTBI may reduce the apical and basal dendritic spine density of pyramidal neurons within the mPFC. This reduction may impair the mPFC's ability to inhibit the amygdala and may explain how mild TBI impairs fear memory extinction and contributes to the development of PTSD.

ABSTRACT

Short- and Long-Term Effects of Repetitive Subconcussive Head Impacts (RSHI) on Cognitive Function

Randy Igbinoba *The University of Texas at Houston Medical School* *Class of 2018*

Sponsored by: Anne B. Sereno, PhD, Department of Neurobiology and Anatomy
Supported by: Anne B. Sereno, PhD, Department of Neurobiology and Anatomy, The University of Texas at Houston Medical School – Office of the Dean
Key Words: Brain Trauma, Adolescent Sports, AntiPoint

The goal was to examine the immediate and longer-term effects of repetitive subconcussive head impacts (RSHI) on sensorimotor and cognitive function of athletes. Much previous research suggests that exercise can immediately enhance task performance, especially for tasks that require executive function. However, RSHI may cause axonal damage or altered neurochemistry indicative of neuroinflammation, which can lead to cognitive decline and neurological dysfunction. A better understanding of changes in cognitive function is key to implement strategies to prevent the development of more serious neurological disorders. We measured both sensorimotor capability (ProPoint task) and cognitive function (AntiPoint task) of athletes with RSHI (soccer players; n=16; mean age=16.0 years) and Control athletes (swimmers and table-tennis; n=14; mean age=15.2) using an iPad application. Each subject was asked to perform the pointing tasks (48 trials each) on the iPad both before and after a workout, for up to 22 sessions across at most a 91-day period (average 8.1 sessions across an average 19 days). During recorded sessions, players in the RSHI group had on average 7.0 head impacts per session (0 for Controls). During the ProPoint task, each subject used an index finger to first touch a center spot until a target appeared in 1 of 4 locations (left, right, up, down) around the center spot, and then had to touch the target as quickly as possible. The AntiPoint task was identical except that the subject was instructed to touch the location directly opposite to the target location. Each trial recorded the subject's response times (RTs). We compared the performance of athletes with and without RSHI, both before and after workouts (immediate changes), as well as across sessions (longer term changes) for both "before" and "after" tests.

All subjects showed significantly lower mean RTs immediately after (compared to before) workouts for both tasks. Further, there was no Group difference in the magnitude of this immediate benefit. Over the course of all sessions (similar findings for both "before" or "after" testing sessions), there was no change in performance on ProPoint but a significant reduction in RTs on AntiPoint. Further, there was a significant interaction with Group. Namely, the RSHI group showed a significantly reduced RT benefit on AntiPoint. Combined these findings suggest that there were no detectable differences (in either sensorimotor or cognitive function) in high-performing athletes immediately following a workout with or without RSHI; however, when comparing performance across a longer time frame (multiple testing sessions), we found that athletes incurring RSHI showed significant RT slowing relative to control athletes on the cognitive task. The study shows that significant decreases in cognitive performance can be detected at longer time scales following RSHI. The iPad app may be useful for early detection or tracking of cognitive function to prevent progression to more serious problems.

ABSTRACT

Targeting NRP1 in Ovarian Cancer Enhances Anti-angiogenesis Therapy

Zachary B. Jenner *The University of Texas at Houston Medical School* *Class of 2018*

Sponsored by: Anil K. Sood, MD, Department of Gynecologic Oncology, The University of Texas MD Anderson Cancer Center

Supported by: NIH P50 CA083639; The University of Texas at Houston Medical School – Office of Educational Programs; The Nanomedicine & Biomedical Engineering Program

Key Words: Ovarian cancer, neuropilin-1, platelet-derived growth factor B

Ovarian cancer remains the most common cause of death from a gynecologic malignancy. Therefore, new treatment approaches are urgently needed. In ovarian cancer and the tumor vasculature, neuropilin expression is increased, and is related to poor outcomes, likely due to enhanced angiogenesis, metastasis, survival, and lymphangiogenesis. In the tumor microenvironment (TME), neuropilin-1 (NRP1) has been shown to interact with platelet-derived growth factor B dimers (PDGF-BB) to increase pericyte migration, promote vascular endothelial growth factor (VEGF) production by pericytes, and modulate endothelial cell proliferation and angiogenesis. PDGF-BB may enhance the proliferative and invasive characteristics of ovarian cancer, in part, through NRP1. Therefore, targeting NRP1 may be a viable therapeutic option to enhance current anti-angiogenesis treatments. In ovarian cancer models, the functional and biological significance of targeting NRP1 with siRNA and the anti-NRP1^{B} monoclonal antibody (mAb), which binds the b1 and b2 extracellular domain. Western blot and RT-PCR were enforced to screen a panel of twelve ovarian cancer cell lines for expression of NRP1, NRP2, PDGFR-α, PDGFR-β, and PDGF-BB, and also to assess NRP1 expression in endothelial and pericyte-like cell lines. In the NRP1-positive SKOV3-ip1 cell line, anti-NRP1^{B} inhibited VEGF-induced migration by 46% ($p<0.05$), whereas the NRP1-null A2780-ip2 cell line migration was not changed by NRP1 blockade. Tumor cell invasiveness was not affected by anti-NRP1^{B}. A sandwich ELISA showed an NRP1-coated plate bound 1.0 nM PDGF-BB. PDGF-BB stimulated migration of pericyte-like cells upon addition of anti-NRP1^{B} resulted in a 63% decrease in tumor cell migration ($p=1x10^{-4}$). The HeyA8 serous ovarian carcinoma cell line, with high NRP1 and PDGF-BB expression, and low or no PDGFR-α and PDGFR-β expression, was transfected with siRNA against NRP1 and/or PDGF-BB. An orthotopic *in vivo* model of ovarian cancer in the NRP1-null ovarian cancer cell line A2780 exhibited a 96% decrease in mean tumor weight when treated with anti-NRP1^{B} and anti-VEGF mAb in combination compared to controls ($p<0.001$), and the addition of anti-NRP1^{B} to anti-VEGF treatment further reduced tumor growth by 61% ($p<0.01$). After therapy, immunohistochemistry of tissue for endothelial cells showed a 71% decrease in micovessel density when treated with anti-NRP1^{B} ($p<0.001$). Tumor cell proliferation, measured by ki67 in the tissue, was decreased by 25% when NRP1 and VEGF blockade were combined ($p=0.007$). The TUNEL assay for apoptotic cells showed no difference

between treatment and non-treatment groups. The following studies are pending completion. Proliferation and migration of an NRP1-positive (HeyA8) and NRP1-null (A2780-ip2) cell line after recombinant PDGF-BB exposure are evaluated in the presence of PDGF-BB neutralizing antibody. Tumor cell proliferation, cell cycle studies, transwell migration/invasion, and apoptosis are evaluated following NRP1 and PDGF-BB knock-down. An orthotopic *in vivo* HeyA8 nude mice model treated with siNRP1, anti-VEGF mAb, or both will be evaluated, with the following biological readouts: tumor weight, metastasis, ascites characteristics, and tissue staining for tumor cell apoptosis, proliferation, and NRP1 expression. Collectively, these data show that NRP1 inhibition sensitizes the TME to anti-VEGF therapy, and that PDGF-BB may be an important mediator of NRP1's pro-angiogenic effects. Therefore, NRP1 blockade may help regain responsiveness to anti-angiogenesis therapy resistant tumors.

ABSTRACT

Role of Multipotent Adult Progenitor Cell Treatment Inducing Neurogenesis after Traumatic Brain Injury: Varying Timing of Dosing Strategy

Margaret Johnson *The University of Texas at Houston Medical School* *Class of 2018*

Sponsored by: Charles S. Cox, Jr. MD, Department of Pediatric Surgery, Supinder S. Bedi, PhD, Department of Pediatric Surgery

Supported by: Charles S. Cox, Jr. MD, Department of Pediatric Surgery, Supinder S. Bedi, PhD, Department of Pediatric Surgery; The University of Texas at Houston Medical School – Office of the Dean

Key Words: TBI, Neurogenesis, MAPC

Multipotent adult progenitor cells (MAPC) are found in the postnatal bone marrow. MAPC promote an influx of T-regulatory lymphocytes to dampen the pro-inflammatory (M1) response as a result of an injury. In this manner, MAPC may be a potential therapy for individuals afflicted with traumatic brain injuries (TBI). MAPC may attenuate the M1 phenotype of microglia following a TBI to provide a milieu favorable for neurogenesis in the adult brain. We hypothesized that MAPC treatment based on specific dosage time will promote neurogenesis in the hippocampus of treated animals following a TBI. Using a rodent model, we tested our hypothesis by intravenous administration of MAPC at 24 alone, 2/24, 6/24, 12/36 and 36/72 hours following a cortical contusion injury. 120 days after the injury, the rat brains were collected and stained with immunohistochemistry for the presence of Doublecortin (DCX) and Ki67 in the ipsilateral and contralateral hippocampus. DCX is a microtubule-associated protein expressed for 30 days in neuroblasts during the rapid proliferation of neuronal precursors and ceases at maturation. Ki67 is a nuclear protein present during all active phases of the cell cycle and used to assess the level of neuroepithelial cell proliferation. There should be an increase in neurogenesis in animals that have received treatment prior to 36 hours as correlated by behavioral changes in spatial learning and memory. Potentially, MAPC treatment increases neurogenesis when administered prior to 36 hours after injury.

ABSTRACT

p120 Catenin is Required for Regeneration of the Exocrine Pancreas in Mice

Neal Jones *The University of Texas at Houston Medical School* *Class of 2018*

Sponsored by: Jennifer Bailey, PhD, Department of Internal Medicine
Supported by: National Institute of Diabetes and Digestive and Kidney Diseases, 2T35DK007676-22
Key Words: Pancreatic cancer, inflammation, regeneration, p120 Catenin

Background: Pancreatic cancer is amongst the most deadly and least treatable form of cancers that inevitably leads to the death of greater than 94% of patients within five years of diagnosis. Chronic pancreatitis is a known risk factor for pancreatic cancer. In pancreatic cancer patients, p120 catenin, an adherens junction protein and inflammatory suppressor, loss or mislocalization of this protein has been correlated with poorer prognosis. **Methods and Results:** Using an acinar cell-specific transgenic mouse model of injury and regeneration, we knocked out p120 catenin and quantified injury sustained and the timeline of regeneration after induction of cerulean mediated acute pancreatitis. Biallelic loss of p120 catenin in the context of acute pancreatitis resulted in significantly increased injury in C iMist1; p120f/f pancreata when compared to C iMist1; p120wt/wt pancreata from Day 3 to Day 11 post cerulean treatment, suggesting that p120 catenin null acinar cells display increased susceptibility to injury. Since p120 catenin is a known regulator of inflammation, we next sought to examine the immune response in C iMist1; p120f/f pancreata. Through IHC staining, we observed that a loss of p120 catenin lead to an increase in the number of F4/80+ macrophages present in the injured pancreas and promotes the retention of pSTAT3. This is consistent with previous published work showing that macrophages can serve as a source for IL-6, an activator of pSTAT3. Further, we observed no change in the number of CD3+ or CD16+ cells observable at the site of injury. The source of this increased GMCSF, a potent recruiter of F4/80+, was determined by immunofluorescence, and appears to be primarily from the acinar cells surrounding areas of injury. These results indicate that p120 catenin regulates pancreatic regeneration by modulating cellautonomous and paracrine inflammatory signaling networks. Continued experimental models to study pancreatic injury will provide insight on new therapeutic treatment strategies for pancreatitis and pancreatic cancer.

ABSTRACT

Analysis of Changes in Levels of ApC/EBP, A Key Downstream Component in the Consolidation of Long-term Facilitation in *Aplysia*

Tahseen J. Karim *The University of Texas at Houston Medical School* *Class of 2018*

Sponsored by: John H. Byrne, PhD, Department of Neurobiology and Anatomy
Supported by: NIH NS019895
Key Words: ApC/EBP, *Aplysia*, Memory, LTF

Background: Memory consolidation is the process during long-term facilitation (LTF) by which new and labile memory becomes stable and persistent. LTF requires de novo mRNA and protein synthesis of several key components. The transcription factor CCAAT enhancer-binding protein (ApC/EBP) is one of these essential proteins produced during the consolidation phase of LTF in *Aplysia californica*. The induction of *ApC/EBP* is regulated by the early phosphorylation and activation of the cAMP response element binding protein, CREB1. This upstream transcriptional regulation along with several other interactions being studied in our lab are important mechanisms for *ApC/EBP* expression and LTF. Upregulation of *ApC/EBP* is both necessary and sufficient for the formation of long-term memory. It has been that shown that specifically timed 5-HT pulses can increase *ApC/EBP* mRNA levels. However, quantification of ApC/EBP protein levels during 5-HT induced consolidation in LTF has yet to be determined. Defining the dynamics of *ApC/EBP* expression can lead to optimization and strengthening of the memory response. Furthermore, expanding on the upstream mechanisms involved in LTF can help predict the effects of downstream mutations leading to increased insight in disease states.

Methods:
Pleural-pedal ganglia were harvested from *Aplysia californica*. One set of ganglia was treated with 5, 5min pulses of a 50 µM 5-HT solution and the other set was treated with 5, 5min pulses of a vehicle solution. After lysis of the ganglia, the protein lysate was analyzed through western blot techniques. Several commercially purchased antibodies based on unique amino acid sequences were used as primary antibodies. Peptide blocking of the antibodies was also implemented during the probing step of the western blots. Image analysis software allowed for the comparison of protein levels on each membrane.

Results:
The western blot results indicated that one antibody in particular had the highest specificity for ApC/EBP. Pre-absorption with a blocking peptide specific to that antibody supported its binding capacity. There was also a pattern of increased ApC/EBP levels after 5-HT treatment when compared to the vehicle treatment. These results in combination with the acquired antibody will be used to further explore the expression of ApC/EBP using cultured neurons and confocal microscopy.

ABSTRACT

A Comparison of the King Vision Channeled, King Vision Non-Channeled, and Cobalt GlideScope Video Intubation Systems in Difficult Intubation Patients

Paden Karnes *The University of Texas at Houston Medical School* *Class of 2018*

Sponsored by: Carin A. Hagberg, MD, Department of Anesthesiology
Supported by: Carin A. Hagberg, MD, Department of Anesthesiology
Key Words: King Vision video laryngsoscope, channeled blade, difficult intubations

Introduction: Endotracheal intubation is essential for maintaining an open airway in patients who are undergoing general anesthesia for a surgical procedure. Direct laryngoscopy during intubation has been standard practice for many years, but new video laryngoscopes have been introduced as a device that could possibly improve the visualization of the patient's laryngeal. Video laryngoscopes allow the laryngoscopist to obtain a superior view of the patient's airway and a better chance to maintain that view during passage of the endotracheal tube. The channeled portion of a laryngoscope is designed to aid in a quicker and more accurate placement of the endotracheal tube into the trachea for proper ventilation, without the need for a stylet. It is hypothesized that the Channeled King Vision Video Laryngoscope is more effective than the Cobalt GlideScope during intubation of patients who have indicators of a difficult intubation. It is also hypothesized that the King Vision Video Laryngoscope with the standard blade is just as efficient as the Cobalt GlideScope.

Methods: A study population of 225 adult patients (> 18 years old) who are scheduled for an elective surgery requiring general anesthesia at either Lyndon B. Johnson General Hospital or Memorial Hermann Hospital (Texas Medical Center) will be split into 3 groups: 75 people randomized to Cobalt GlideScope, 75 randomized to the King Vision Video Laryngoscope with the channeled blade, and 75 randomized to the King Vision Video Laryngoscope with the standard blade. A conventional endotracheal tube will be used. Subjects are selected based on meeting at least two of the following criteria: Mallampati III-IV, neck circumference > 43 cm, thyromental distance < 6 cm, or a mouth opening < 4 cm. After anesthesia is administered and ventilation of the patient begins, a resident of anesthesiology will perform the intubation. The results of the number of attempts and the intubation time will be recorded. The resident will have up to two attempts to successfully intubate a patient with their assigned laryngoscope. After two unsuccessful attempts of intubation, the attending anesthesiologist will attempt the intubation with the same laryngoscope. If the attempt is still unsuccessful, then the attending may use the laryngoscope of his or her choosing and the case is recorded as a failure.

Results:

Device	Count	Optimal View	First CO2	Total Time
GS	46	10.18391304	37.3321	47.51601
KVNch	47	9.664042553	32.66859	42.33263
KVCh	40	15.874	30.37479	46.24879

The non-channeled King Vision had the fastest optimal view and total time. Although the channeled King Vision was 5 seconds slower than the non-channeled King Vision in total time, it was 2.3 seconds faster in obtaining the first CO2 wave form. Other metrics are still undergoing data analysis.

ABSTRACT

The Role of Endothelial–to–Mesenchymal Transition in Renal and Cardiac Fibrosis

Sharmistha Lahiri *The University of Texas at Houston Medical School* *Class of 2018*

Sponsored by: Raghu Kalluri, MD, PhD, Department of Cancer Biology, The University of Texas MD Anderson Cancer Center

Supported by: National Institute of Diabetes and Digestive and Kidney Diseases, 2T35DK007676-22

Key Words: Renal fibrosis, cardiac fibrosis, endothelial mesenchymal transition, EndMT, unilateral ureter obstruction, UUO, aortic banding, Twist, Snail, myofibroblast

Introduction: Organ fibrosis is characterized by the accumulation of excessive fibroblasts and the deposition of large amounts of matrix proteins. A hallmark of renal fibrosis (RF) is interstitial fibrosis along with the presence of an immune infiltrate. Cardiac fibrosis (CF) typically starts as an adaptive response to left ventricular pressure overload in an effort to preserve regular cardiac function and, if left untreated, this progresses on to replacement fibrosis, which is characterized by cardiomyocyte hypertrophy followed by necrosis. Fate-mapping studies have demonstrated that up to 30% and 10% of myofibroblasts involved in CF and RF, respectively, arise from endothelial cells through the process of endothelial–to–mesenchymal transition (EndMT). In EndMT, endothelial cells gradually acquire a mesenchymal phenotype, a transition induced by TGF-□ signaling. We investigated the functional contribution of EndMT to RF and CF by conditionally knocking down the transcription factors Twist and Snail, both master regulators of EndMT, in endothelial cells in models of kidney or heart fibrosis.

Methods: Mice with targeted floxed alleles for Twist were bred with mice having the Cre-recombinase expressed under the control of the CDH5/VE-cadherin promoter and having the Cre-loxP-mediated expression of enhanced yellow fluorescence protein (Rosa26-LSL-EYFP) to obtain lineage tracing of endothelial cells. 12-14 weeks old WT and TwistcKO mice were subjected to unilateral ureteral obstruction (UUO), which is known to produce RF, and sacrificed 10 days later. Another cohort of WT and TwistcKO mice was sacrificed at 24-28 weeks of age, and their tissue examined for evidence of baseline CF. Paraffin-embedded tissue sections underwent a histological evaluation using H&E, Masson Trichrome (MT) and Sirius Red (SR) staining to evaluate fibrosis. The aged mice underwent MRI scans to record the baseline ejection fraction and their post-mortem heart weight was measured.

Results: Preliminary results indicated no significant fibrotic differences between the WT and TwistcKO contralateral (control) kidneys in the UUO model. However, in the UUO kidneys, there was a 16% reduction in interstitial RF as evaluated in SR staining and a 62% enhanced tubular health as evaluated by H&E staining in the TwistcKO mice. Our results on CF in the

aged mice showed no overt histological difference but recorded a reduced ejection fraction and a 33% increased heart-body weight ratio in the TwistcKO compared to WT mice, indicating a potential developmental defect. There was a marginal reduction in the interstitial basal collagen content in the TwistcKO (3.1%) compared to WT (5.4%) mice, as evaluated in SR staining.

Conclusions and Future Directions: Endothelial-specific deletion of the positive EndMT regulator Twist limits interstitial fibrosis and tubular atrophy in the UUO model and induces a cardiac defect in aged mice. The next step to evaluate the functional contribution of EndMT in CF is to image a cohort of WT, TwistcKO and SnailcKOmice, followed by aortic banding at 10-12 weeks of age, re-imaging and sacrificing 4 weeks later and analyzing paraffin sections of their tissue for CF. For RF, the next step is to analyze paraffin sections of another cohort of WT and SnailcKOmice that underwent UUO at 12 weeks.

ABSTRACT

Activation of p90 Ribosomal S6 Kinase (pRSK) and CCAAT Enhancer-binding Protein (ApC/EBP) 45 Minutes Following Serotonin Treatment

Victor Liu *The University of Texas at Houston Medical School* *Class of 2018*

Sponsored by: John H. Byrne, PhD, Department of Neurobiology and Anatomy
Supported by: National Institutes of Health grant NS019895
Key Words: p90 Ribosomal S6 Kinase, CCAAT enhancer-binding protein, long-term memory

The induction of long-term memory (LTM) mechanisms in *Aplysia* relies upon activation of multiple protein cascades that depend upon binding of the neurotransmitter serotonin (5-HT) released from modulatory interneurons. 5-HT transiently activates the cAMP-dependent pathway in which PKA phosphorylates the transcription factor cAMP responsive element binding protein (CREB1). In other animal models, pRSK can also phosphorylate CREB1 at the same site, but this component of the model has not been confirmed in *Aplysia*. CREB1 then goes on to stimulate production of ApC/EBP, a downstream transcription factor also necessary for long-term memory. The aim of this project was to explore the possibility of activation of both pRSK and ApC/EBP 45 minutes following 5-HT treatment.

Before comparing pRSK and ApC/EBP levels following serotonin and vehicle treatments, it was first necessary to establish the sensitivity and specificity of antibodies for the two proteins. For pRSK, I used a mammalian antibody, as there is no commercially available antibody for *Aplysia* and the projected sequence of *Aplysia* pRSK contains the same binding sequence for the antibody. However, following several western blot trials using different batches of anti-pRSK antibody and different lysates from *Aplysia* pleural-pedal ganglia, I concluded that the antibody was not able to specifically detect pRSK in *Aplysia* as there was no protein detected that corresponded to the size of the predicted *Aplysia* pRSK protein and a strong band at a different molecular weight.

Specificity of the *Aplysia* ApC/EBP antibody was previously confirmed in experiments conducted by another medical student in the lab, Tahseen Karim. I used cell lysates of ganglia that had been treated with a 5 minute pulse of 5-HT or vehicle and then frozen 45 minutes following initiation of the 5-HT pulse to observe ApC/EBP levels via western blot. In the only experiment concluded thus far, 5-HT had the effect of increasing ApC/EBP levels 45 minutes following 5-HT treatment. Further experiments will be required to establish significance of elevated ApC/EBP levels 45 minutes following 5-HT treatment.

ABSTRACT

Outcomes of Chest Wall Sarcoma Resections in Pediatric Patients

Carmen Lopez *The University of Texas at Houston Medical School* *Class of 2018*

Sponsored by: Andrea Hayes-Jordan, MD, Department of Pediatric Surgery
Supported by: Andrea Hayes-Jordan, MD, Department of Pediatric Surgery
Key Words: pediatric, sarcomas, chest wall tumors

Background: Chest wall tumors are rare, accounting for only 1-2% of all cancers. A large proportion of these chest wall tumors are sarcomas and can include soft tissue tumors like rhabdomyosarcoma or bony tumors like osteosarcoma and Ewing sarcoma. Despite combinations of chemotherapy, radiation therapy and surgery, prognoses remain poor. Survival rates for most chest wall sarcomas remain at 60%. An inevitability for these children is the surgical removal of anywhere from 1-7 ribs. The removal of multiple ribs typically leaves defect that must be repaired in order to maintain proper stability and function of the chest wall. A variety of natural and prosthetic materials exist to cover these defects.
Purpose: This retrospective study aims to evaluate the survival and quality of life outcomes like in pediatric patients who have undergone chest wall resections secondary to sarcomas.
Methods: A retrospective chart review was performed on patients, 18 years of age and under, who underwent chest wall resections for sarcomas between 1999 and 2014 and were seen at MD Anderson Cancer Center. In addition to demographics, ribs involved, ribs resected, position of tumor on ribs, surgical margins, material used for reconstruction, radiation, time to local and distant recurrence, postoperative complications, incidence of scoliosis, activity restrictions and time to death were recorded.
Results: Of 44 patients, age ranged from 4-18 years (median 15years). The most common diagnoses were Ewing sarcoma (n=18) and osteosarcoma (n=16). Other sarcomas (n=10) included synovial sarcoma, chondrosarcoma, rhabdomyosarcoma. The average number of ribs resected was 2.95 ± 0.74. Gore-Tex® mesh was used in 14 cases, a marlex mesh and methyl methacrylate sandwich was used in 8 patients and 9 children did not require any reconstruction. With regards to activity restrictions, 24 (54.5%) patients had no problems with normal activity, 3 (6.8%) had occasional discomfort, 2 (4.5%) had pain impairing function, 7(15.9%) required medication or physical therapy for impairment and 8 (18.2%) needed additional surgery. Five children (11.4%) developed scoliosis all of whom had tumors on the posterior portion of the ribs. These patients each had resections of 3 or more ribs while 3 also had radiation to the posterior chest wall. Histology (p=0.003), location of tumor on the ribs (p=0.007) and surgical margins (p=0.011) were significantly associated with overall survival. Patients with osteosarcoma had the lowest survival rate at 31%. Tumors on the middle (p=0.003) and posterior (p=0.032) portions of the ribs had a much lower chance of death than those with tumors on the anterior part of the chest wall. Patients with R2 surgical margins (p=0.005) also had poor survival rates. There was no significant correlation between number of ribs resected or position of tumor on the ribs and activity restrictions (p=0.215). Nor were there

any individual factors that significantly led to recurrence. Median overall survival for the entire cohort was 73.46 ± 11.37 months while median time to death was 36.48 ± 5.19 months.
Discussion: Poor outcomes in children with chest wall sarcomas are likely due to a combination of many different factors. Persistent pain and breathing impairment may be possibilities when treating chest wall sarcomas but vary on a case-by-case basis and do not have a significant links to the type of material used in resection or number of ribs resected. Scoliosis is also a possibility as a result of posterior rib resections in younger children or in those who receive radiation to the posterior chest wall. Histology, the location of the tumor and surgical margins can have significant impact on overall survival, however, recurrence is harder to predict.

ABSTRACT

Resuscitative Endovascular Balloon Occlusion of the Aorta (REBOA) for Control of Non-Compressible Torso Hemorrhage

Clay D. Martin *The University of Texas at Houston Medical School* *Class of 2018*

Sponsored by: Laura J Moore, MD, FACS, Department of Surgery

Supported by: Center for Translational Injury Research (CeTIR), The University of Texas at Houston Medical School—Office of The Dean

Key Words: REBOA, hemorrhage, trauma, aortic occlusion

Background: Trauma patients with non-compressible torso hemorrhage are at high risk of exsanguinating before potentially life-saving surgical interventions can be performed. Temporary aortic occlusion augments systolic blood pressure (SBP) and perfusion to the heart and brain in these patients. The traditional method for temporary aortic occlusion is via Resuscitative Thoracotomy (RT) with aortic cross clamping. While effective, RT is highly invasive and may worsen blood loss, hypothermia, and coagulopathy by opening an otherwise uninjured body cavity. Resuscitative Endovascular Balloon Occlusion of the Aorta (REBOA) provides an alternative means of temporary aortic occlusion. Our purpose is to describe our experience with the implementation of REBOA at our Level 1 trauma center.

Methods: A retrospective case series describing all cases of REBOA performed at the Texas Trauma Institute between October 2011 and September 2015. The inclusion criteria were any patient that received a REBOA procedure in the acute phases following injury. There were no exclusion criteria. Data was collected from electronic medical records and the Memorial Hermann Hospital Trauma Registry.

Results: A total of 31 patients underwent REBOA during the study period. The median age of REBOA patients was 47 (IQR 27-63) and 77% were male. A majority (87%) sustained blunt trauma. The median Injury Severity Score of 34 (IQR 22-42). The overall survival rate was 32% but varied greatly between subgroups. Survival was highest (53.8%) in patients who had vital signs present at the time of REBOA inflation in zone III (n=13), and lowest (0%) in patients receiving active CPR during a zone I occlusion (n=6). Balloon inflation resulted in a median increase in systolic blood pressure of 55 mmHg (IQR 33-60), in cases where the data was available (n=20). A return of spontaneous circulation (ROSC) was noted in 55% of patients who had arrested prior to REBOA (n=11). Overall, early death by hemorrhage was 28% with only 2 deaths in the Emergency Department prior to reaching the OR.

Conclusions: REBOA is an effective method for achieving temporary aortic occlusion in trauma patients with non-compressible torso hemorrhage. Balloon inflation resulted in an increase in SBP with ROSC in over half of patients.

ABSTRACT

Clinical Analysis of Flap Expansion with Use of ¾ Z-Plasty in Burn Contracture Release

Madison D. McMenemy *The University of Texas at Houston Medical School* *Class of 2018*

Sponsored by David J. Wainwright, MD, Department of Plastic Surgery

Supported by: David J. Wainwright, MD, Department of Plastic Surgery

Key Words: ¾ Z-Plasty, Flap, Burn contracture release

Introduction: Scar contractures may develop across joints following deep burns to the adjacent, periarticular skin, leading to significant functional impairments. A variety of methods are available for management of this problem. The long term effectiveness of many techniques is compromised by the incorporation of skin grafts or scar tissue for resurfacing of the released area. A 3/4 Z-plasty is a reconstructive tool where a transposition flap (usually fasciocutaneous) of adjacent uninjured skin is rotated 90° into a scar release site. It has been our observation that a 3/4 Z-plasty provides superior maintenance of the release and actual improvement with time as the flap's uninjured tissue has the potential to stretch. Objective data is lacking to substantiate this observation so the purpose of the current study was to prospectively evaluate the results and dimensions of the flap with time.

Methods: Patients in whom a 3/4 Z-plasty was to be performed were entered into the study. Appropriate candidates for a 3/4 Z-plasty met the following criteria: 1) A burn scar contracture across a joint resulting in a functional impairment. 2) Available uninjured skin adjacent to the scar contracture. 3) The scar contracture was not a simple linear band. The patient's demographics, burn details and specifics of the burn contracture (site, range of motion) were recorded. The flap's height and width (base of flap) were measured at the time of surgery ("in situ" design before incision and following transposition and suturing into place) and at follow up visits in our burn office. All measurements were performed with the effected joint in a standardized position (eg. Elbow - full extension). Areas for flaps were roughly calculated using each width and height measurements in a triangular area formula. Using photos from each clinical visit, areas for flaps were more accurately measured with image computing software (ImageJ).

Results: Twenty-seven ¾ Z-Plasty flaps sites were available for evaluation in sixteen patients. The average age was 32.6 years at surgery (range 4-66 yrs) and the original burn size was 35% (range 2-65.5%). The joints involved included the axilla (13 sites), elbow (5), wrist (4), neck (2), ankle (1), and chest (1). Average follow-up was 20.7 months (range 0-110). All patients had a normal range of motion of the effected joint at the time of their last evaluation. The average increase in the base width of the ¾ Z-Plasty flap was calculated to be 68.6% (range: -25% to 170%). The increase in the measured flap area was significant (87.6%), reflecting loss of height, gain in width, and reshaping of the flap from triangular to rectangular.

Conclusions: The ¾ Z-Plasty flap is an effective reconstructive tool in selected deformities. It provides an immediate contracture release and has the potential to achieve additional gains with time, in our series averaging almost 70% the original width. This effect is likely through "tissue expansion" of healthy tissue flaps under the influence of adjacent scar tension and stretching exercises.

ABSTRACT

Missed Opportunities for Intervention Prior to Fall in Elderly Patients

Chris D. Minifee *The University of Texas at Houston Medical School* *Class of 2018*

Sponsored by: Sasha D. Adams, MD, The Center for Translational Injury Research
Supported by: The Center for Translational Injury Research (CeTIR)
Key Words: Falls, Elderly, Trauma, Education, Prevention

Background: Approximately 33% of elderly people (aged ≥ 65 years) experience a fall each year. With the rapidly aging population, the incidence of injury from ground level falls has surpassed that for motor vehicle crashes. Although most falls cause minor injuries, 20-30% are severe resulting in significant physical impairment, and elderly hospitalized for severe fall-related injuries have a 50% mortality rate. Many health and environmental factors contribute to fall risk in the elderly, however the most predictive risk factor is a prior fall. The CDC has emphasized the importance of injury prevention through identification of risk and intervention. In patients with severe injuries due to a fall, we determined the incidence of fall assessment and prevention during previous hospital encounters.

Methods: We performed a retrospective review of adult (≥65 years of age) trauma patients with severe injury (any AIS ≥ 3) admitted to our Level I center after a ground-level fall in 2014. We reviewed inpatient and clinic records to identify patients with previous admissions to our hospital, and recorded fall risk assessments and prevention efforts.

Results: Of 5448 admissions, 214 patients met the inclusion criteria. The median age was 79 (65-98), and 47% were male with an average ISS of 21 (16-42) and mortality 22%. After chart review, previous admissions were found in 39 (18%), most within 10 years. All 2014 admissions were for severe head injury (AIS ≥ 3) and had a median length of stay of 6 days. Median age was 80 (65-98), 54% were male, and the average ISS was 22 with mortality of 10%. The 39 patients had a total of 66 prior encounters, an average of 1.7 per patient. Prior admissions were for injuries (fall, MVC, stroke) and medical illness (cardiac, cancer, infection). Fall education or intervention was not documented in 68% of the patient encounters and in 4 of the 12 patients with a known history of falls.

Conclusion: As people age, physiological changes and illness affect gate and balance, increasing the risk for falls. Patients with falls are known to be at highest risk for subsequent falls, and potentially fatal injury. We have demonstrated that our institution only documented appropriate risk identification and intervention in 46% of high risk patients. Many elderly patients presenting with a major fall-related injury had not received appropriate intervention during previous encounters, which demonstrates a missed opportunity for injury prevention.

ABSTRACT

Improving Teamwork in the Pediatric Operating Room

Andrew N. Minzenmayer *The University of Texas at Houston Medical School* *Class of 2018*

Sponsored by: Akemi L. Kawaguchi, MD, Department of Pediatric Surgery
Supported by: Akemi L. Kawaguchi, MD, Department of Pediatric Surgery
Key Words: Teamwork, OTAS, Pediatric Surgery

Background: In 1999, the Institute of Medicine observed that a major cause of medical error is due to a failure of systems rather than individuals. A vital component of the healthcare system is the healthcare team, and infrequent teamwork behavior in the adult operating room is associated with a higher risk of patient death or complications. We anticipate that higher quality teamwork behavior in the pediatric operating room will be correlated with improved pediatric surgical patient outcomes.
Methods: Teamwork behaviors in the pediatric operating room were evaluated using the previously validated Observational Teamwork Assessment for Surgery (OTAS). This tool was used to assess five teamwork behaviors including communication, coordination, cooperation, leadership, and situational awareness for surgical, nursing, anesthesia, and scrub tech teams. These teamwork behaviors were evaluated across three operative stages using a 0 to 6-point scale, where 0 represents the lowest teamwork behavior and 6 represents the highest teamwork behavior.
Results: 214 cases were observed from June 1-July 28, 2015. The mean teamwork score was 3.93 ± 0.74. Among the three operative stages, the post-operative stage received the lowest mean score of 3.81 ± 0.71. Intra-operative surgery communication received the highest mean score of 4.44 ± 0.78, and scrub tech post-operative leadership received the lowest mean score of 3.40 ± 0.55.
Conclusion: Our baseline results indicate that overall teamwork in the pediatric operating room is good. Areas for improvement include cooperation and awareness during surgical debriefing as well as leadership among anesthesia, nursing, and scrub tech teams. We will correlate the observed teamwork scores with 30-day patient outcomes. We will also use this data to target future training programs aimed at improving teamwork behavior.

ABSTRACT

Nicholas C. Mitchell *The University of Texas at Houston Medical School* *Class of 2018*

Sponsored by: Richard A. Johnston, PhD, Department of Pediatrics
Supported by: Richard A. Johnston, PhD, Department of Pediatrics; The University of Texas at Houston Medical School—Office of The Dean
Key Words: asthma, chemerin, obesity, ChemR23, and airway hyperresponsiveness

Rationale. Air pollution and obesity are some of the most pressing public health concerns being faced in the developed and developing world. Obesity increases the airway responsiveness to methacholine following exposure to ozone (O3), which is a common air pollutant and asthma trigger. Currently the mechanism through which obesity potentiates airway responsiveness is unknown. The Johnston Lab has previously shown evidence that chemerin may serve a protective role in dampening lung dysfunction related to obesity. Chemerin is hormone and cytokine that is secreted by adipocytes. Due to the increased number of adipocytes in obese individuals, the levels of chemerin are increased in the serum of obese individuals. In addition elevated levels of chemerin can be found in the lungs following O3 exposure. We hypothesize that the receptor which mediates this effect is the ChemR23 receptor. In order to test our hypothesis, we measured airway responsiveness to methacholine in mice genetically deficient in the ChemR23 receptor (chemR23-deficient mice) and lean, wild-type (C57BL/6) mice.

Methods. Male chemR23-deficient mice and age- and gender-matched, wild-type C57BL/6 control mice were exposed to either filtered room air (air) or O3 [2 parts/million] for three hours. Twenty-four hours following the cessation of exposure, the mice were anesthetized and instrumented for the measurement of airway responsiveness to methacholine using the forced oscillation technique. To assess airway responsiveness, we used indices of airway [airway resistance (Raw)] and lung parenchymal [the coefficient of lung tissue damping (G) and the coefficient of lung tissue elastance (H)] oscillation mechanics.

Results. Following exposure to air, responses to methacholine for Raw, G, and H were similar in chemR23-deficient as compared to wild-type mice through the entirety of the methacholine dose response curve. The same results were found following O3 exposure. While exposure to O3 significantly increased responses to methacholine for Raw, G, and H as compared to air exposure, there was little difference in response between the ChemR23-deficient mice and the wild-type mice.

Conclusion. Contrary to our hypothesis, these results demonstrate that it is unlikely that the effects of chemerin in relationship to asthma and obesity are mediated through the ChemR23 receptor. However, even these negative results serve to narrow down the list of possible receptors through which chemerin acts to preserve lung function.

ABSTRACT

Do Risk Calculators Accurately Predict Surgical Site Infection and Surgical Site Occurrence in Ventral Hernia Repair?

Thomas O. Mitchell *The University of Texas at Houston Medical School* *Class of 2018*

Sponsored by: Lillian S. Kao, MD, MS, Mike K. Liang, MD, Department of General Surgery

Supported by: Lillian S. Kao, MD, MS, Mike K. Liang, MD, Department of General Surgery; The University of Texas at Houston Medical School – Office of Educational Programs

Key Words: Ventral hernia repair, surgical site occurrence, surgical site infection, risk calculator

Background: Current risk assessment models for surgical site occurrence (SSO) and surgical site infection (SSI) following ventral hernia repair (VHR) have limited external validation. Our aim was to determine 1) if existing models stratify patients into groups by risk and 2) which model best predicts the rate of SSO and SSI.

Study Design: Patients who underwent VHR and were followed for at least one month were included. Using two datasets--a retrospective multicenter database (Ventral Hernia Outcomes Collaborative; VHOC) and a single-center prospective database (Prospective)--each patient was assigned a predicted risk with each of the following models: Ventral Hernia Risk Score (VHRS), Ventral Hernia Working Group (VHWG), Centers for Disease Control (CDC) Wound Class, and Hernia Wound Risk Assessment Tool (HW-RAT). Patients in the Prospective database were also assigned a predicted risk from the American College of Surgeons National Surgical Quality Improvement Project (ACS-NSQIP). Areas under the receiver operating characteristic (ROC) curve (AUC) were compared to assess the predictive accuracy of the models for SSO and SSI. Pearson's Chi-Square was used to determine which models were able to risk-stratify patients into groups with significantly differing rates of actual SSO and SSI.

Results: The VHOC database (n=795) had an overall SSO and SSI rate of 23% and 17%. The AUCs were low for SSO (0.56, 0.54, 0.52, 0.60) and SSI (0.55, 0.53, 0.50, 0.58). The VHRS ($p=0.01$) and HW-RAT ($p<0.01$) significantly stratified patients into tiers for SSO while the VHWG ($p<0.05$) and HW-RAT ($p<0.05$) stratified for SSI. In the Prospective database (n=88), 14% and 8% developed a SSO and SSI. The AUC were low for SSO (0.63, 0.54, 0.50, 0.57, 0.69) and modest for SSI (0.81, 0.64, 0.55, 0.62, 0.73). The ACS-NSQIP ($p<0.01$) stratified for SSO while the VHRS ($p<0.01$) and ACS-NSQIP ($p<0.05$) stratified for SSI. In both databases VHRS, VHWG, and CDC overestimated risk of SSO and SSI while HW-RAT and ACS-NSQIP underestimated risk for all groups.

Conclusions: All five existing predictive models have limited ability to risk-stratify patients and accurately assess risk of SSO. However, both the VHRS and ACS-NSQIP demonstrate modest success in identifying patients at risk for SSI. Continued model refinement is needed to improve upon the two highest performing models (VHRS and ACS-NSQIP) along with investigation to determine if modifications to perioperative management based on risk stratification can improve outcomes.

ABSTRACT

Generation of an Hsc70cb Mutant with Compromised Substrate Binding Activity

Justin V. Nguyen *The University of Texas at Houston Medical School* *Class of 2018*

Sponsored by: Kevin A. Morano, PhD, Department of Microbiology and Molecular Genetics
Supported by: National Institute of Diabetes and Digestive and Kidney Diseases, 2T35DK007676-22
Key Words: Heat Shock Proteins, Amyloidosis, Hsc70cb

Background: Amyloidosis is a protein misfolding disease that frequently affects the kidneys, leading to organ dysfunction and end stage renal disease in untreated individuals. Studies conducted in various animal models have revealed that Hsp110 chaperones are effective at averting the progression of protein misfolding disorders. In Drosophila melanogaster, Hsp110 is represented by Hsc70cb and is a potent inhibitor of cytotoxicity resulting from expression of polyQ proteins, which have a propensity to aggregate. Proteins of the Hsp110 family are highly conserved nucleotide exchange factors that interact with Hsp70 to fulfill nucleotide exchange function. Additionally, they possess protein "holdase" activity by sequestering but not refolding amyloidogenic proteins. We hypothesized that Hsc70cb can avert the symptoms of polyQ expression due to its holdase ability and set out to test this model by creating Hsc70cb alleles compromised in holdase activity.
Methods: Mutants in the yeast homolog of Hsc70cb that independently impair nucleotide exchange function or holdase activity were previously generated and characterized. We created the homologous mutations in D. melanogaster Hsc70cb (dmHsp110) using overlap PCR site-directed mutagenesis and homologous recombination in yeast. dmHSP110NBD1 and dmHSP110SBD1 were designed to target the nucleotide exchange function and holdase function, respectively. Recombinant wild-type dmHsp110 protein was purified from Escherichia coli and its ability to interact with the D. melanogaster Hsp70 (dmHsp70) was assessed.
Results: dmHsp110 and dmHsp70 were shown to interact in a heterodimeric protein complex. dmHSP110NBD1 was successfully generated and we are currently exploring alternative options to build dmHSP110SBD1 after experiencing cloning difficulties . We determined that the dmHsp110 wild type and dmHSP110NBD1 proteins are stable when expressed in E. coli, a prerequisite to performing in vitro chaperone assays.
Conclusion: Once dmHSP110SBD1 is constructed, the substrate binding capability of all the dmHsp110 proteins will be tested using model misfolded proteins in a dynamic light scattering assay. We expect that the wild-type and mutant dmHsp110 alleles will replicate the findings with yeast Hsp110, pacing the way for generation of dmHSP110SBD1 flies for phenotypic analysis. This will allow for the discrimination between nucleotide exchange function and holdase activity at the tissue and organ level, providing future therapeutic targets and treatment for amyloidosis.

ABSTRACT

Supporting Vascular Function by Directed Splicing Manipulation of α1 Soluble Guanylyl Cyclase Gene

Sagar Patel *The University of Texas at Houston Medical School* *Class of 2018*

Sponsored by: Iraida G. Sharina, PhD, Department of Internal Medicine, Cardiology
Supported by: Iraida G. Sharina, PhD, Department of Internal Medicine, Cardiology
Key Words: Nitric Oxide (NO), Soluble Guanylyl Cyclase (sGC), Morphinoino Oligonucleotides

A major regulator of vascular plasticity is the endogenous molecule, Nitric Oxide (NO), which is largely dependent on the expression and activity of the enzyme, soluble Guanylyl Cyclase (sGC). sGC functions in arterial walls to mediate active vasodilation in times of vascular inflammation, thus playing a significant role in the regulation of hypertension. Decreases in sGC expression are known to exacerbate vascular stiffness leading to contraction of the vascular smooth muscle cells and an increase in blood pressure, potentially leading to acute congestive heart failure. Nitric oxide is synthesized intracellulary in vascular endothelial cells by an enzyme known as nitric oxide synthase (NOS). NOS converts the substrate, L-Arginine, into both Citrulline and NO, and NO diffuses freely across the membrane and binds to a heme moiety of the enzyme soluble guanylyl cyclase (sGC) in order to activate it. sGC produces ubiquitous secondary messenger cGMP which activates Protein Kinase G, a central component in vascular smooth muscle relaxation. Oxidative stress, which tends to increase with age, has been demonstrated to decrease sGC protein level in vascular tissue. Under oxidative stress, the sGC heme group is susceptible to oxidation, which blunts its sensitivity to NO and eventually targets the sGC protein for ubiquitin-dependent degradation. Prevention of the progressive loss of the sGC protein induced by oxidative stress provides a new potential therapeutic strategy to support vascular function. Previous work revealed the complexity of alternative splicing of sGC genes and demonstrated its importance in regulation of sGC function[8]. Several sGC splice variants were identified and characterized including the C-α1 (Isoform B) sGC[9-11]. This project was set to validate the approach of the splicing manipulation of the α1 sGC gene by the use of morpholino oligonucleotides in mammalian cell cultures. Human neuroblastoma BE2 cells were cultured and underwent RNA purification and reverse transcription to create cDNA in order to analyze and verify the expression of the C-α1 sGC sequence. Protein lysates were also obtained to verify the expression of C-α1 sGC in BE2 cells using western blot analysis. A subsequent experiment utilizing a similar methodology followed in which the BE2 cells were treated with various oxidants in order to demonstrate the regulation of C-α1 sGC protein levels by these oxidants. The oxidants included treatment of H_2O_2, ODQ, BSO, HEDS, and LPS. The change of ratio was observed between protein isoforms of sGC in these particular treatments due to oxidative degradation of canonical α1 but not the C-α1 splice form. Validation of BE2 cells as an appropriate cell model and verifying the effect of an oxidizer were important initial steps in this experiment. The final goal of this project is to transfect the BE2 cells with liposomes containing morpholino oligonucleotides specifically designed to block the major 3′ prime diverting spliceosomes to the alternative site. Additional experimentation utilizing the morpholino oligonucleotides is underway.

ABSTRACT

The Effect of PAK1 Knockout on the Efficacy of Metoclopramide Therapy in a Murine Model of Postoperative Ileus

Travis Peery *The University of Texas at Houston Medical School* *Class of 2018*

Sponsored by: Karen Uray, PhD, Department of Pediatric Surgery

Supported by: Karen Uray, PhD, Department of Pediatric Surgery; The University of Texas at Houston Medical School—Office of The Dean

Key Words: Ileus, PAK1, Metoclopramide, Contractility

Background: Postoperative ileus (POI) is characterized as a decrease in gastrointestinal motility following a surgical procedure. POI is one of the most common postoperative complications in the United States and presents a considerable cost in both financial terms and patient morbidity.

Significance: Metoclopramide (Reglan) is a gastroprokinetic agent which antagonizes D2 receptors in the enteric nervous system (ENS) and is currently employed to treat POI. Reviews of the literature have shown metoclopramide to be ineffective in the treatment of POI, possibly due to elevated activity of PAK1 kinases within the smooth muscle cells of the affected intestine. PAK1 negatively regulates phosphorylation of myosin light chains and therefore negatively regulates smooth muscle contraction at the cellular level, downstream of neuronal influence. Knocking out PAK1 in mice has been shown to improve gut contractility in models of POI.

Hypothesis: If elevated PAK1 inhibits smooth muscle contraction at the cellular level, then knocking out PAK1 will increase the efficacy of metoclopramide treatment of POI.

Experimental Design: C57BL/6 mice were used for all experiments. To compare the effect of PAK1 knockout against controls, PAK1 homozygous knockout strains and wildtype mice of both sexes were used. The mouse strains were each divided into four groups. 1) Received sham surgery and placebo; 2) Received POI inducing surgery and placebo; 3) Received sham surgery and 0.1mg/kg body weight of metoclopramide; 4) Received POI inducing surgery and 0.1mg/kg body weight of metoclopramide. 1 cm sections of whole ileum were harvested 24 hours post-surgery and suspended in 37°C buffered Krebs solution while muscle contractility was measured.

Results/Data: Amplitude, frequency, tone, and integral were recorded while the tissue was exposed to increasing concentrations of carbachol. As expected, a significant decrease in baseline integral, max integral, and max tone was observed in the POI groups as compared to the sham surgery groups. Contractility tended to improve in PAK1 knockout and metoclopramide treated groups; however, the differences were not significant.

Conclusions: Though we failed to demonstrate a significant benefit of metoclopramide/PAK1 combination therapy, the qualitative improvements observed did support our hypothesis. We plan to investigate this observed difference by continuing to gather data until we attain a statistical power sufficient to confidently accept or reject the hypothesis.

ABSTRACT

McGRATH MAC Video Laryngoscope – Direct vs Indirect Laryngoscopy in Difficult Airway Management

Tyler J. Poi *The University of Texas at Houston Medical School* *Class of 2018*

Sponsor: Carin A. Hagberg, MD, Kenneth Hiller, MD, Kathrine Normand, MD, Department of Anesthesiology

Supported by: Carin A. Hagberg, MD, Kenneth Hiller, MD, Kathrine Normand, MD, Department of Anesthesiology; The University of Texas at Houston Medical School – Office of Educational Programs

Key Words: Difficult Airway, Direct VS Indirect Laryngoscopy, McGrath Laryngoscope

Introduction: An anesthesiologist's ability to visualize laryngeal anatomy during laryngoscopy is very important to gain access to the airway and perform a successful intubation. Visualization of the airway in patients whose anatomical structures create a "difficult airway" can prove especially challenging and poor visualization can lead to problematic or unsuccessful intubations. Advances in laryngoscope technology such as video laryngoscopes have been useful tools for anesthesiologists, specifically for patients with a predicted difficult airway. This study investigates the success rate of both direct and indirect laryngoscopy in patients who present with potentially difficult airways, in an effort to determine the added value of indirect laryngoscopy.

Methods: This study will be performed on consenting adult patients requiring general anesthesia for elective surgery, who all have potentially difficult airways based off certain metrics such as Mallampatti score, ect… After standard pre-surgical procedures, initial vital signs will be recorded and the laryngoscopist will attempt to intubate the patients using the McGRATH® MAC video laryngoscope via the direct visualization technique (no use of the camera). If the direct intubation attempt is unsuccessful, the intubation will be attempted using the indirect view (with the camera). In the event that a patient presents with a Cormack-Lehane (C-L) grade of 4 during direct laryngoscopy, the indirect technique will be immediately utilized. Variables such as C-L glottis view (determined by the laryngoscopist), time for laryngoscopy, time for intubation, number of intubation attempts, lifting force required, and additional subjective measurements will be recorded during the intubation.

Results: As of 8/2015 data has been collected on 20/100 patients and is ongoing. Preliminary trials show a 100% success rate of both direct (n=10) and indirect (n=10) intubations, thus indicating a C-L grade 4 view has been the primary reason for indirect laryngoscopy. With that said, indirect laryngoscopy reduced the total intubation time ($\bar{x}$= 25.27 s , S= 11.93 s) compared to direct laryngoscopy ($\bar{x}$= 32.03 s , S= 13.89 s). Patients that were intubated indirectly were less likely to need external manipulation than patients intubated directly (20% compared to 70%,

respectively). Additionally, subjective metrics such as "difficulty of ETT delivery" improved with indirect laryngoscopy despite having to overcome the C-L grade 4 view.

Discussion: Preliminary results start to show the added value of using indirect laryngoscopy. In addition to anticipated difficult airways, indirect laryngoscopy could also prove extremely useful in C-spine patients where external manipulation needs to be extremely limited. Additional data collection will strengthen the current statistical figures and possibly uncover specific pre-operative metrics that predict the necessity of indirect laryngoscopy.

ABSTRACT

Risk Factors for Fascial Dehiscence Following Emergent Trauma Laparotomy

James A. Price *The University of Texas at Houston Medical School* *Class of 2018*

Sponsored by: John Harvin, MD, Department of Surgery, CeTIR
Supported by: John Harvin, MD, Department of Surgery, CeTIR
Key Words: Surgery, trauma, exploratory laparotomy, fascial dehiscence

Introduction: Fascial dehiscence (FD) following emergent trauma laparotomy occurs in 10% of patients. FD is associated with longer hospital stays and may require a second operation to repair the incisional hernia. While organ/space surgical site infection (SSI) has been associated with FD, no factors available to the surgeon prior to fascial closure have been reported. The aim of this study is to identify risk factors for FD in patients undergoing emergent trauma laparotomy.

Methods: A retrospective study was performed from 1/1/2011-3/31/2015. An institutional trauma registry was queried for patients ≥ 16 years of age undergoing emergent trauma laparotomy – defined as ED directly to OR or ED to IR to OR. Patients who did not achieve fascial closure during hospitalization were excluded. The cohort was then divided into those undergoing definitive (DEF) and damage control laparotomy (DCL); univariate analysis was performed to compare those with FD to those without for both groups. A purposeful multiple logistic regression model was then constructed using variables chosen based on existing literature (age, mechanism, BMI, previous laparotomy, and DCL) and those found to be both clinically and statistically different.

Results: A total of 19,506 patients were admitted over the study period. 871 underwent emergent trauma laparotomy, including 291 (34%) DCL, 562 (65%) DEF, and 18 (2%) intraoperative deaths. In the DEF group, 1 had a skin only closure, leaving 561 patients to analyze, of which 18 (3%) had FD. The DEF patients with FD had a more severe abdominal injuries (median AIS abdomen 3, IQR [2, 4] vs 3, IQR [2, 3], p=0.03) and a higher rate of postoperative vasopressor use (22% versus 6%, p=0.02). Of the 291 patients undergoing DCL, 69 (24%) did not attain fascial closure, leaving 222 patients to analyze, 34 (15%) with FD. The DCL group with FD had no significant differences in demographics, Injury Severity Score (ISS), or intraoperative vital signs and resuscitation. The patients with FD had a higher rate of intestinal discontinuity (59% versus 34%, p<0.01), longer time to fascial closure (median 38 hours, IQR [32, 65] versus 34 hours, IQR [26, 47], p=0.02), and more re-laparotomies to closure (median 1, IQR [1, 2] versus 1, IQR [1, 1], p=0.03). In both the DEF and DCL groups, patients with FD had significantly higher rates of enteric suture line failure, superficial SSI, and organ/space SSI. On multiple linear regression analysis, older age (OR 1.03, 95% CI 1.00-1.06, p=0.03) and DCL (OR

7.03, 95% CI 2.29-21.62, $p<0.01$) were independently associated with FD.

Conclusion: Patients undergoing both definitive and damage control emergent trauma laparotomy who develop FD are highly likely to have an abdominal infectious process at the time of FD. In this retrospective analysis, age and DCL were independently associated with the development of FD following emergent trauma laparotomy.

ABSTRACT

Predictive Value of Fecal Testing for Clostridium Difficile Toxins A/B in Successful Fecal Microbiota Transplantation (FMT) of Patients with Multiple Recurrences of *C. difficile* Infections (CDI)

Justin Riojas *The University of Texas at Houston Medical School* *Class of 2019*

Sponsored by: Herbert L. DuPont, MD, Center for Infectious Diseases, University of Texas-Houston School of Public Heath

Supported by: Herbert L. DuPont, MD, Center for Infectious Diseases, University of Texas-Houston School of Public Heath The University of Texas at Houston Medical School – Office of The Dean

Key Words: *C. difficile,* Fecal Microbiota Transplant, fecal calprotectin

The rates of CDI have tripled during the past decade. CDI is currently the most common hospital-acquired infection in the United States. Despite the first-line traditional antibiotic treatments for CDI, many patients have one bout of infection after the other responding only to FMT. The primary defect in patients with multiple recurrences is loss of intestinal microbial flora diversity due in large part by the recurrent exposure to flora-damaging antibiotics in susceptible people. FMT reestablishes intestinal flora diversity and leads to intestinal colonization resistance against strains of *C. difficile*. Patients treated with FMT demonstrate approximately 90% cure rate. The novel parts of the present study are: study of commercial tests for *C. difficile* and *C. difficile* toxins to see which is/are most predictive of successful FMT; availability of multiple stool samples for study from a large number of FM-treated subject in one of the few centers in the U.S. organized to perform FMT in patients with multiply recurrent CDI. To test for inflammatory response, fecal calprotectin (FC) will be tested to document the bowel conditions. Another very sensitive screening test for *C. difficile* is the glutamine dehydrogenase (GDH), a metabolic enzyme found in all *C. difficile* strains and a few other bacteria. Twenty-three patients were tested for GDH levels; Average levels before FMT, after day 7, day 14, and day 30 were (9.10±3.79ng/mL, 14.52±4.74ng/mL, 13.98±2.24ng/mL, and 14.42±3.02ng/mL) and range 3.46-10.93ng/mL, 8.91-31.18ng/mL, 10.82-19.01ng/mL, and 9.54-20.19ng/mL respectively. Thirty-one patents were tested for Calprotectin; mean measurements before FMT, after day 7, day 14, and day 30 were (211.78±357.58 ng/mL, 124.11±205.96ng/mL, 153.20±288.66ng/mL, and 128.62±207.95ng/mL) and range (2.61-1365.79ng/mL, 1.25-971.57ng/mL, 2.03-1147.90ng/mL, 0-578.29ng/mL) respectively. GDH levels were taken from three FMT failures and 20 successful FMTs with mean levels 11.67±3.59ng/mL, and 13.16±2.47ng/mL for 3 FMT failures. Calprotectin was recorded from 4 failures and 29 successful FMTs with average levels of 104.80±125.25ng/mL (range 3.61-1113.00) and 162.22±248.13ng/mL (range 2.39-1368.40). GDH data did show significant difference between before FMT and three collection dates after (all $p<0.05$). Calprotectin did not show predictive value early however there was a significant difference (p=. 042) at 30 days after FMT. In the

future to compare the diversity of flora in recipient stool before and after FMT, a metagenomic analysis will be finished using 16 S rRNA methods on samples. This data will help further our understanding of what predicts successful FMTs.

ABSTRACT

The Role of PAK1 on Leukocyte Chemotaxis in a Postoperative Ileus Model

Orlyn Rivas *The University of Texas at Houston Medical School* *Class of 2018*

Sponsored by: Karen L. Uray, PhD, Department of Pediatric Surgery
Supported by: National Institute of Diabetes and Digestive and Kidney Diseases, 2T35DK007676-22
Key Words: PAK1 Postoperative Ileus Leukocytes Migration

INTRODUCTION: Postoperative ileus (POI) following abdominal surgery contributes to increased patient complications including: increased hospital stay, increased nosocomial infections, discomfort from gastrointestinal symptoms, and prevention of enteral feeding. There is currently no routine treatment for POI. Inflammation, use of certain pharmacological drugs, and edema have all been proposed as mechanisms for the formation of POI. PAK1 is a protein that is partly mediated by cytokines, and is involved in cytoskeletal rearrangement and leukocyte chemotaxis. The role of PAK1 in mediating neutrophil and macrophage chemotaxis into the intestinal layers is not fully understood. Therefore, we hypothesize that knocking out PAK1 in a POI mouse model would result in decreased leukocyte chemotaxis into the intestinal layers.
METHODS: A published gut manipulation (GM) model was used in C57BL/6 mice. Mice were subdivided into the following categories: GM PAK1 knockout, sham PAK1 knockout, GM wildtype, and sham wildtype. GM was induced by first rolling the small intestines three times between cotton applicators, then repackaging the bowel. Control mice underwent a sham operation in which only a midline incision was made, followed by immediate closure. Twenty-four hours later, the peritoneal fluid and blood were collected from each set of mice. Neutrophils and macrophages were isolated from each fluid and labeled using Calcein AM dye. Chemotaxis was assessed using a 12-well chemotaxis system combined with chemotactic factors CINC-1, MCP-1, and IL-8. A negative control was used that contained no chemotactic factor.
RESULTS: The project is still ongoing. A total of 5 experiment sets were performed. Preliminary results show an increase number of macrophages in both the GM wildtype mice and GM knockout mice. There appears to be no change in chemotaxis in both neutrophils and macrophages. MCP-1 activity, indicating mast cell activation, is increased in the GM mice sets, but no apparent difference between the wildtype and knockout genotypes exist.
CONCLUSION: No definite conclusion can be made regarding PAK1 and its role in leukocyte chemotaxis at this time. There is a known increase in neutrophils and macrophages in the intestinal layers, but it does not appear to be due to changes in chemotaxis. This research project on PAK1 is still ongoing, and further studies are required in order to formulate a conclusion.

ABSTRACT

Characterization of the Mechanical Conflict-Avoidance System with a Stimulus-Response Assessment

Marvin Rivera *The University of Texas at Houston Medical School* *Class of 2018*

Sponsored by: Scott D. Olson, PhD, Department of Pediatric Surgery
Supported by: Scott D. Olson, PhD, Department of Pediatric Surgery
Key Words: Mechanical Conflict-Avoidance System, Operant pain test

Background: The Mechanical Conflict-Avoidance System (MCS) is an operant method of pain testing that utilizes the cognitive component of pain that many reflexive pain tests lack. The purpose of this study is to determine the optimal testing parameters for experiments by performing a stimulus-response assessment that assesses operant pain in rats with a traumatic brain or spinal cord injury.
Methods: The MCS is comprised of a rectangular box divided into three sections: 1) light chamber, 2) probe chamber, and 3) escape chamber. Panels, or 'doors', are placed between each chamber and are raised and lowered according to testing protocol. The light source in the light chamber may be switched on to act as an aversive stimulus. The probe chamber contains nociceptive probes, which may be raised to various heights (0mm – 5mm), providing an additional aversive stimulus. Rodents were acclimated to the apparatus in a 5-minute introductory period during which they were allowed to move freely between chambers with no aversive stimuli in place. The rats were tested over a period of eight consecutive days. On day 1, rats were acclimated to the MCS. On each of the remaining days, however, animals were tested with a pretrial at 0 mm and 3 test trials at the specific probe height for that day (0, 0.5, 1, 2, 3, 4, and 5 mm, respectively). Mean latency to exit the light chamber and the duration spent in the probe chamber were recorded.
Results: At a probe height of 0.5 mm or greater, the latency to leave the light chamber remained 23.25 seconds on average. Mean latency to exit the probe chamber was similar at probe heights of 0.5 mm to 3 mm (9.61 secs). A decrease in exit latency was observed, however, with probe heights of 4 mm and 5 mm. A one-way ANOVA failed to reveal statistical significance.
Conclusion: This study suggests that a probe height of 3 mm is optimal when testing operant pain in animals post-injury with the MCS. At this probe height, animals begin to exhibit decreased duration in the probe chamber. Due to a lack of statistical significance, however, further testing should be done with more animals to better characterize the MCS. After optimal testing parameters have been determined, the MCS may be used in future experiments to determine how mesenchymal stem cell or drug treatments affect operant pain behavior in rodents.

ABSTRACT

Retrospective Review Comparing Clinical Outcomes for Robotic and Laparoscopic Ventral Hernia Repair

Monica Rosales Santillan *The University of Texas at Houston Medical School* *Class of 2018*

Sponsored by: Peter Walker, MD, Department of Surgery

Supported by: Peter Walker, MD, Department of Surgery; The University of Texas at Houston Medical School—Office of the Dean

Key Words: Hernia repair, da Vinci robot, laparoscopic, recurrence, infection

Background: The da Vinci Surgical System is a patented surgical platform that is utilized for an array of surgical procedures including hernia repair. Robotic assistance during laparoscopic hernia repair adds multiple degrees of freedom, which can potentially avoid the need for surgical tacks and transfascial suture placement. Some case series describing robotic assisted hernia repair have been published; however, to date, there is limited data comparing outcomes with laparoscopic repair. Our retrospective study examined outcomes in order to determine whether there is an advantage to using the robotic platform.

Methods: We reviewed a retrospective database of hernia repair patients from multiple institutions associated with UT Houston Medical School between 2010-2014. Our study focused on hernia repair patients who received robotic-assisted laparoscopic and laparoscopic primary ventral and incisional hernia repair. We reviewed patient EMRs to examine outcomes data in order to compare differing surgical techniques. The primary outcomes included length of stay, recurrence, and surgical site occurrence. The secondary outcomes included perioperative narcotic utilization.

Results: The retrospective data of 91 robotic hernia repair patients and 43 laparoscopic hernia repair patients were reviewed. No difference was observed in length of stay (robot- 1.6 days, lap- 0.8 day) or hernia recurrence (robot- 3.3%, lap- 2.5%; p=0.8). A significant decrease in surgical site occurrence was observed (robot- 12.2%, lap- 32.5%; p= 0.006) likely secondary to decreased incidence of seroma formation (robot- 11.1%, lap- 27.5%; p= 0.005).

Conclusion: Our results demonstrate that robotic-assisted hernia repair could potentially lead to an improvement in patient outcomes following ventral hernia repair. Additional prospective studies are required to more clearly evaluate cost effectiveness as well as the specific patient populations, which would receive the most benefit from robotic assisted repair.

ABSTRACT

Measuring Large-Scale Single Neuron Activity of a Small Brain System with Voltage-Sensitive Dyes

Samantha Royalty *The University of Texas at Houston Medical School* *Class of 2018*

Sponsored by: John H. Byrne, PhD, Department of Neurobiology and Anatomy
Supported by: Waggoner Endowment Fund
Key Words: Voltage-sensitive dye, *Aplysia*

Background: Voltage Sensitive Dyes (VSDs) bind to the membranes of cells and provide a measure of membrane potential and therefore of neuronal activity of potentially hundreds of neurons simultaneously. Previous studies used RH155, a VSD which changes absorbance, to study activity in the ganglia of marine mollusks *Aplysia* and *Tritonia*, small-brain systems that have served as useful models for understanding neuronal pathways in more complicated organisms. Another dye RH795, a fluorescent VSD, was recently found to produce a strong signal with a large signal-to-noise ratio when used with ganglia from the crab *Cancer pagurus,* indicating that it might provide signals in *Aplysia* which are superior to those made using RH155. To test this hypothesis, I compared the effectiveness of RH155 and RH795 in the buccal ganglion of *Aplysia* focusing on the signal to noise (S/N) ratio of each dye and its concentration dependency. A greater S/N ratio would increase the number of neurons that can be studied.
Methods: The buccal ganglia were removed and stained with either RH155 or RH795 at various concentrations. The BN2 nerve was stimulated to produce activity in the ganglia using a WPI A300 stimulus generator with a WPI 1850A stimulus isolator. To record changes in absorbance of multiple neurons in RH155 stained ganglia, an Olympus BX51WI fixed stage microscope and Neuroplex acquisition software were used with a Redshirt 128 CMOS camera. For RH795 stained ganglia, the same setup was used with a NeuroCCD SM256 camera to capture changes in fluorescence. Statistical analysis was performed with Microsoft Excel 2010 and MATLAB 2013. S/N ratios were calculated by averaging the amplitude of three spikes for each neuron that produced a signal, dividing by the standard deviation, and averaging the S/N ratios for each experiment.
Results: Different staining concentrations of the absorbance dye RH155 did not result in significantly different S/N ratios, but there was a trend towards increasing S/N ratio with increasing dye concentration (One-way ANOVA, $p>0.05$); S/N ratios, 4.97 ± 0.58, n = 3 for 0.05 mM; 4.19 ± 0.44, n=3 for 0.10 mM; and 6.60 ± 1.00, n = 3 for 0.25 mM. Different concentrations of the fluorescent dye RH795 did not result in significantly different S/N ratios either, but also showed a trend towards increasing S/N ratio with increasing dye concentration (One-way ANOVA, $p>0.05$); S/N ratios, 5.38 ± 0.37, n=3 for 0.05 mM; 5.58 ± 0.20, n=3 for 0.10 mM; and 5.68 ± 0.21, n=3 for 0.2 mM. The largest S/N ratio for RH155, 6.60 ± 1.00 (n=3), was not significantly different from the largest S/N ratio for RH795, 5.68 ± 0.21 (n=3) (t-test, $p>0.05$).
Conclusion: Voltage-sensitive dyes allow for a more complete picture of neural circuits than

intracellular recordings. Both RH155 and RH795 resulted in S/N ratios sufficient for recording neural activity in some cells. Our recordings with the fluorescent dye, RH795, did not have a greater S/N ratio than the absorbance dye, RH155. This is most likely due to limitations of our NeuroCCD SM256 camera. The S/N ratio of the fluorescent dyes could be improved with a camera that could record at a higher frequency. It is also possible that staining concentrations higher than those tested could improve the S/N ratio of both dyes.

ABSTRACT

The Effects of Defective STIM1 Mediated Store-Operated Calcium Entry on Reactive Oxygen Species Production in Rat Macrophages

Corey Sadd *The University of Texas at Houston Medical School* *Class of 2018*

Sponsored by: Peter A. Doris PhD, The Brown Foundation Institute of Molecular Medicine
Supported by: National Institute of Diabetes and Digestive and Kidney Diseases, 2T35DK007676-22
Key Words: Hypertension, Kidney Disease, Reactive Oxygen Species, Store-Operated Calcium Entry

The underlying factors that lead to hypertension and hypertension-related end-organ disease remain unknown. Hypertension may contribute to renal injury by elevating blood pressure above the autoregulatory range. The kidney relies on vascular autoregulation to regulate perfusion. As blood pressure rises the elastic components of the renal vasculature stretch, this initiates a reflex vasoconstriction so that renal perfusion is maintained constant. In hypertension, the autoregulatory range may be exceeded disrupting perfusion and resulting in both ischemia and reactive hyperperfusion. This produces an initiating mechanism for renal injury and initiates the activation of inflammation and the influx of cells of the immune system into the kidney. Recent work in models of autoimmune disease have provided insight into genetic mechanisms by which the normal wound healing mechanism can be disrupted and non-resolving inflammation can lead to progressively worsening inflammatory disease. Macrophages appear to play a critical role in the resolution of inflammation and genetic defects specific to macrophage function are implicated in non-resolving inflammation. Reactive Oxygen Species production by macrophages may play a critical role in the resolution of inflammation. In our study, two Spontaneously-hypertensive rat strains were used; SHR-B2 with normal STIM-1 Protein and SHR-A3 with defective STIM-1 protein. STIM-1 is responsible for Store-Operated Calcium Entry. Macrophages were isolated from the Rat by stimulating macrophage proliferation with Concanavilin A. Macrophages were collected from the peritoneal cavity. The Western Blot performed showed an absence of the C-terminus of the STIM-1 Protein in the SHR-A3 strain but not in the SHR-B2 strain. This finding demonstrates that the STIM-1 protein is unable to communicate with the ORAI1 channel which is responsible for Store-Operated Calcium Entry. An ROS assay was performed to measure the difference in production of ROS between SHR-B2 and SHR-A3. In the SHR-A3 strain, ROS production was negligible. In the SHR-B2 strain, there was an ROS production fluorescent signal of 140 MFI. In conclusion, the negligible production of ROS in the SHR-A3 strain compared to the SHR-B2 strain may indicate the important role of ROS in down regulating inflammation.

ABSTRACT

Treatment with Multipotent Adult Progenitor Cells in Traumatic Brain Injury: a Time Course Study of Microglia/Macrophage Activation

Walter Schiffer *The University of Texas at Houston Medical School* *Class of 2018*

Sponsored by: Charles Cox, MD, Department of Pediatric Surgery

Supported by: Charles Cox, MD, Department of Pediatric Surgery; The University of Texas at Houston Medical School – Office of Educational Programs

Key Words: Multipotent adult progenitor cells, traumatic brain injury, microglia

After previously demonstrating that IV administration of multipotent adult progenitor cells (MAPC) helps to mitigate brain inflammation after traumatic brain injury (TBI), the next critical step is to discern the optimum time scale for therapeutic administration. Additionally, therapeutic outcome will be correlated to secondary inflammation as measured by the ratio of inactive microglia/ macrophages (M2) to active microglia/ macrophages (M1). Rats underwent a cortical contusion injury (CCI) and then received saline IV (CCI-Alone), or MAPCs (CCI-Tx). Rats in the CCI-Tx group were then subdivided according to time course of MAPC administration: 24 hours, 2 and 24 hours, 6 and 24 hours, 12 and 36 hours, 24 and 48 hours, or 36 and 72 hours. All doses were given at a concentration of 10 million/kg. Spatial learning was assessed by measuring latency to platform in the Morris Water Maze (MWM). Brains were harvested and prepped for immunohistochemistry studies and each group was stained with IBA1 and P2Y12. Approximately 5 pictures were taken at 20X from each of three hippocampal areas: dentate gyrus, CA1 and CA3 Hippocampus; and quantitative and statistical analysis were used to determine ratio of M2/M1 cells. Administration of MAPCs resulted in a significant decrease in latency to the platform in the 2/24 and 6/24 hour groups, while the 2/24, 12/36, and 24 hour alone groups spent significantly more time in the region proximal to the platform. This therapeutic effect, however, was not observed in the 12/36 and 36/72 hour groups. Improved spatial learning is expected to correlate with increased M2/M1 ratios in the hippocampus. The preliminary data suggests that there is a critical time interval MAPC administration at 24 hours post-TBI during which secondary damage due to activated microglia/ macrophages may be mitigated.

ABSTRACT

Neuropsychological Impairment in West Nile Virus

Nicole Schrock *The University of Texas at Houston Medical School* *Class of 2018*

Sponsored by: Rodrigo Hasbun, MD, MPH, Department of Infectious Disease
Supported by: Rodrigo Hasbun, MD, MPH, Department of Infectious Disease; Steven P. Woods, Psy.D., University of Houston Cognitive Neuropsychology of Daily Life Laboratory
Key Words: West Nile Virus, Neuroinvasive, Neuropsychological impairment, RBANS

BACKGROUND: Emerging data suggests that West Nile Virus is associated with Central Nervous System complications, including neurocognitive impairment. However, little is known about the demographic (e.g. age), psychiatric (e.g. depression), and everyday functioning (e.g. quality of life) factors in WNV-associated neurocognitive impairment. The present study used a large, well-characterized cohort of WNV patients to evaluate these issues.
METHODS: In this cross-sectional, observational study 110 patients were enrolled and underwent comprehensive medical, laboratory, and neuropsychological evaluations. We excluded participants with major CNS disease (e.g. stroke, dementia). Participants were classified as neurocognitively impaired on the basis of the Repeatable Battery for the Assessment of Neuropsychological Status (RBANS). Measures of learning, memory, visuoconstruction, language, and attention were assessed for each subgroup. Impairment in each domain was defined as one standard deviation below the mean based on published normative data. Consistent with DSM V, global neurocognitive impairment was defined as having two or more domains falling one standard deviation below the mean. The patients were stratified into two groups based on neurocognitive status, and confounders across neuropsychological status were compared. Predictors of neuropsychological impairment were determined for each group using WNV neuroinvasive disease status, as well as scores from the Beck Depression Inventory and Multidimensional Fatigue Inventory. Downstream consequences of impairment were examined using scores from the Short Form 36 Health Survey (SF-36) and Barthel ADL Index. Analyses were conducted using independent sample T tests and chi square tests with critical alpha of 0.05.
RESULTS: An analysis of the RBANS scores suggests that the higher than normal cognitive impairment is driven by difficulty in the acquisition of new verbal information. The neurocognitively impaired and neurocognitively normal groups did not differ significantly in age, education, or gender. The neurocognitively impaired group was 37% non-Caucasian compared to 8.4% non-Caucasian in the neurocognitively normal group. However, further statistical analysis showed that the findings are not better explained by demographic differences. Mood, fatigue, and neuroinvasive disease diagnosis were all shown to be significant predictors ($p<0.05$) of neuropsychological impairment. Measures of everyday functioning (SF-36 and ADL) suggest a lower quality of life in those with WNV neurocognitive impairment but no differences in activities of daily living.

CONCLUSIONS: Cognitive impairment as an expression of brain involvement of WNV is related to_non-Caucasian ethnicity, neuroinvasive disease, lower quality of life, higher depression, and higher fatigue. Findings may shape patient care and introduce therapies aimed at improving or compensating for cognitive deficits in patients with WNV CNS disease.

ABSTRACT

Endocrine and Behavioral Indices of PTSD Susceptibility in Recent Trauma Patients

Andrew Schroeder *The University of Texas at Houston Medical School* *Class of 2018*

Sponsored by: Nicholas J. Justice, PhD, Institute of Molecular Medicine for the Prevention of Human Diseases

Key Words: PTSD, HPA axis, startle, trauma

Post-Traumatic Stress Disorder (PTSD) is characterized by severe anxiety, nightmares, and flashbacks involving a traumatic event that occurred in a person's life. Although relatively common in trauma patients, PTSD is rarely diagnosed early in the onset of the condition. Studies show patients receiving early intervention often have better prognoses improving their quality of life. The objective of our research is to determine if we can identify measurements of trauma patients' psychological status, Hypothalamic Pituitary Adrenal (HPA) axis activity, and startle reactivity, measured <14 day from admission that correlate with subsequent development of PTSD. Psychological state in recently hospitalized trauma patients was gauged based on PCL-5, LEC-5, BAI and BDI-II scores derived from a compiled survey. The enrolled patients' startle reactivity was individually evaluated based on prepulse inhibition (PPI) of their blink-startle response delay and magnitude of blink to an auditory stimulus. HPA axis activity was measured in plasma samples assayed for cortisol and ACTH levels as well as various additional biomarkers. Patients with PCL-5 scores >30 were compared to those with PCL-5 scores <30 in regards to their 74dB, 78dB and 82dB prepulse inhibited response to an 110dB stimulus. There was no significant correlation found between these two data sets. Patients will be contacted to return for the same battery of tests after three months, at which point they will be evaluated for PTSD symptoms. Back correlation of the data collected at each time point, along with other contributing factors (e.g. drug regimen), will be used to establish if behavioral and endocrine measurements can predict later development of PTSD. Success in establishing behavioral or endocrine biomarkers in trauma exposed populations will aid in determining which patients would likely benefit from early intervention and prevention treatments to prevent chronic PTSD.

ABSTRACT

Complementation of LiaYZ in *Enterococcus feacalis* OG1RF

Bruce W. Sharp *The University of Texas at Houston Medical School* *Class of 2018*

Sponsored by: Cesar A. Arias, MD, MSc, PhD, Department of Internal Medicine
Supported by: Cesar A. Arias, MD, MSc, PhD, Department of Internal Medicine; The University of Texas at Houston Medical School – Office of Educational Programs
Key Words: *liaYZ, E. faecalis,* Daptomycin, Antibiotic Resistance

Background: A key "front-line" intervention in severe vancomycin-resistant enterococcal (VRE) infections is daptomycin (DAP). Although not FDA approved for the treatment of VRE, DAP has *in vitro* bactericidal activity against these organisms and is frequently used to treat serious VRE infections. DAP is a lipopeptide antibiotic that inserts into the cell membrane (CM) of bacteria at the division septum through a calcium-dependent mechanism and is thought to form a pore structure that ultimately results in cell death. Of interest, clinical VRE isolates have been noted to develop resistance to DAP (DAP-R) during therapy. Bacteria have a network of specialized signaling pathways composed of membrane associated sensor kinases and cytoplasmic transcriptional regulators, which work together to alter gene expression in response to changes in the extracellular environment, including antimicrobial attack. In *Enterococcus faecalis*, changes in one such regulatory system, LiaFSR, were associated with the DAP-R phenotype. This study focuses on a predicted operon of three genes, *liaXYZ*, which is a target of the LiaR response regulator, and consists of a putative periplasmic protein (LiaX) and two predicted membrane-associated proteins (LiaYZ). Previous work had generated a nonpolar deletion of *liaYZ* in the laboratory *E. faecalis* strain OG1RF (OG1RFΔ*liaYZ*). This mutant exhibited an increase in the minimum inhibitory concentration (MIC) of DAP from 2µg/ml to 6µg/ml (clinical breakpoint for resistance is 4 µg/ml). The aim of this work was to complement these two genes in the OG1RFΔ*liaYZ* mutant which we hypothesized would restore the original MIC.

Methodology: Two different complementation methods were performed to restore *liaYZ* to OG1RFΔ*liaYZ*. First, we attempted to complement in *cis* using a *pheS** counter-selection system. Primers were designed in flanking regions to produce a fragment using the crossover PCR strategy. The insert and plasmid (pHOU1) were digested using BamHI and SphI then ligated together. This ligated product was transformed into chemically competent EC1000 cells and plated on Luria Bertani (LB) plates with gentamicin (25mg/ml) and Xgal (80µg/ml). Second, to complement in *trans*, we initially used a high copy number vector pBluescript (pBS), which allows white/blue screening, to clone the *liaYZ* genes with restriction sites for SacI and XbaI. The ligation reaction was transformed in *E. coli* TG1 and plated on LB agar supplemented with ampicillin 100ug/ml and Xgal (80µg/ml). The white colonies were recovered and the insert was confirmed by PCR and sequence. The genes *liaYZ* were subcloned in a low copy number vector pAT392 (using SacI and XbaI enzyme) under the control of the P2 promoter to allow constitutive

expression of the gene products into the vector. The selection of the recombinant colonies was performed on LB agar with gentamicin 25µg/ml.

Results: We were unsuccessful at obtaining colonies from *E. coli* using the *pheS** counter-selection. We instead used the strategy of complementation in *trans* using the pAT392 vector. We obtained 100 colonies in *E. coli* TG1, of which we screened 50 colonies by PCR to determine the presence of the insert in pBS. Out of 50 colonies, 40 were positive for the insert by PCR and two colonies were chosen for sequencing to confirm the insert. The sequence of the *liaYZ* was correct and the plasmid was isolated and used for further subcloning in pAT392. The confirmation of the insert (*liaYZ*) in this vector is still under process.

Conclusions: We were unsuccessful in obtaining the restoration of the genes *liaYZ* in *cis* in OG1RFΔ*liaYZ*. We are in the process of confirmation of the complementation in *trans* using the pAT392 vector.

ABSTRACT

Mesenchymal Stem Cells Delivered Intravenously and Intrathecally Attenuate Hypersensitivity Following Spinal Cord Contusion

Jacob Shaw *The University of Texas at Houston Medical School* *Class of 2018*

Sponsored by: Scott Olson, PhD, Department of Pediatric Surgery
Supported by: Scott Olson, PhD, Department of Pediatric Surgery
Key Words: Spinal cord injury, stem cells, rat

Background: Traumatic Spinal Cord Injury (SCI) is a debilitating injury leaving the approximately 273,000 people, as of 2013, who were affected by it with an enormous physical and financial burden that for many of them will last the remainder of their lives.[1] The physical manifestations range from neuropathic pain and numbness to complete and incomplete paraplegia or tetraplegia.[1] In the hours and days following an SCI, there is the potential for secondary injury from activated inflammatory cells (microglia, monocytes and T cells) leading to possible hemorrhage and blood-spinal cord barrier disruption.[1] While it was once thought that multipotent stem cells (MSC) could be used for regeneration of any type of tissue they have proved more useful in immune regulation.[2] Previously, MSCs have been shown to be therapeutically effective in modulation of the immune system in treatment of graft vs host disease following bone marrow transplant.[2] The benefits of MSCs can therefore be used in the modulation of immune cells, particularly microglia, and, by extension, can potentially reduce the threat of secondary injury following SCI.[2]
Significance: The *long-term goal* is to develop a novel therapy which is easily utilized in a patient population presenting with acute trauma. We would hope that this therapy is able to minimize the threat of secondary injury and neuropathic pain while simultaneously maximizing locomotor recovery.
Hypothesis: We hypothesize that rats treated with MSCs 24 hours after spinal cord injury will demonstrate less mechanical sensitivity, decreased thermal sensitivity and improved locomotor recovery when compared to injured rats receiving vehicle treatment.
Methods: Rats receive either sham or contusion spinal cord injury at level T10 followed by intravenous and intrathecal injection of either PBS (vehicle) or MSC at 24 hours post-injury Locomotor recovery was scored using the Basso, Beattie and Bresnahan (BBB) Locomotor Rating at 1, 2, 3, 5, 7, 10 and 14 days post-injury. Thermal sensitivity of hind paws was measured using the Hargreaves[3] apparatus set to 32°C. Mechanical sensitivity of hind paws was measured using Von Frey filaments and scored using the Dixon Up-Down method. Mechanical sensitivity of the torso was also tested using Von Frey filaments of 2g and 26g. Both thermal and mechanical sensitivity was measured at 7, 14, 21 and 28 days.
Results: Treated rats exhibited a significantly increased threshold to mechanical stimuli in the Von Frey test when compared to untreated animals at 7, 21 and 28 days post-injury. There was no significant difference between treated and untreated groups in performance of the thermal, girdle or BBB tests.

Conclusion: The results of the Von Frey test are consistent with our hypothesis, indicating a therapeutic effect of MSC after SCI. We expect increasing the numbers of animals in this study will reveal significance in the other tests as well. We will use ELISA to determine if the MSCs effectively reduce pro-inflammatory cytokines (TNF-α and IL1-β) therefore decreasing the threat of secondary injury.

[1] Dasari, Vankeeta R., Krishna K. Veeravalli, and Dzung H. Dinh. "Mesenchymal Stem Cells in the Treatment of Spinal Cord Injury: A Review." *World Journal of Stem Cells* 6.2 (2014): 120-33. Web.

[2] Singer, Nora G., and Arnold I. Caplan. "Mesenchymal Stem Cells: Mechanisms of Inflammation." *Annual Review of Pathology: Mechanisms of Disease* 6.1 (2011): 457-78. Web.

[3] Hargreaves K, Dubner R, Brown F, Flores C, Joris J. A new and sensitive method for measuring thermal nociception in cutaneous hyperalgesia. Pain. 1988; 32: 77–88.

ABSTRACT

SEEKing to Improve Care: A Follow-up Study of a Project to Improve Screening for Psychosocial Stressors in a Pediatric Clinic

Ankita Tewari *The University of Texas at Houston Medical School* *Class of 2018*

Sponsored by: Rachael J. Keefe, MD, MPH; Department of Pediatrics
Contributors: Michelle Barratt, MD, MPH; Christine Ellis, MD; Department of Pediatrics
Key Words: primary care pediatrics, psychosocial stressors, quality improvement

Background: In 2011, the Safe Environment for Every Kid (SEEK) questionnaire was shown to be a reliable methodology in private practice to improve physician screening for risk factors in child healthcare. Our clinic had no formal screening tool to ensure a reduction in psychosocial stressors and prevent child maltreatment, one of the resident continuity clinics decided to incorporate the SEEK questionnaire into their practice. Since then, the SEEK screening questionnaire is implemented regularly with a goal of 90% for our well child visits at 4, 15, and 30 months.
This follow up research project created a method to evaluate the effectiveness of the SEEK screening by speaking with the caregivers over the telephone after each visit to better understand how we can improve on our current methodology. The areas in the metroplex that can be labeled as high-risk will be identified and it will be determined how we can best help those families. The aim is find out if the caregivers received the care they were looking for and how the SEEK process can be further improved. By speaking with the caregivers on the phone, any needs that were left unmet or any concerns that were not brought up during the well visit can be addressed. By performing this study, it will be determined whether SEEK screening is meeting our patients' needs in the best way possible.

Methods: Starting in June 2015, the clinic implemented a "permission slip" with the well child checkup forms that the caregiver fills out during the appointment. This form asks the parent whether they would be okay with answering questions regarding their child's care with someone over the phone. The process of calling the caregivers about one week after their visit to the clinic was conducted in order to follow up with the questionnaire and check the efficacy of the resources they received while in clinic.

Results: Over the summer we consented a total of 38 patients into the study. This included nineteen 4-month checkups, nine 15-month checkups, and eight 30-month checkups. Our patient population is mainly Medicaid funded and a majority identify themselves as African American or Hispanic. By conducting the in-clinic surveys and follow up phone calls, it was determined that the most concerning needs for the caregivers of our patients are: need for the poison control number, smoking around the child, food insecurity, and insurance needs.

Conclusion: Although our study is limited by a small sample size and is ongoing, overall, parents felt that the screening for psychosocial needs in the pediatric primary care clinic was useful and reported that they benefited from the resources provided. Due to the positive response, we will continue to administer the SEEK survey in our clinic. Next steps include geographical mapping of patient's addresses in order to identify if the patients with certain needs lived in similar locations within the city to potentially address these concerns at a broader public health level.

ABSTRACT

Determining the Stability of Frozen and Lyophilized Fecal Microbiota Transplant (FMT) Product used to Treat Patients with Multiple Bouts of *Clostridium difficile* Infection (CDI) to Provide Data on Storage Life

Evangelia Valilis *The University of Texas at Houston Medical School* *Class of 2018*

Sponsored by: Herbert L. DuPont, MD, Department of Epidemiology
Supported by: National Institute of Diabetes and Digestive and Kidney Diseases, 2T35DK007676-22
Key Words: *Clostridium difficile*, recurrent CDI, fecal microbiota transplant, frozen stool, lyophilized stool

OBJECTIVES: Fecal microbiota transplant (FMT) is the most effective therapy in treating patients suffering from recurrent *Clostridium difficile* infection (CDI). This study determined the stability of FMT bacterial product stored for variable times past three months. Collecting and freezing samples is an expensive task considering the cost of screening donors. Determining if frozen and/or lyophilized samples are stable after 3 months of storage would be a significant savings and would allow treatment of greater numbers of patients.

METHODS: To determine the microbial stability of 50 frozen samples and 16 lyophilized microbiota products from different time points, quantitative polymerase chain reaction (qPCR) was used on extracted fecal DNA to enumerate the bacterial genera present in the human gut: *Bacteroidetes, Clostridium, Escherichia coli, Bifidobacterium, Lactobacillus.* Mean number of 16S rRNA sequences per µg of sample DNA was compared between each time point using non-parametric Mann-Whitney test.

RESULTS: The frozen samples were significantly different from each other across all time points and bacterial genera ($p<0.001$). The same was true for lyophilized samples ($p<0.001$). Among frozen and lyophilized samples, levels of *Bifidobacterium* increased over time. The microbial diversity of frozen and lyophilized were statistically different among the genera *Bacteriodetes* ($p=0.0060$), *Bifidobacterium* ($p<0.0001$), *E. coli* ($p=0.0029$) and *Lactobacillus* ($p=0.0003$) with lower counts of these genera in lyophilized samples. *Clostridium* species had statistically similar levels between frozen and lyophilized samples ($p=0.6531$).

CONCLUSIONS: Analysis of qPCR results show that microbial content was marginally different across all time points among frozen and lyophilized samples. These differences may be attributed to the large diversity of flora across healthy donors. Frozen samples maintained greater microbial stability than lyophilized samples providing evidence that frozen FMT product has a longer storage lifetime. Viability studies are being planned to compliment these studies.

ABSTRACT

Zebrafish Avoid Odor Associated with Caudal Fin Injury

Alexandra van Brummen *The University of Texas at Houston Medical School* *Class of 2018*

Sponsored by: Edgar, T. Walters, PhD, Carmen Dessauer, PhD, Gislain Breton, PhD, Department of Integrative Biology and Pharmacology

Supported by: Edgar, T. Walters, PhD, Carmen Dessauer, PhD, Gislain Breton, PhD, Department of Integrative Biology and Pharmacology; The University of Texas at Houston Medical School—Office of the Dean

Key Words: Aversive Conditioning, Pain, Nocifensive Behavior, Mechanical Stimulation, Zebrafish, Escape Response

Background/Significance: Neither pain mechanisms nor their evolution are understood. Rodents are commonly used to investigate pain mechanisms, but zebrafish may also be a useful model for addressing pain-like mechanisms because of their genetic advantages and well characterized avoidance and escape behaviors. Avoidance is demonstrated by locomotion away from an aversive stimulus. An escape behavior is the C-start, a rapid flexion of the body into a C-shape that is used to abruptly change the direction of movement, thus promoting escape from threatening stimuli. Sensitization of the C-start escape behavior, increased animal vigilance after injury, and avoidance of signals associated with injury are likely adaptive responses to avoid predators in an injured state. Understanding these adaptive behaviors after injury in non-mammalian vertebrates like zebrafish may provide clues about the evolution of pain and lead to advantageous new models to discover pain-related mechanisms and treatments in humans.
Hypothesis: I predict that 1) zebrafish will show sensitization of escape responses after peripheral injury, and 2) the fish will learn and remember olfactory stimuli associated with peripheral injury, expressed as avoidance of the injury-associated odor.
Experimental Design: Injured zebrafish were given a minor injury to the tail on the dorsal portion of their caudal fin after being anesthetized with 0.02% MS-222 (tricaine). Control zebrafish were anesthetized with no fin clip, following the same procedure as the clipped fish. The zebrafish were then put in a recovery tank for 5 min containing 0.5 ml of the odor source to be conditioned (carrot juice) in 1050 ml of water. The fish was then placed in a 1050 ml clean water tank. The movement of the fish was then videorecorded for five min. Repeated C-starts were elicited by 18 vibratory stimuli applied every 5 sec. To test conditioned avoidance, 0.5 ml of carrot juice was added to the back right corner of the chamber and the behavior recorded for another 5 min. The C-start and avoidance tests were repeated 24 hr later. Ethovision XT software was used to track and analyze the zebrafish's movements.
Results: With 7 injured fish and 7 control fish, a trend was found for the injured fish to have more C-starts than uninjured animals, indicating sensitization of this escape response after injury. The most important finding was in the avoidance test 24 hr after injury. Compared to controls, injured fish spent substantially more time near the bottom (a known defensive response of zebrafish) and on the opposite side of the chamber from the carrot juice. These

results indicate a persistent conditioned aversion to the carrot juice produced by the tail injury. If the results are replicated, they would provide the first demonstration in any fish of an aversive memory of injury, and would provide perhaps the clearest demonstration yet of pain-like behavior in fish.

ABSTRACT

Use of StO2 Monitoring in Conjunction with a Sepsis Screening Tool to Improve Early Recognition of Sepsis

Natacha C. Villegas *The University of Texas at Houston Medical School* *Class of 2018*

Sponsored by: Laura J. Moore, MD, Center for Translational Injury Research (CeTIR)
Supported by: Laura J. Moore, MD, Center for Translational Injury Research (CeTIR)
Key Words: Sepsis, StO_2 monitor, ICU, hypoperfusion, near infrared spectroscopy, systemic inflammatory response syndrome, STICU

Background: Sepsis is defined as a systemic inflammatory response to an infection which, if not treated early, can progress to organ failure and eventually death. In the United States in 2011 there were over a million cases of sepsis with an associated cost of $16.4 billion. Time is essential for sepsis treatment as early interventions are associated with better outcomes, thus the goal of this study is to improve early detection of sepsis.
Sepsis leads to cardiovascular abnormalities that in turn cause hypoperfusion, which is one of the markers of the disease. Therefore, we hypothesized that a point-of-care device that has been developed to measure tissue perfusion, called StO_2 monitor, can be utilized to improve the early detection of sepsis in conjunction with a sepsis screening tool that has already been validated.
Methods: Data were collected prospectively during a 10 week period, at the Memorial Hermann Shock Trauma Intensive Care Unit (STICU), including collection of sepsis screening sheets filled by the STICU personnel and measurement of StO_2 values with the monitor. Afterwards, data were collected retrospectively through the Care4 electronic medical record database, to determine whether the patient developed sepsis. Finally, a statistical analysis was performed with the DT ComPair statistical package on the R software.
Results: 91 patients were screened at the STICU's 23 beds for a period of 10 weeks. Out of the total 244 data entries (one per patient per day), 174 were considered for the study as entries were not taken into account after diagnosis of sepsis. The age mean was 47 and 36% of the patients were female. The most frequent microorganisms causing infections were *Klebsiella*, *Staphylococcus aureus*, *Escherichia coli*, and *non-enterococcus Streptococcus*. The most frequent sources of infection were lungs, blood and urine. 26% of the population sample developed sepsis.
The screening tool alone yielded a sensitivity of 76%, specificity of 83%, positive predictive value (PPV) of 43% and negative predictive value (NPV) of 95%. Whereas the combined use of the StO_2 monitor and the screening tool yielded a sensitivity of 52%, specificity of 95%, PPV of 68% and NPV of 92%.
Discussion: the results show that the combined use of the StO_2 monitor and the screening tool has a statistically significant higher specificity and positive predictive value. This evidence suggests that the StO_2 monitor might be a good addition to the screening tool for the early recognition of sepsis, producing better outcomes due to earlier interventions.

ABSTRACT

Replication of Common Variant Associations with Bicuspid Aortic Valve

Margaret Wang *The University of Texas at Houston Medical School* *Class of 2018*

Sponsored by: Siddharth K. Prakash, MD, PhD, Department of Internal Medicine
Supported by: Siddharth K. Prakash, MD, PhD, Department of Internal Medicine
Key Words: Bicuspid Aortic Valve, Congenital Cardiovascular Defect, Single Nucleotide Polymorphisms, Next generation qPCR, Genome Wide Association Studies

Background: Bicuspid Aortic Valve (BAV), the most common congenital cardiovascular disorder in adults, is found in 1% of the adult population and is associated with life-threatening Thoracic Aortic Aneurysms and Dissections (TAAD) and aortic valve dysfunction requiring valve replacement. We hypothesize that common genetic variants contribute to BAV. Previously, we validated this hypothesis by identifying common variants that are consistently associated with BAV in a meta-analysis of genome-wide (GWA) data from diverse European-American cohorts with isolated BAV (n = 455), Turner syndrome (n=435), TAAD (n=1068) and left-ventricular outflow tract obstructive defects (n=1651).

Methods: To replicate these observations, I designed and implemented protocols to genotype 12 top candidate GWA SNPs using Taqman reagents in dynamic microfluidic arrays (Fluidigm BioMark). The replication cohort (Dr. Hector Michelena, Mayo Clinic) included 198 sporadic BAV cases with age and gender-matched controls. I quantitated genomic DNAs using PicoGreen and dispensed assay reagents using a custom-programmed liquid handling robot (Eppendorf EpMotion 5075). After appropriate quality controls and manual reclustering of the raw SNP data, I compared allele frequencies using chi-squared tests, assuming an additive genetic model.

Results: The minor allele frequencies (MAF) of all 12 candidate SNPs approximated reported values for European populations. The minor allele of one SNP in the ANKRD28 locus (rs924753, MAF = 0.4) was enriched in BAV cases (OR=1.4, 95% CI 1.0-1.8) with the same direction of effect as in the discovery cohort, but this difference narrowly missed statistical significance (p = 0.07).

Conclusion: In a follow-up of GWA peaks, I detected a promising replication signal in ANKRD28, a novel candidate gene for BAV. ANKRD28 encodes an aortic endothelial protein that interacts with CRK and CRKL, known mediators of left ventricular outflow tract and aortic valve development. ANKRD28 was also the most significant locus in our meta-analysis. Additional validation studies of independent BAV cohorts are in progress.

ABSTRACT

Trismus Dose-response Assessment using Quantitative Volumetric Measures in Head and Neck Radiotherapy

Benjamin W. Warren *The University of Texas at Houston Medical School* *Class of 2018*

Sponsored by: Clifton D. Fuller, MD, PhD, Department of Radiation Oncology, The University of Texas MD Anderson Cancer Center

Key Words: Trismus, intensity modulated radiotherapy, masseter, pterygoid

Objective: The objective of this study was to investigate a potential dose-toxicity relationship between radiation delivered to muscles of mastication and subsequent trismus development in patients receiving intensity modulated radiotherapy (IMRT) for oropharyngeal squamous cell carcinoma (OPSCC).

Methods: Retrospective data from 324 patients treated with IMRT for OPSCC at MD Anderson Cancer Center between 2004 and 2011 were analyzed via an IRB-approved protocol. For each patient, clinical data were extracted from electronic medical records, and incidences of trismus occurring after the onset of treatment were recorded using a binary variable. Regions of interest (ROIs), namely masseter (M), medial pterygoid (MP), and lateral pterygoid (LP) muscles, were segmented on planning CT images using an automatic segmentation algorithm and defined as ipsilateral (I) or contralateral (C) to the primary tumor. Radiation dose plans were then retrieved and dose volume histograms (DVHs) generated for ROIs. Dose-response assessment was performed using logistic regression and Wilcoxon rank-sum test with Bonferroni correction for multiple comparisons. Cumulative group DVHs were generated to visualize differences in continuous dose distributions between trismus and asymptomatic patient groups. Dose-threshold candidates were selected via a bootstrap forest technique.

Results: A total of 324 patients treated with IMRT were evaluated for trismus. For the purposes of exploratory statistics, mean dose to CMP, and maximum dose to CMP and ILP between trismus and asymptomatic groups were significantly different ($p<0.05$) using Wilcoxon rank-sum test but did not retain this significance after Bonferroni correction. Nevertheless, cumulative group DVHs dichotomized by the trismus variable allowed for visualization of differences between groups for each ROI across all doses. The top dose-threshold candidate determined by bootstrap forest was IM V_{59} (volume of the ipsilateral masseter receiving 59 Gy).

Conclusion: Trismus is a well-known sequela of radiotherapy treatment for head and neck cancers that negatively impacts quality of life and presents a problem to both patients and healthcare providers. However, certain dosimetric parameters are associated with increased probability of trismus, and thus, through further investigation and risk stratification, present potential opportunities to either modify dose to specific structures when possible or identify at-risk patients for early intervention.

ABSTRACT

Dynamically Changing Neuronal Networks in the Prefrontal Cortex

Ashley Webb *The University of Texas at Houston Medical School* *Class of 2018*

Sponsored by: Valentin Dragoi, PhD, Department of Neurobiology and Anatomy
Supported by: Valentin Dragoi, PhD, Department of Neurobiology and Anatomy; The University of Texas at Houston Medical School—Office of the Dean
Key Words: Prefrontal cortex

INTRODUCTION: In order to survive in a dynamically changing environment, we must be able to not only make decisions, but also be able to rapidly change our decisions when presented with new information**.** The dorsolateral prefrontal cortex plays a vital role in learning the rules of how to respond to different stimuli and executing these rules. Specific neurons respond preferentially to different portions of a given task in order to encode associations between stimuli and their corresponding motor response according to the learned rule. Together, these neurons form a complex network in the prefrontal cortex to allow us to make decisions and respond appropriately to different situations. The purpose of this experiment was to identify neurons firing preferentially when two conflicting stimuli are subsequently presented and the planned course of action must be changed. Analysis of these neurons can be used to determine how the network of neurons learns to represent a rule and how the network dynamically changes when the rule is switched.

METHODS: To study how the dorsolateral prefrontal cortex (dlPFC) learns to encode rules, we used multi-electrode arrays to record the activity of multiple dlPFC neurons while a monkey (*Macaca mulatta*) performed a simple association task. The task required the monkey to learn which of two saccade directions would result in a juice reward following presentation of two different visual stimuli (natural images presented on a computer screen). To study how the neuronal network dynamically changes between rules, a second set of experiments will be conducted, in which a small subset of trials ("oddball trials") will be randomly interweaved. In these oddball trials, two different stimuli will be subsequently presented, requiring the monkey to change the planned direction of the saccade. To analyze the completed recordings, we compared firing rates at different parts of the task ($P<0.05$, Wilcoxon rank-sum test). This comparison was used to classify cells according to the specific portion of the task to which they are encoding. Additional analysis of each session involved comparing early versus late trials in order to quantitatively observe the process of learning by measuring differences in firing rates across trials ($P<0.05$, Kruskal-Wallis test).

RESULTS: Analysis of the neuron firing rates of approximately thirty neurons indicated that 27% of cells were responding to the visual stimulus, 22% were responding during the delay period, and 51% were responding prior to saccade initiation. Analysis of the firing rate across trials showed that although firing rates for certain neurons changed over time, the nature of the

change, whether increased or decreased, was dependent on the individual neuron.

CONCLUSION: Neurons in the dlPFC work in synchrony to allow complex decision-making tasks to be performed and for responses to be quickly altered when new information is presented. Over time, these cortical networks dynamically change in order to adapt to new situations by changing individual neuron firing rates and responsiveness to different stimuli in order to best meet the needs of the organism in a constantly changing environment.

ABSTRACT

Determining Potency Factors Associated with Mesenchymal Stem Cells

Austin Wheeler *The University of Texas at Houston Medical School* *Class of 2018*

Sponsored by: Scott D. Olson, PhD, Department of Pediatric Surgery
Supported by: Scott D. Olson, PhD, Department of Pediatric Surgery
Key Words: Mesenchymal Stem Cells, TNF-α, IFN-γ, Anti-inflammatory

Background: Despite advances in clinical care, traumatic brain injury (TBI) remains the leading cause of death and disability in patients from 0 to 44 years of age. The increasing role of neuroinflammation as a major secondary injury following TBI has encouraged the use of mesenchymal stem cells (MSCs). MSCs have the ability to suppress the activation and proliferation of T lymphocytes and macrophages. However, the precise mechanisms governing MSC-immune cells interactions remain largely elusive. It is known that MSCs can be activated in response to environmental cues, including pro-inflammatory cytokines, toll-like receptor agonists and hypoxia. Often in response to these cues, MSCs secrete immunomodulatory factors, including TSG-6, PGE2, and IDO. In this study, we hypothesize that MSC pre-conditioning with particular cues increases their ability to suppress immune cell activation in vitro, and that the specific expression of PGE2, IDO and TSG-6 functions as indexes that will determine the potency and efficacy of isolated MSCs.
Methods: Frozen MSCs from donor bone marrow (BM) and amniotic fluid (AF) were allowed to recover for 3 days in culture media. Cells were then lifted and exposed to a variety of preconditioning protocols, which included the addition of inflammatory mediators such as lipopolysaccharide (LPS), POLY I:C, TNF-α, IFN-γ, TNF-α+IFN-γ, different osmolarities, and hypoxia. MSCs were exposed to these conditions for either 24 h or 1 h. Following pre-conditioning, MSCs were plated in a 96 well plate and rat splenocytes were added at a 20:1 ratio (splenocytes:MSC). To determine the effects of pre-conditioning on the immunomodulatory potential of MSCs, LPS or Concanavalin A (ConA) were added to the MSC/splenocyte co-culture to activate the macrophages, B cells, and dendritic cells (LPS) or the T cells (ConA). Culture supernatant was collected 24 h after LPS and 48 h after ConA treatment and samples analyzed utilizing TNF-α and IFN-γ ELISA kits following manufacturer's protocol. Finally, we determined expression of three different genes: COX, IDO, and TSG-6 in MSCs pre-conditioned for 24h using Real-Time PCR.
Results: Previous results from the Olson lab have shown that BM-MSCs are superior immunomodulators when compared to AF-MSC both in vitro and in vivo. In this study, despite instigating significant changes in gene expression of COX-2 and IDO, pre-conditioning of BM-MSC had marginal effects in the ability of these cells to inhibit inflammatory responses in vitro. However, pre-conditioning of AF-MSC with Poly I:C, TNF-α and a hyperosmolar media significantly improves the anti-inflammatory activity of AF-MSCs.
Conclusions: MSC pre-conditioning approaches can improve the anti-inflammatory properties of AF-MSCs. This improvement could be applicable not only for TBI treatment, but also for a myriad of conditions in which a strong inflammatory response plays a significant role.

ABSTRACT

Investigation of Platelet Function Defects in Patients Presenting for Liver Transplantation and Patients with Cirrhosis

Joanna Wu *The University of Texas at Houston Medical School* *Class of 2018*

Sponsored by: Evan G. Pivalizza, MD, Department of Anesthesiology
Supported by: Evan G. Pivalizza, MD, Department of Anesthesiology; The University of Texas at Houston Medical School – Office of Educational Programs
Key Words: TEG, thrombeloastograph, platelet mapping, cirrhosis

Patients with cirrhosis and end-stage liver disease have multiple potential defects in coagulation and hemostasis, including thrombocytopenia, dysfibrinogenemia, accelerated fibrinolysis, and platelet dysfunction. This puts them at risk for increased bleeding during procedures or surgery. For such patients, overall balance of coagulation, with appreciation for potential risks of increased thrombosis, is crucial. One tool for global assessment of thrombin formation is the thrombelastograph (TEG). In addition, there is a recent FDA-approved modification to the TEG, Platelet Mapping (PM), which was originally designed as a method to evaluate for the effects of antiplatelet agents (aspirin and clopidogrel) by arachidonic acid and ADP agonists respectively. The TEG is often used during surgery for patients with liver disease, but this project aimed to investigate TEG-PM analysis in liver transplant (LT) patients and patients with cirrhosis who are presenting for surgical procedures or liver associated procedures. About 10 ml of blood was taken from each patient from an existing intravenous line whenever possible, or from a single need stick. Standard TEG parameters were measured, including 1) R time (min- time from start to a set point of fibrin formation), 2) K time (min- clot strengthening), 3) angle (degrees- clot strengthening), 4) MA maximum amplitude (mm- clot strength, reflecting platelet function), and 5) G (dynes/sec- shear strength derived from MA with significant platelet contribution). Platelet mapping was performed with three additional samples: heparinized sample with activator, heparinized sample + activator and ADP agonist, and heparinized sample + activator and arachidonic acid (AA) agonist. 15 patients were enrolled in the study – 6 were undergoing liver transplants, 7 ERCPs, and 2 surgical procedures. Liver function tests (AST, ALT, ALP, and total bilirubin) were all outside normal ranges, and platelet count was low (118.1 ± 79.2). TEG parameters were all within normal ranges. However, platelet mapping results showed that platelet inhibition to both AA (70.6 ± 18.9%) and ADP (64.1 ± 14.1%) were above 50%. Although PM was designed to measure response to anti-platelet agents, the data suggested that platelet dysfunction might be underappreciated in patients with pre-existing thrombocytopenia. Platelet inhibition was observed in patients with end stage liver disease despite the discontinuation of antiplatelet agents. This data suggests that PM analysis may be a useful tool to detect platelet dysfunction in patients with liver disease who already have significant other risk factors for coagulopathy.

ABSTRACT

Role of SIK1 on Insulin Resistance in Skeletal Muscle

Albert Xiao *The University of Texas at Houston Medical School* *Class of 2018*

Sponsored by: Rebecca Berdeaux, PhD, Department of Integrative Biology and Pharmacology
Supported by: National Institute of Diabetes and Digestive and Kidney Diseases, 2T35DK007676-22; and R01-DK092590
Key Words: Glucose Transport, Diabetes, Insulin Resistance

Background: Type 2 diabetes mellitus is a major epidemic that is characterized by insulin resistance. The attenuated insulin response can be due to decreased insulin production and secretion, decreased downstream insulin signaling, or a combination of the two. Because there are multiple mechanisms involved in the etiology of this disease, developing new treatments for diabetes is complex. SIK1, salt inducible kinase 1, is a protein kinase that can regulate certain metabolic transcription factors such as CRTCs, CREB regulated transcription coactivators. CREB/CRTCs have been shown to improve insulin sensitivity in liver by inducing expression of proteins involved in insulin signaling. The Berdeaux lab previously demonstrated that mice lacking the *Sik1* gene specifically in skeletal muscle (SIK1-MKO) are more glucose tolerant than wild type controls after high fat diet feeding. The aim of this project is to determine the molecular mechanism of increased glucose tolerance observed in SIK1-MKO mice. We hypothesize that SIK1 conditional knock out mice have increased glucose tolerance due to activation of downstream insulin signaling pathways that ultimately increase GLUT4 translocation. This mechanism could involve increased CRTC/CREB activation.
Methods: To identify the mechanism by which SIK1 promotes insulin resistance in obesity, muscle tissues from wild type and SIK1-MKO mice were isolated and protein amounts and relative gel mobility (reflecting activation) of CRTC1, CRTC2, and CRTC3 were examined by Western blot and normalized with HSP90 loading control. Phosphoinositide 3-Kinase (PI3K) activity was also measured using competitive kinase ELISA. Glycogen assays were performed to determine whether obese SIK1-MKO mice have increased glucose storage. Literature review revealed additional proteins involved in insulin signaling that could potentially be phosphorylated by SIK1.
Results: There were no statistically significant changes in CRTC levels or phosphorylation based on western blotting. Preliminary results indicated that PI3K activity might be elevated in insulin-stimulated SIK1-knockout muscle cells, but the protocol requires optimization in muscle tissue. Further testing is planned to increase sample size. There was no significant difference in glycogen storage in obese *ad libitum* fed SIK1-MKO mice, indicating that the extra glucose taken up is likely oxidized rather than stored as glycogen.
Conclusion: The data show that SIK1 MKO mice exhibit higher glucose tolerance when rendered obese due to high fat diet feeding. The search for the mechanism of how SIK1 increases glucose intolerance is still under study. The *in vivo* data indicate that SIK1 could be a potential new drug target for treatment of insulin resistance and diabetes.

ABSTRACT

Reference Values for Rapid Thrombelastography for Injured Pediatric and Adult Patients

Rayce Yanney *The University of Texas at Houston Medical School* *Class of 2018*

Sponsored by: Bryan A. Cotton, MD, MPH, Department of Surgery (CeTIR)
Supported by: Bryan A. Cotton, MD, MPH, Department of Surgery (CeTIR)
Key Words: Trauma, injury, coagulation, thromboelastography

Introduction: Rapid thrombelastography (rTEG) is a whole blood assay that evaluates properties of clot formation. Its application to the injured and critically ill patient has expanded greatly among US civilian trauma centers in recent years. However, reference values for these patients have come primarily from small validation studies and/or healthy volunteers. Given the experience here at UTH with critical values that often fall within the manufacturer's "normal" reference range, we set out with a purpose to identify and evaluate rTEG reference values for critically injured children and adults at our trauma center.

Methods: Following IRB approval, we performed a retrospective study in which we identified all trauma admissions that met highest-level trauma activation criteria between 07/2009 and 04/2015. After excluding those patients that received blood products in the first 4 hours, had a severe brain injury (head AIS>3), were on known anti-coagulants or died from hemorrhage or head injury, we obtained 90% reference ranges for the individual components of the rTEG assay. These included the activated clotting time (ACT), r-value, split point, k-time, α-angle, maximum amplitude, and percent fibrinolysis after 30 minutes (Ly30). We performed this analysis on both adults (>17 years of age) and children (0-17 years of age). Analyses were repeated on mechanism, gender and race differences.

Results: Of the 8472 patients with admission rTEG values, 4302 patients met study criteria. 3681 were adults and 621 were children or adolescents. The median age for adults was 37 (IQR 25, 53), 75% were male and 50% were white. Of these, 73% were blunt and had a median ISS of 14 (IQR 4, 25). Ranges for initial r-TEG values are listed in the TABLE below. The median age for children was 14 (IQR 6, 16), 65% were male and 36% were white. Of these, 72% were blunt and had a median ISS of 14 (IQR 5, 25). Pediatric ranges for initial r-TEG values are listed in the TABLE below as well. There were no significant differences among mechanisms, gender, or race.

Conclusion: We present the first description of references ranges for injured adults and children among those patients who are not actively bleeding or coagulopathic on arrival. Very small differences exist between adults and children with respect to their reference values in injured patients.

TABLE

	5th tile	10th tile	25th tile	50th tile	75th tile	90th tile	95th tile
ADULT REFERENCE RANGES							
ACT, sec	85	97	105	113	121	128	136
r-value, min	0.4	0.5	0.6	0.7	0.8	0.8	0.9
Split point, min	0.3	0.4	0.5	0.6	0.7	0.8	0.8
k-time, min	0.8	0.8	1.1	1.3	1.8	2.1	2.2
α-angle, degrees	63	66	70	74	76	77	79
mA, mm	53	56	60	64	68	70	72
G-value, dynes/sec	5.6	6.3	7.5	8.9	10.7	11.3	12.6
LY-30, %	0.0	0.0	0.3	1.2	2.5	3.3	4.2
PEDIATRIC/ADOLSCENT REFERENCE RANGES							
ACT, sec	89	97	105	113	121	128	136
r-value, min	0.4	0.5	0.6	0.7	0.8	0.8	0.9
Split point, min	0.3	0.4	0.5	0.6	0.7	0.8	0.8
k-time, min	0.8	0.8	1.1	1.3	1.6	1.8	2.2
α-angle, degrees	65	68	71	74	77	79	80
mA, mm	55	57	60	64	68	70	72
G-value, dynes/sec	6.1	6.3	7.6	8.9	10.7	11.3	12.6
LY-30, %	0.0	0.2	0.9	2.1	2.6	3.4	5.0

ABSTRACT

Studies of Lymphangiogenesis on Tumor Progression in PDPN-tk Mice

Chen Yao *The University of Texas at Houston Medical School* *Class of 2018*

Sponsored by: Raghu Kalluri, MD, PhD; Department of Cancer Biology, MDACC
Supported by: National Institute of Diabetes and Digestive and Kidney Diseases, 2T35DK007676-22
Key Words: Lymphangiogenesis, metastasis

The lymphatic system is an essential regulator of body fluid homeostasis, immunocyte trafficking, and immunological surveillance. Lymphangiogenesis, the formation of new lymphatic vessels, has been widely studied in the context of solid tumors for its relationship with tumor metastasis. Lymphatic vessels, composed of thin-layer endothelium that lack adequate basement membrane or pericyte coverage, are thought to provide an accessible route for tumor dissemination to lymph nodes and/or distant organs. However, multiple key questions in this field still remain to be further elucidated, such as whether tumor lymphangiogenesis-related metastasis is induced by pre-existing lymphatic vessels and/or newly-formed ones and whether intratumoral lymphatic vessels are functional. Through these studies, we can then better target tumor lymphangiogenesis as a promising therapeutic strategy. Our study aimed at examining the specific role of lymphangiogenesis, apart from angiogenesis, by ablating proliferating podoplanin (PDPN)-positive lymphatic endothelial cells. For this study, our lab had previously generated novel transgenic mice that express the HSV thymidine kinase (tk) under control of the PDPN-promoter (PDPN-tk mice), a lymphatic marker. Upon ganciclovir (GCV) treatment, the PDPN-positive cells were irreversibly arrested in DNA replication, resulting in the selective ablation of proliferating PDPN-positive cells. Our previous results have demonstrated that, upon GCV treatment, PDPN-tk system can efficiently ablate the proliferating PDPN-positive lymphatic endothelial cells (in vitro assays) and lymphatic vessels (in vivo assays). In the context of orthotopic 4T1 breast cancer, our current results show that PDPN-tk mice, as compared with WT mice, exhibited significantly decreased lung metastasis (56% decrease), whereas the growth of primary tumor was not altered. Through the utilization of the new transgenic mouse model to specifically deplete the proliferating lymphatic endothelial cells, our results validate the notion that lymphangiogenesis is indeed correlated with tumor metastasis, although its influence on tumor growth is not as significant.

ABSTRACT

Viabahn Stents for the Treatment of Femoral Popliteal Peripheral Arterial Disease

Laila Yazdani *The University of Texas at Houston Medical School* *Class of 2018*

Sponsored by: Ali Azizzadeh, MD, Department of Cardiothoracic and Vascular Surgery

Supported by: Ali Azizzadeh, MD, Department of Cardiothoracic and Vascular Surgery; The University of Texas at Houston Medical School – Office of Educational Programs

Key Words: Viabahn stents and femoral popliteal disease

Objectives: Endovascular interventions for treatment of occlusive disease of the superficial femoral artery (SFA) have been in evolution. The use of self-expanding covered stents has grown, and today, many interventionists favor an "endovascular first" approach to long-segment SFA stenosis or occlusion. We specifically evaluated the use of Viabahn stents for de novo treatment of femoropopliteal stenosis and occlusion.

Methods: All patients treated with Viabahn stents in the SFA, between January 2006 and June 2015, were included in the study. Rutherford category, pre- and post-operative ankle-brachial indices, and follow-up duplex ultrasound scans at 1, 6, 12, 24, and 36 months were retrospectively analyzed. Primary end points of the study included 3-year primary, primary-assisted, and secondary patency rates, postoperative ABI, and amputation-free survival.

Results: A total of 64 SFAs in 55 patients were treated with Viabahn stents during the study period. Approximately one-half were male (N = 34, 53%). The mean age was 64 years (range, 13-96). The indication for treatment was severe claudication (Rutherford category 3) in 56%, ischemic rest pain (category 4) in 19%, non-healing ulcers (category 5) in 14%, and major tissue loss (category 6) in 11%. The mean lesion length was 18.3cm (range, 2.5 to 45cm), and 64% were classified TransAtlantic Inter-Society Consensus (TASC) II types C and D. Technical success was 92.2%. In 58% of cases one stent was deployed; 36% had 2 stents, and 6% had 3 stents. The mean pre- and post-operative ABI was 0.7 and 0.8, respectively. The median follow-up was 3.5 months (range, 0.03-61.1). The 3-year primary, primary-assisted, and secondary patency rates were 20%, 46%, and 53%, respectively. The overall 3-year amputation-free survival was 23%.

Conclusions: Viabahn stents for de novo treatment of femoropoliteal stenosis and occlusion, particularly TASC II types C and D, demonstrate acceptable short-term outcomes, with high technical success and comparable patency rates to open surgical revascularization.

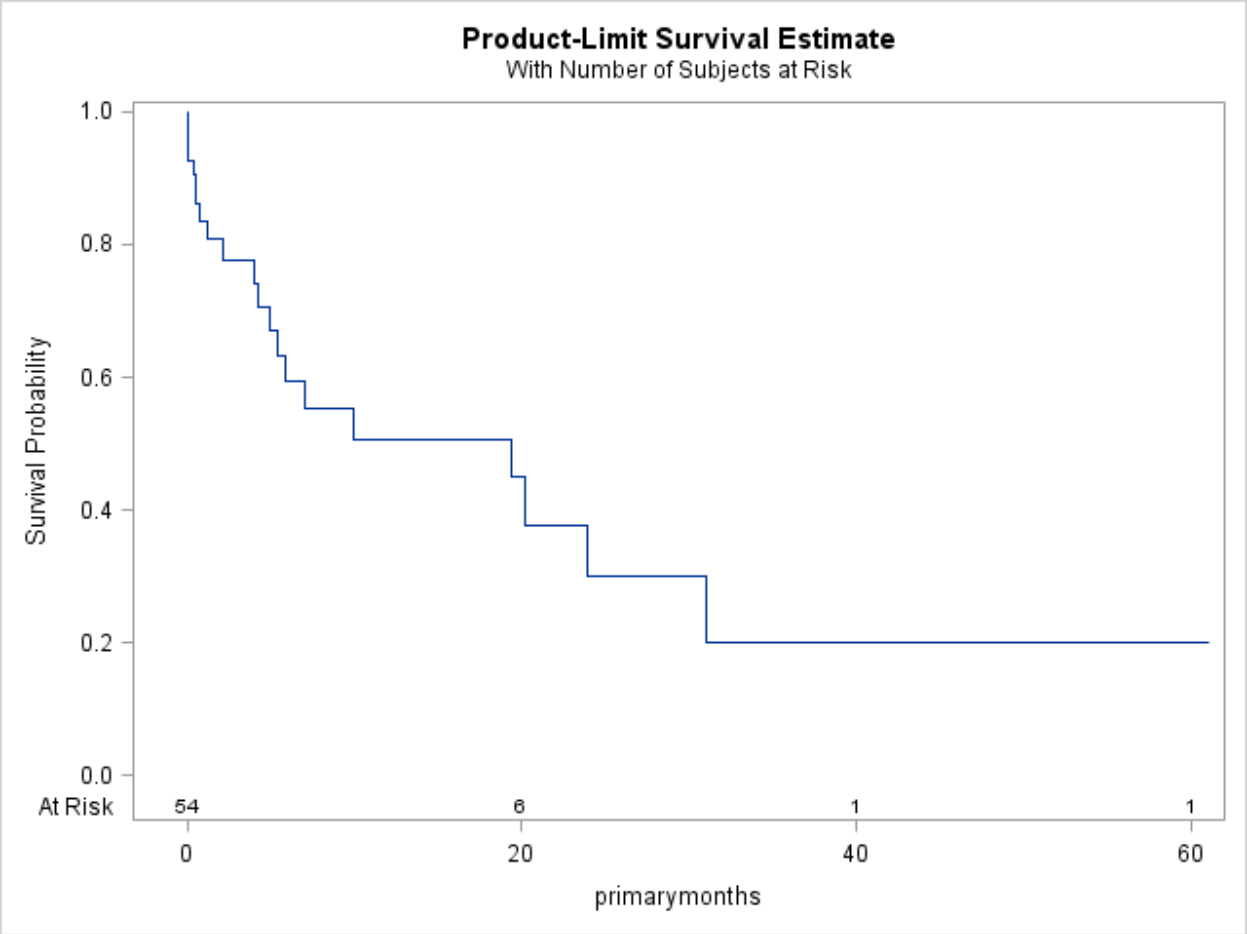
Product-Limit Survival Estimate
With Number of Subjects at Risk
Survival Probability
1.0
0.8
0.6
0.4
0.2
0.0
At Risk
54
6
1
1
0
20
40
60
primarymonths

ABSTRACT

Quantitative Analysis of an in vitro Model of Implant-associated Osteomyelitis in Diabetic Patients

Joshua Zuniga *The University of Texas at Houston Medical School* *Class of 2018*

Sponsored by: Heidi B. Kaplan, PhD, Department of Microbiology and Molecular Genetics; Catherine G. Ambrose, PhD, Department of Orthopaedic Surgery

Supported by: National Institute of Diabetes and Digestive and Kidney Diseases, 2T35DK007676-22

Key Words: Biofilm, *Staphylococcus aureus*, diabetes, osteomyelitis

Implant-associated osteomyelitis biofilm-infections among the 29.1 million diabetic Americans are a growing concern as these patients are among the large number of individuals undergoing orthopedic surgery and they are at high risk for more negative outcomes due to higher infection rates. Biofilm infections pose significant risks to patients as they are quite resistant to antibiotics and often necessitate additional surgeries which can result in increased morbidity and mortality, and create excess healthcare costs, with one estimate at $50,000 per patient and $250 million nationwide. An *in vitro* biofilm model developed previously in the Kaplan laboratory was adapted to mimic conditions of osteomyelitis due to *Staphylococcus aureus* or *S. epidermidis* in diabetic patients by modulating glucose levels in synthetic synovial fluid (SSF) medium with the intent of determining if biofilms display increased growth in cases of increased hyperglycemia. Ethylene oxide sterilized poly-methyl methacrylate (PMMA, bone cement) discs representing orthopedic materials used in arthroplasty procedures were placed in the bottom of a 24-well plate and statically incubated at 4℃ in carbonate buffer containing 20% fetal bovine serum (FBS) for a period of 24 hours. Following this period, carbonate buffer was removed by pipet and wells were inoculated with 10^6 cells in SSF containing 95 mg/dL, 135 mg/dL, or 175 mg/dL glucose and statically incubated at 37℃. Every 24 hours, SSF was removed by pipet and replaced with sterile SSF to provide new growth media. At intervals of 72, 120, and 168 hours, half of the experimental discs were stained with a BAClight live/dead stain and imaged via fluorescence microscopy, while the remaining discs were used to quantitate the number of cells attached to PMMA per cm^2 via DNA isolation and subsequent qRT-PCR using SYBR green dye. qRT-PCR data for *S. aureus* indicate that there is a trend towards more growth in 175 mg/dL glucose compared to 95 mg/dL glucose at 72 hours incubation but there were no significant differences between biofilms incubated in differential glucose media at 72 or 120 hours. Fluorescence microscopy images indicate that for both *S. aureus* and *S. epidermidis*, there are small microcolonies of cells attached to PMMA at 72 hours incubation, and at 120 hours these microcolonies coalesce to form a uniform lawn of cells. *S. epidermidis* appears to form a more complete lawn of cells by 120 hours than does *S. aureus*, but with more dead cells present than *S. aureus*. These preliminary data indicate that decreased control of a patient's blood glucose levels may facilitate increased attachment of cells to orthopedic implants. Further study will be required to elucidate whether control of glycemia has a significant effect on biofilm growth.

UTHealth™ | Medical School

The University of Texas
Health Science Center at Houston

Undergraduate Students

ABSTRACT

Alexander Alexander *Rice University* *Class of 20*

Sponsored by: Pamela Wenzel, PhD, Department of Pediatric Surgery
Supported by: Pamela Wenzel, PhD, Department of Pediatric Surgery
Key Words:

Excessive inflammation can cause or exacerbate multiple types of diseases and injuries, including traumatic brain injury (TBI). Mesenchymal stromal cells (MSCs) can display immunoregulatory functions to combat this inflammation by releasing cytokines that signal macrophages and other immune cells such as microglia in the brain to convert to anti-inflammatory phenotypes. To exert these effects, MSCs must first be activated, or licensed. Wall shear stress (WSS) have recently been shown to be an effective method of licensing MSCs to display an anti-inflammatory phenotype. In this study, we attempted to demonstrate the immunoregulatory effect of sheared MSCs *in vivo* in a rat controlled cortical impact (CCI) model. Sprague Dawley rats were split into sham, CCI, and cell therapy groups. CCI and cell therapy rats were injured, then 24 hours later received tail vein injections of either PBS vehicle (CCI condition), MSCs that were not sheared (static condition), or sheared MSCs (WSS condition). 24 hours later, the rats' brains were collected, fixed, frozen, and sectioned. The brain sections were stained using immunohistochemistry for Iba1, a marker for microglia. Amoeboid (pro-inflammatory) and ramified (anti-inflammatory) microglia in the CA1 region of the hippocampus were counted. Significantly less amoeboid microglia were found in the cell therapy animals than in the CCI control, suggesting that MSCs had an anti-inflammatory effect. Significantly more ramified microglia were found in the WSS animals than in the sham rats, but not as much as in the CCI animals. We proceeded to use immunofluorescence staining to determine whether these additional ramified microglia in the CCI animals were apoptotic. We stained using anti-Iba1 and anti-cleaved caspase 3 (an apoptosis marker). Preliminary results shows more non-apoptotic ramified microglia in the WSS animals, suggesting that shear stress is an effective method in pre-licensing MSCs. Future work will involve corroborating cell count obtained from IF staining and staining for neurogenesis markers and additional types of immune cells.

ABSTRACT

Role of LiaX in a Daptomycin Resistant *E. faecium*

Ebore Awano *Rice University* *Class of 2017*

Sponsored by: Cesar A. Arias, PhD, Department of Biochemistry and Molecular Biology
Supported by: The University of Texas MD Anderson Cancer Center and The University of Texas Health Science Center at Houston (UTHealth) Graduate School of Biomedical Sciences
Key Words: Daptomycin, E. *faecium*, LiaX, LiaXYZ, LiaFSR

Background: The emergence of drug resistance, including the lipopeptide antibiotic daptomycin, has made the treatment of enteroccocal infections a pressing global health issue. Previous studies have shown that the LiaFSR gene system functions to organize the cells response to cell membrane stress in E. *faecal*is. The *liaR* gene activates the *liaXYZ* operon in response to cationic antimicrobial peptides. In E. *faecalis*, an adaptive mutation of the *liaX* gene is associated with increased resistance to daptomycin [1]. The LiaXYZ system is not well studied in E. *faecium*. By observing the phenotype of *liaX* deletion we can gain a better understanding of this genes function in E. *faecium*.
Methodology: In order to develop the *liaX* deletion mutant, the upstream (700 bp) and downstream fragments (700 bp) of the *liaX* gene were amplified by crossover PCR strategy and cloned into the pHOU1 plasmid. The pHOU1 plasmid was introduced into *E. coli* EC1000 cells by transformation. The pHOU1 plasmid contains the *pheS* gene which has a high affinity for p-Cl-Phenylalanyl which is toxic to enterococcus cells.[2] This allows for negative selection. The pHOU1 plasmid also contains an *aph2*-ID gene which confers resistance to gentamycin allowing for positive selection. The recombinant plasmid was extracted from E. *coli* EC1000 cells and introduced into E. *faecalis* CK111 cells by electroporation. Subsequently, the recombinant plasmid will be introduced into E. *faecium* R497 by filter mating with E. *faecalis* CK111 as the donor. The E. *faecium* R497 cells will be screened by PCR and the mutated region will be sequenced to confirm the deletion.
Results: We have successfully cloned-the upstream and downstream regions of the *liaX* gene into pHOU1 plasmid and transformed this plasmid into E. *coli* EC1000 competent cells. The insert was confirmed by sequencing. The plasmid was successfully electroporated into E. *faecalis* CK111 cells.
Conclusions: We are currently carrying out the recombination process.

1) Milya Davlieava, Yiwen Shi, Paul G. Leonard et al: **A variable DNA recognition site organization establishes the LiaR-mediated cell envelope stress response of enterococci to daptomycin.** Oxford Medical Journal 2015, 4758-4773
2) Diana Panesso, Maria C Montealegre, Sandra Rincon et. al:**The *hyl*$_{Efm}$ gene in pHyl$_{Efm}$ of Enterococcus faecium is not required in pathogenesis of murine peritonitis.** BMC Microbiology 2011,1171-2180

ABSTRACT

Expression of Cancer Stem Cell Markers in OSCC Cells

Kelvin Barahona *University of Houston - Downtown* *Class of 2016*

Sponsored by: Kalu U. E. Ogbureke, BDS, MSc, DMSc, JD, FRCPath, Diagnostic & Biomedical Sciences

Supported by: UTHealth School of Dentistry, Department of Diagnostic and Biomedical Sciences; UT School of Dentistry at Houston Research Office

Key Words: Oral Squamous Carcinoma, Cancer Stem Cells, DSPP, MMP20, Cisplatin

Background: Oral cancer represents about 3% of all cancers worldwide. Oral squamous cell carcinoma (OSCC) accounts for over 90% of oral cancers. Surgery remains the mainstay of treatment for OSCC patients because of the lack of effective chemotherapeutic regimens that may either complement surgery, or act solely to eliminate oral cancer cells. While minimal success is achieved with some chemotherapeutic agents, overall long-term effects in achieving cure/recurrence-free status have been disappointing. This is because, while chemotherapy may effectively target established OSCC cell, they have minimal anti-cancer effect on oral cancer stem cells (OCSCs). Our recent findings show that dentin sialophosphoprotein (DSPP) and matrix metalloproteinase (MMP) 20 silencing abrogate several phenotypic hallmarks of oral cancer cells. The objective of this study therefore was to determine the effects of DSPP-MMP20 gene silencing on OCSCs in the OSCC cell line, OSC2, as well as the effect of silencing on OCSC sensitivity to cisplatin treatment.

Methods: Proportions of OCSCs in the OSCC cell line, OSC2, and DSPP/MMP20-silenced OSC2 cells were analyzed by western blot (WB) and flow cytometry by assaying the following well-established OCSC marker: ATP-binding Cassette half transporter protein (ABCG2); Aldehyde dehydrogenase 1 (ALDH1); Prominin 2(CD133); CD44; BMi-1; LGR4; Met; and Podoplanin. WB was performed on whole cell extracts with appropriate positive and negative controls. The effect of DSPP-MMP20 silencing on the sensitivity of OCSCs to cisplatin was determined by WB and flow cytometry. For flow cytometry analysis, fluorescence emission from 10,000 cells was measured with a FACS Calibur (Becton Dickinson, San Jose, CA) using Cell Quest Software.

Results: There was a 5-fold reduction in DSPP-MMP20-silenced OSC2 cells expressing ABCG2, 2-fold reduction in cells expressing ALDH1, 3-fold reduction in cells expressing CD133, 2-fold reduction in CD44-expressing cells, one-fold reduction in BMi-1-expressing cells, 3-fold reduction in cells expressing LGR4, 2-fold reduction in cells expressing Met, and 1.6-fold reduction in podoplanin-expressing cells, compared to levels in parent and scrambled OSC2 cells. Furthermore, WB and flow cytometry analyses showed a 5-8 fold increased sensitivity of OCSCs to cisplastin at an optimal dose of 10μM in DSPP-MMP20-silenced OSC2 cells compared to parent and scrambled OSCC controls within 72hrs.

Conclusion: OCSC population in OSCC is significantly reduced following DSPP-MMP20 silencing in OSC2 cells. There is a significant increase in the sensitivity of OCSC in DSPP-MMP20-silenced OSCC cells to cisplatin. MMP-20-DSPP silencing in OSCC cells may reduce OCSC population, while increasing overall sensitivity to chemotherapeutic agents such as cisplatin.

ABSTRACT

Development of a Novel Translocation Assay to Monitor Substrate Delivery to the Donor Cell Periplasm

Kylie S. Borden *Southwestern University* *Class of 2017*

Sponsored by: Peter J. Christie, PhD, Department of Microbiology and Molecular Genetics

Supported by: The University of Texas MD Anderson Cancer Center and The University of Texas Health Science Center at Houston (UTHealth) Graduate School of Biomedical Sciences

Key Words: Type IV secretion; Conjugation; Translocation

Type IV secretion systems (T4SSs) function to deliver protein and DNA substrates to other cells. These machines increase genetic variability among bacterial species and are also responsible for disseminating antibiotic resistance and virulence traits to other bacteria, and delivering virulence effector proteins to eukaryotic host cells. The archetypal Gram-negative T4SS is that of *Agrobacterium tumefaciens* which is comprised of 12 proteins, VirB1-VirB11, and the VirD4 substrate recruitment protein. A phylogenetically related T4SS encoded by *Escherichia coli* plasmid pKM101 is comprised of Tra homologs of the 11 VirB subunits and the VirD4-like TraJ substrate receptor. In Gram-negative bacteria, T4SSs must deliver the substrates across the inner and outer membranes. While the proteins that span both membranes have been identified, the exact route of translocation is unclear. By using a chimeric T4SS to deliver effector proteins that are active only in the periplasm, we developed an assay to monitor substrate delivery specifically across the inner membrane to the periplasm of donor cells. We created the system by using three components: i) a chimeric substrate recruitment protein made by fusing the soluble domain of a VirD4 homolog from *Xanthomonas* and the transmembrane domain of *E. coli* pKM101 TraJ, ii) cell wall hydrolases fused to a translocation signal carried by *Xanthomonas* effectors, and iii) the pKM101 T4SS lacking TraJ. Using this combination of T4SS components, we detected substrate transfer to the periplasm as monitored by toxic effects on cell growth and morphological aberrations consistent with cell wall degradation. This assay will now be used to define the minimal subunit and energetic requirements for transporting substrates across the inner membrane via a T4SS.

ABSTRACT

Socioeconomic Factors Predict Walk-in Clinic and Primary Care Provider Locations

Alissa Chen *Class of 2015*

Sponsored by: Frances Lee Revere, PhD, MHA, School of Public Health
Supported by: The University of Texas at Houston Medical School – Office of the Dean
Key Words: Primary care physicians, walk-in clinics, urgent care clinics, retail clinics

Background: The United States overall has a lack in primary care physicians (PCPs), and those who are of lower income and are minorities are more likely to lack access to a primary care physician (Huang & Finegold, 2013). Meanwhile, alternative pathways to primary care, like walk-in clinics, have become available. Walk-in clinics have been found to be a less expensive alternative than visiting the emergency room, which often occurs when a patient does not have access to primary care (Mehrotra et al., 2009). It could be a possible avenue to decrease the gap in primary care for those of lower socioeconomic status.

Objective: To assess the relationship between the availability of walk-in clinics and the supply of PCPs and the impact of race and economic factors on said availability.

Methods: Using data from the Census Bureau's American Fact Finder, each zip code in Harris County was profiled on economic factors and race factors. A database of walk-in clinics was made using Google Maps, the Urgent Care Association of America's database, and urgentcarelocations.com. The list of PCPs in Harris County was found using the database from the Texas Medical Board, and the ratio of PCPs per 10,000 in each zip code was calculated. Linear regressions were used to explain the variation of the PCPs per 10,000 with economic and race factors. Logistic regressions were used to determine walk-in clinic presence varied with economic and race factors. A T-test was used to determine if zip codes with walk-in clinics had different ratios of PCPs per 10,000 than zip codes without walk-in clinics.

Key Findings: The most predictive economic factor for the ratio of PCPs per 10,000 and walk-in clinic presence was percent of the population on Medicaid (p-value < 0.001, $r^2 = 0.11$; p-value < 0.001 , pseudo $r^2 = 0.10$). The most predictive race factor for the ratio of PCPs per 10,000 ratio was percent Hispanic (p-value = 0.0005, $r^2 = 0.09$), and the most predictive race factor for walk-in clinic presence was percent African American (p-value < 0.001 , pseudo $r^2 = 0.06$). Zip codes with walk-in clinics had a higher concentration of PCPs (p-value = 0.001).

Conclusions: These results suggest that walk-in clinics are placed in similar locations as PCPs, so they may be in competition with PCPs. Though the Affordable Care Act has increased insurance coverage for those of low income, PCPs and walk-in clinics are less likely to be located in areas with low socioeconomic status.

ABSTRACT

From Pre-Clinical Development of Wharton's Jelly-based Autologous Tissue Engineering Applications to Clinical Grade cGMP-compliant Manufacturing: A Translational Research Experience

Matteo Costantini *Rice University* *Class of 2017*

Sponsored by: Fabio Triolo, DdR, MPhil, PhD, Department of Pediatric Surgery
Supported by: Fabio Triolo, DdR, MPhil, PhD, Department of Pediatric Surgery; The University of Texas at Houston Medical School – Office of the Dean
Key Words: Wharton's Jelly, Cleft Palate, cGMP

The objective of my experience in Dr. Triolo's cellular therapy core laboratories was to be exposed to multiple phases of the translational research cycle within the field of regenerative medicine. In particular, my activities were focused on the preclinical development of an innovative tissue-engineering of cell-based products for clinical applications of regenerative medicine.

At a pre-clinical level, I was involved in a project aimed at investigating the potential use of native Wharton's jelly (WJ) in repair of primary cleft lip and palate (CLP), which represent nearly 1/3 of all birth defects. The underlying rationale of the project is that autologous bone grafts are the gold standard treatment, but are invasive and have potentially serious complications that lead to the need of additional surgeries. Another strategy based on using biomaterials seeded with bone marrow (BM) stem cells has proven promising, but BM harvest is too invasive to use in CLP repair in newborns, thus alternative strategies are needed. WJ, the connective tissue matrix of the umbilical cord, is a gelatinous substance comprised of proteoglycans and various isoforms of collagen and is rich in perinatal stem cells. It is a natural "tissue engineering" construct that provides a scaffold derived from the recipient's own molecules, naturally seeded with the recipient's own stem cells, and is thus immunologically inert. Since WJ is typically discarded as post-delivery medical waste, its use does not pose ethical concerns and its harvest is completely non-invasive. Our hypothesis is that inclusion of WJ in the alveolar pocket of CLP patients at the time of palate repair will enhance bone growth and accelerate healing, proving to be an ideal adjunct to orofacial cleft repair. I participated in investigating the use of native WJ in the repair of CLP in a critical-size alveolar bone defect model in the rat.

At a clinical level, I was trained in cellular therapy manufacturing in compliance with current Good Manufacturing Practice (cGMP) guidelines of the FDA. Following the theoretical portion of the training, I participated in the processing of human bone marrow to prepare

enriched fractions of BM-derived mononuclear cells within a Phase II clinical study aimed at evaluating whether bone marrow-derived cells preserve injured brain tissue after traumatic injury in children, and if so, whether such preservation is associated with improvement in functional and cognitive outcomes. In addition, I also participated in the preparation of placebo within a randomized, blinded, placebo-controlled, cross-over Phase II clinical study designed to compare the effects of autologous bone marrow-derived versus autologous umbilical cord blood-derived mononuclear cells on pediatric patients with cerebral palsy. My training in cGMP processing was aimed at integrating quality assurance (QA) and quality control (QC) in my current education in order to fill the gap between fundamental science and clinical insight. This is not a trivial aspect, as most academic centers, in fact, have excellent stem cell research laboratories and are able to offer specialized services for a part of the translational research phase but are, however, unable to bring a cell therapy and/or tissue engineering product - with all scientific, pharmaceutical, technical and regulatory documents and data - to the registration phase. The reason is that they do not have the knowledge on product development, regulations, quality control and assurance, as well as specialized personnel able to manage all aspects for the development of current (cell therapy, tissue engineering products) and new biologics.

ABSTRACT

Effects of AHCC (Active Hexose Correlated Compound) on Inflammation-Induced Oxidative Stress in Rats

Sundar Devakottai *Rensselaer Polytechnic Institute* *Class of 2018*

Sponsored by: Marie-Francoise Doursout, PhD, Department of Anesthesiology
Supported by: Marie-Francoise Doursout, PhD, Department of Anesthesiology; The University of Texas at Houston Medical School – Office of the Dean
Key Words: Active Hexose Correlated Compound (AHCC), Inflammation, Lung Lavage

Hypertension and cancer are two main causes of mortality worldwide and are linked to inflammation. Active Hexose Correlated Compound (AHCC), a supplement made from mycelium extract obtained from liquid culture of *Lentinula edodes*, is a supplement for the treatment of hypertension and cancer in Japan and China. Lipopolysaccharides (LPS) induce inflammation and oxidative stress and have some deleterious effects in the lung. AHCC is thought to reduce oxidative stress/inflammation.

We hypothesize that AHCC restores immune function in the rat. Thirteen male Sprague-Dawley rats were anesthetized to implant catheters into the femoral artery and vein to record mean arterial blood pressure (MAP) and heart rate (HR). After recovery from surgery, animals were divided into 3 groups. Group 1 (n=6) was treated with LPS alone (20mg/kg IV) to induce inflammation, group 2 (n=4) was treated with 10% AHCC in drinking water 3 days prior to being subjected to LPS, and group 3 (n=3) was treated with 10% AHCC in drinking water 3 days prior to experiment day. MAP and HR were continuously recorded for 3 hours following LPS or saline administration. Blood samples were taken hourly starting with 0 hours for nitric oxide (NO) and cytokine production. Animals were sacrificed at 3 hours. Group 1 tissue samples of the kidney, spleen, liver, heart, and small intestine were frozen and preserved in formalin. For all 3 groups, the lungs were taken out and a bronchalveolar lavage (BAL) fluid was made using 50 mL cold saline solution. The lavage solution was centrifuged at 300g and 4 degrees Celsius for 5 minutes. Once centrifuged, the liquid in the tube was dispersed of, and 1 mL cold saline was pipetted into the tube. The tube was then vortexed and from there a diluted 0.1 mL lavage fluid was made using cold saline. This solution was cyto-centrifuged onto slides which were stained to count macrophage percentages. BD Unopette Reservoirs were then used for white blood cell count.

Final results have yet to be determined, however from observation there are apparent differences in MAP drop between the groups, suggesting the AHCC attenuates the drastic drop in MAP induced by the LPS. No significant differences in macrophage or white blood cell count from the lavage fluid was observed. Nitrate/nitrite assays will be run and further experimentation will follow.

ABSTRACT

Protein Kinase C alpha Expression in the Goldfish Retina in Response to Light Adaptation

Nhi Dinh *Earlham College* *Class of 2016*

Sponsored by: Ruth Heidelberger MD, PhD, Department of Neurobiology and Anatomy
Supported by: Ruth Heidelberger MD, PhD, Department of Neurobiology and Anatomy; The University of Texas at Houston Medical School – Office of the Dean
Key Words: Protein Kinase C alpha, Rod Bipolar Cells, Visual system

Protein Kinase C (PKC) has been well studied as a marker of rod bipolar cells in the retina of a variety of vertebrate species. In rats, the expression of PKC in rod bipolar cells increased significantly at 15 days postnatal, when their eyes opened (Zhang, 1991), suggesting the important role of PKC in the visual system. When mice and goldfish were exposed to light after being in the dark, the rod bipolar cells depolarized, diacylglycerol (DAG) and calcium activated PKC and translocated it from the soma to the axon terminal (Vaquero, 1996; Gabriel, 2001; Germain, 2001). The PKCα in particular influenced the activation and the termination of the bipolar cell light response, as the PKCα mutant mice responded slower to light comparing to the wild-type mice and the PKCβ isoform could not compensate for the lack of PKCα function in retinal activity (Ruether, 2009). PKCα expression in the rod bipolar cells were not fixed but rather fluctuated according to light-dark cycle (Gabriel, 2001). However, the pattern of PKCα expression in relation to the amount and length of exposure to light remained unclear. Using immunohistochemistry (IHC), we studied this pattern of PKCα expression in relation to light exposure in the ON-rod bipolar cells of goldfish retina. We hypothesized that the translocation of PKC alpha from the soma to the axon terminal would increase the longer the goldfish would be exposed to light, and thus increase the ratio of terminal/soma PKCα labeling. All experimental animals were adapted in complete darkness for two hours. After the dark adaptation period, animals were divided in four conditions: no exposure to light, exposure to light of 1200-1600 lux, similar to the light source from the goldfish living environment, for two minutes, 15 minutes, and 60 minutes. We utilized a mouse monoclonal antibody against PKCα as primary antibody and a Cy3 donkey anti-mouse (DAM) antibody as secondary antibody. Tissues were sectioned to 30μm slide with a cryostat; sections were incubated for one hour in a 5% donkey serum blocking solution. The primary antibody (1:200) was left on slides overnight at room temperature in a moisturized IHC chamber. Afterward, slides were incubated in the Cy3 DAM antibody (1:200) for two hours at room temperature, then mounted with Gold anti fade reagent with DAPI. Slides were visualized using Zeiss 510 confocal laser-scanning microscope and images were processed with Zen 2009 and Simple PCI. We did not find a pattern of translocation from the soma to the axon terminal in PKCα expression across four conditions. We concluded that the fluctuation of PKCα expression in ON-rod bipolar cells in response to light might be controlled by the circadian cycle specifically (Gabriel, 2001) and not by light adaptation alone. However, a changing pattern of PKCα expression in response to light activity alone might be observed if the goldfish were exposed to light for more than 60 minutes.

ABSTRACT

The Role of *Irf6* in Salivary Gland and Pancreas Development

Megan Do *Agnes Scott College* *Class of 2017*

Sponsored by: Walid D. Fakhouri, MSc, PhD, UTHealth School of Dentistry, Department of Diagnostic and Biomedical Sciences

Supported by: Walid D. Fakhouri, MSc, PhD, UTHealth School of Dentistry, Department of Diagnostic and Biomedical Sciences; UT School of Dentistry at Houston Research Office

Key Words: IRF6, salivary glands, pancreas, histopathology, immunofluorescence staining, cleft lip and palate, lip pits, Van der Woude Syndrome

Background: Interferon Regulatory Factor 6 (IRF6) encodes for transcription factor that regulates expression of interferons and other signaling proteins that are critical for proper immune functions and biological processes during craniofacial and ectodermal development. Mutations in *IRF6* cause Van der Woude and Popliteal Ptrygium syndromes and contribute to the risk of the non-syndromic cleft lip and palate. Van der Woude Syndrome is characterized by lip pits, cleft lip and palate and has been associated with accessory salivary glands. *Irf6* null mice are born with abnormal skin, limb, and craniofacial. Our data showed that the mutant pups have shorter mandible which is similar to what is seen in humans for Van der Woude Syndrome. The aim of this project was to determine if *Irf6* is expressed in salivary glands, particularly the submandibular gland, and pancreas and to analyze the pathology of both exocrine glands in *Irf6* null mice.

Methods: We performed phenotypic analysis on newborn wild type and *Irf6* null (*Irf6 -/-)* pups as well as histological and immunofluorescent staining for the transcription factors *Irf6, p63,* and *Twist1*.

Results: H&E staining showed a clear difference in terms of organization and cell types. The salivary glands in *Irf6* null mice were disorganized and had almost no mucous acinar cells relative to their wild type littermates. Immunofluorescent staining also showed a difference in antigen location and expression. In wild type salivary glands, *Irf6* was located in the cytosol of mucus and serous acinar cells, *p63* was located in the nucleus of ductile cells, and *Twist1* was not expressed. However, in *Irf6* null, neither *Irf6* nor *Twist1* were expressed but *p63* was overexpressed leading to cell proliferation. In *Irf6* null pancreas, H&E staining showed abnormal morphology and disorganization of acinar cells, as well as large spatial arrangement between them compared to their wild type littermates.

Conclusion: Our findings indicate that *Irf6* is critical in the development of salivary glands and pancreas. These results suggest that DNA variations in IRF6 contribute to the risk of salivary gland and pancreatic disorders in humans. Our future goals are to understand the molecular role of IRF6 and translate these findings into the clinic to identify genetic risk factors in salivary gland and pancreas disorders.

ABSTRACT

A Randomized Double Blind Phase III Placebo Controlled Trial of LUMINENZ - AT™ In Children with Autism

Darlene Estrada *University of Houston* *Class of 2016*

Sponsored by: Deborah A. Pearson, PhD, Department of Psychiatry and Behavioral Sciences

Supported by: Grant entitled "A Phase III Randomized Double Blind Placebo Controlled Trial of LUMINENZ- AT™ (CM-AT) In Children with Autism", sponsored by Curemark, LLC; The University of Texas at Houston Medical School – Office of the Dean

Key Words: Autism Spectrum Disorder (ASD), Pancreatic Enzyme Concentrate (PEC), Intestinal hyperpermeability , LUMINENZ- AT™ (CM-AT), Chymotrypsin

Autism Spectrum Disorder (ASD) is a neurodevelopmental disorder characterized by varying degrees of impaired social interaction, delayed speech and communication, and restricted or repetitive behaviors. ASD can also be associated with gastrointestinal disturbances, leading researchers to investigate the relationship between digestion and the core symptoms of ASD. Curemark, the sponsor of this study, found in a previous study that a significant portion of children with ASD express low levels of chymotrypsin. Chymotrypsin is a serine protease that cleaves essential amino acids that are necessary for optimal brain functioning. Research conducted by Curemark has suggested that enzyme therapy with LUMINENZ-AT™ (CM-AT), a lipid-encapsulated pancreatic enzyme concentrate (PEC) intended to release proteases into the small intestine, may improve gastrointestinal function, which in turn may be associated with enhanced cognitive and behavioral function. The purpose of this study was to determine the safety and efficacy of CM-AT in the treatment of symptoms linked to ASD. Children between ages 3 and 8 with a diagnosis of ASD participated in an initial screening to determine whether or not they were eligible to be included in the study. Qualifying children were then randomized and given either active or placebo study drug for the duration of twelve-weeks. At each study visit, changes in behavior and symptoms were measured through parent questionnaires and interviews, behavioral scales, stool tests, and a brief physical exam. Data collection has been completed and analysis of data is ongoing. At the conclusion of the 12-week double-blind study, the children were invited to participate in an open-label extension of this project; some of these children continue to be seen in the open-label trial several years later. If CM-AT is approved for pediatric use, it may help children with ASD by improving their ability to digest dietary protein and thus enhance the availability of necessary amino acids, which may ultimately improve cognitive and behavioral function in these children.

ABSTRACT

Fetal vs Postnatal Repair of Myelomeningocele at Children's Memorial Hermann Hospital in comparison to MOMS Trial

Madeline Folkerts *The University of Texas at Austin* *Class of 2018*

Sponsored by: KuoJen Tsao, MD, Department of Pediatric Surgery, The Fetal Center

Supported by: KuoJen Tsao, MD, Department of Pediatric Surgery, The Fetal Center; The University of Texas at Houston Medical School – Office of the Dean

Key Words: Myelomeningocele, Spina bifida, Fetal intervention, MOMS Trial

Background: The Management of Myelomeningocele Study (MOMS Trial) showed that fetal repair of myelomeningocele (MMC) yields better neurological outcomes than postnatal repair. We analyzed and compared fetal and postnatal MMC-repair outcomes at Children's Memorial Hermann Hospital (CMHH) with the standards set by the MOMS Trial.

Methods: Prenatal, maternal, and neonatal outcome data was retrospectively collected on spina bifida cases evaluated at the Fetal Center at CMHH, and entered into a registry via REDCap (Research Electronic Data Capture). 13 patients were included in the fetal-repair group and 30 patients were included in the postnatal-repair group. Data at 1 year of age was obtained from records of pediatric follow-up performed at CMHH for 14 patients in the postnatal-repair group.

Results: Both MOMS Trial and CMHH cohorts had similar gestational ages at delivery; the CMHH fetal-repair group delivered significantly earlier than the postnatal-repair group ($p<0.001$). Chorioamniotic membrane separation during pregnancy occurred at a significantly higher rate in the fetal-repair group of the MOMS Trial while it was not observed in either repair group at CMHH. Spontaneous rupture of membranes during pregnancy occurred in 46% of fetal-repairs in the MOMS Trial while it occurred in 38% of fetal-repairs at CMHH. Hysterotomy sites from fetal repairs remained intact at a higher rate at CMHH than in the MOMS Trial. In both repair groups, neonatal respiratory distress syndrome (RDS) was observed at a slightly higher rate at CMHH than in the MOMS Trial; the CMHH fetal-repair group developed RDS at a higher rate than the postnatal-repair group ($p=0.07$). Neonatal lower extremity function was not reported in the MOMS Trial; however, this additional data set was captured for the CMHH cohort. Normal lower extremity movement and reflexes were reported at a greater rate in the fetal-repair group versus the postnatal-repair group ($p=0.03$ and $p=0.01$, respectively). Reversal of hindbrain herniation occurred at a greater rate in the fetal-repair group versus the postnatal-repair group ($p=0.001$). At one year, 57% reported shunts, 64% reported normal lower extremity movement, and 57% reported normal lower extremity reflexes in the postnatal-repair group; this data set is not currently available for the fetal-repair group.

Conclusions: Though this study has limited sample sizes and outcome data, overall, CMHH meets the standards set by the MOMS Trial. Fetal-repairs at CMHH demonstrated significant improvement in lower extremity function and reversal of hindbrain herniation at NICU discharge in comparison to postnatal-repairs. The next step is gathering external medical records and obtaining long-term pediatric follow-up information through this registry and collaboration with the North American Fetal Therapy Network.

Abstract

Lactoferrin as an Immunomodulator in Granulomatous Response to Tuberculosis Infection

Ron Gadot *Brandeis University* *Class of 2018*

Sponsored by: Jeffrey K. Actor, PhD, Department of Pathology and Laboratory Medicine
Supported by: NIH-NIAID #1R41-AI117990-01
Key Words: Tuberculosis, TDM, Granulomas, Lactoferrin, Cytokine Production

Introduction: Tuberculosis is a global pandemic estimated to affect nearly one third of the world's population. *Mycobacterium tuberculosis (*MTB*)* is the second leading infectious killer of adults worldwide, placing only behind HIV/AIDS. Adjunct therapeutics that allow modification of lung pathology in such a way so as to promote drug targeting of tuberculosis infectious organisms would be greatly beneficial. The iron-binding glycoprotein Lactoferrin (LF) has been shown to serve as an immunomodulator that could modulate the body's proinflammatory response to MTB infection, thereby allowing affected tissue to be more receptive to drug therapy. This concept may be tested in a granuloma model system based upon reactivity using the MTB glycolipid trehalose 6,6′ dimycolate (TDM or cord factor), which is a major contributor to early proinflammatory responses post infection.
Methods: BALB/C (n=20) and C57BL6 (n=20) mice were injected with 25 µg TDM formulated in emulsion to induce mycobacterial pulmonary granulomas that mimic TB-induced pathology. Mice were treated with either 1 or 2 mg bovine (bLF) or recombinant human LF (rHLF) given by oral administration on days 4 and 6 post TDM injection. Lungs were examined at day 7 post granuloma induction and samples were assessed by histology and overall inflammatory response in the lung, and by ex-vivo cytokine production as measured by ELISA. Experiments were repeated 2-3 times, and compared to naïve or TDM alone groups.
Results: Mice given TDM alone demonstrated strong granulomatous responses with classical monocytic foci. Treatment with all Lactoferrins led to a uniform change in the structure of TDM induced granulomas, with mice exhibiting less focal response and decreased Lung Weight Indexes. Mice given TDM alone also saw marked and significant increased production of proinflammatory cytokines TNF-α, IL-6, IL-1β, IL-12p40, and KC. Treatment with bovine LF at 1 or 2 mg led to significant reduction ($p < 0.05$) in aforementioned cytokine levels in BALB/c mice with more variation in C57BL6 mice. In a similar manner, recombinant human LF given at 1 or 2 mg doses also showed significant reduction in all of the above cytokines across both strains ($p < 0.01$), which was superior to the significance seen with the bLF. In particular, the 1 mg dosage of recombinant LF showed the most consistency in its ability to control (reduce) production of proinflammatory cytokines.
Conclusion: These results indicate that adjunct therapy with Lactoferrin may be beneficial in modulating immunogenic responses during MTB infection so as to reduce inflammatory foci in the lung. This would potentially allow more effective drug delivery and treatment of infection.

ABSTRACT

Dynamic Mechanical Analysis (DMA) of Dental Polymer Fillings to Investigate Degradation Factors

Heather Haeberle *The University of Texas at Austin* *Class of 2016*

Sponsored by: Catherine G. Ambrose, PhD, Department of Orthopaedic Surgery
Supported by: Department of Orthopaedic Surgery; NIH NIDCR grant R01DE021394-01; The University of Texas at Houston Medical School – Office of the Dean
Key Words: dental filling, Dynamic Mechanical Analysis, three-point bending, dental caries

INTRODUCTION Polymer resins potentially provide a safer and more aesthetically pleasing alternative to amalgam fillings for dental caries, but have shown a high risk of complication and failure within the first five years of implantation. This study aims to investigate the factors contributing to the failure of these materials in order to evaluate their use in dental applications. Possible factors contributing to material breakdown include moisture, salivary components, acidic surroundings, and the growth of bacteria on the surface of the filling materials.
METHODS In order to isolate the possible effects of moisture, low pH, and biofilm growth, we tested the viscoelastic mechanical properties of three polymer resin materials dry and after one week exposure to four conditions: PBS, artificial saliva, conditioned artificial saliva, and biofilm. Our collaborators have previously demonstrated that the *in vitro* biofilm conditions created using four species of oral bacteria mimic those seen in dental caries. Five specimens were tested for each material and condition, and each specimen was tested in a three-point bending apparatus using a Dynamic Mechanical Analysis (DMA) program which applied a cyclic displacement at a range of frequencies from 0.1 Hz to 20 Hz. This range of frequencies was chosen as it is centered around the average human chewing frequency of approximately 2 Hz. This testing recorded several material properties at each frequency including the storage modulus (E′), loss modulus (E″), and tangent of delta (tanδ).
RESULTS & CONCLUSIONS Mechanical properties were significantly degraded after exposure to moisture and the property degradation was frequency dependent. There was a general trend of loss moduli decreasing as frequency increased. The major exception to this was in the biofilm condition, in which the E″ at 0.1 Hz was significantly less than that at 0.25 Hz for two of the three materials. This indicates the possibility that the properties of these materials at low frequencies were significantly impacted by the growth of the biofilm. Additional data analysis, including an impedance-based electrical model of each material, is ongoing.

ABSTRACT

Determining the Role of Globins in the Oxidative Stress Response of *Caenorhabditis elegans*

Sarah Hanif *Cornell University* *Class of 2018*

Sponsored by: Danielle A. Garsin, PhD, Department of Microbiology and Molecular Genetics
Supported by: NIH/NIAID R01076406 The Role of ROS in Innate Immunity to Danielle A. Garsin, PhD
Key Words: *C. elegans*, globin, oxidative stress

Oxidative homeostasis is the state in which an organism is able to sense and respond to reactive forms of oxygen. Organisms that are unable to maintain oxidative homeostasis are at higher risk for developing several neurological and cardiovascular diseases, as well as cancers that progress with age. Our lab studies the mechanisms of oxidative homeostasis in the model organism *Caenorhabditis elegans.* This nematode produces reactive oxygen species as a defense mechanism against pathogens, as do many mammalian species. In *C. elegans,* the dual oxidase Ce-Duox1/BLI-3 activates SKN-1, the major oxidative stress response transcription factor that is crucial in initiating the protective response. Recent literature suggests that globins, which have a high affinity for oxygen, may also play a role in the oxidative stress response of this nematode. The *C. elegans* genome contains 33 putative globins, and homologs of these proteins are present in many mammalian species. Recently, *glb-1*, *glb-5*, and *glb-13* were demonstrated to play a beneficial role in resistance against oxidative stress-induced toxicity. *glb-1* and *glb-5* have an extremely high affinity for oxygen compared to their mammalian homologs and are up regulated during hypoxia, suggesting that these globins play an important role in the metabolism of molecular oxygen. The mRNA level of *glb-13* was significantly up regulated during paraquat exposure, and the mutant strain indicated sensitivity to paraquat-induced oxidative stress. Because oxidative stress is present during pathogen infection, we hypothesized that additional members of the globin family would play a protective role during infection with pathogen. In support of this hypothesis, we have screened through six globins of *C. elegans* using RNAi and susceptibility assays. Nematodes that expressed decreased levels of *glb-5, glb-13, glb-10, glb-16,* and *glb-17* showed increased sensitivity to the human pathogen *Enterococcus faecalis*. These results suggest that certain globins are indeed protective during infection, perhaps due to a role in maintenance of oxidative homeostasis and resistance against oxidative stress-induced toxicity. Future studies will focus on defining the mechanism by which these globins are protective, examining the hypothesis that they affect SKN-1 activity, the major oxidative stress response transcription factor found in *C. elegans.*

ABSTRACT

Evaluation of Hemodynamic Transesophageal Echocardiography for use in Burn Patient Resuscitation

Jane Hayes *The University of Texas at Austin* *Class of 2016*

Sponsored by: Ryan Lawless, MD, Department of Surgery

Supported by: Charles Wade, PhD, Department of Surgery, Center for Translational Injury Research (CeTIR); The University of Texas Medical School at Houston—Office of the Dean

Key Words: Burn, resuscitation, Hemodynamic Transesophageal Echocardiography, fluid balance, KMAC value, urine output, Brooke formula, Parkland formula

Background: Patients with severe burn injuries to more than 20% of their total body surface area experience burn shock, which must be immediately treated to prevent devastating outcomes. Burn shock is characterized by hemodynamic changes including decreased extracellular fluid, decreased cardiac output, decreased plasma volume, and oliguria. Patients in burn shock need to be resuscitated with fluid in order to counterbalance these fluid shifts and restore tissue perfusion to prevent ischemia and cellular death. Administering the proper volume of fluid is made difficult by the fact that each patient reacts uniquely to burn injuries depending on their age, preexisting comorbidities, BMI, percent of body area burned, and depth of burn among other factors. Therefore general burn formulas that only take into account the patient's weight and percentage of skin burned should merely serve as guidelines because these formulas cannot provide a personalized assessment of proper volume administration. Traditionally urine output has been used to help titrate the amount of fluid given to a patient but this may not be a reliable measurement of resuscitation as kidney function secondary to injury is highly variable from patient to patient. The Hemodynamic Transesophageal Echocardiogram (HTEE) may serve as a better method to assess volume and titrate resuscitation efforts as it allows the physician to measure cardiac filling and gain a real time assessment of volume status.

Hypothesis: Using Hemodynamic Transesophageal Echocardiography results to guide fluid administration in burn patients will decrease under-resuscitation and over-resuscitation in the first 24 hours.

Methods: Historical data was collected in the Memorial Hermann John S. Dunn Burn Center from July 2013 through April 2015 to conduct a retrospective study. The data was then used to compare burn patients who had an HTEE to assess fluid resuscitation in a 1:3 ratio with matched burn patients who received the standard of care. The patients were matched on factors including age, BMI, and percentage of total body surface area burned. KMAC values, which are a measure of fluid balance, were then calculated for each patient and these values will be used to determine which patient population was better resuscitated.

Results: As of 7/30/15, data collection and analysis is ongoing, therefore no results are available at this time.

ABSTRACT

The Effect of Human Polyomavirus 7 Small T Antigen on Cell Signaling Pathways

Thomas Hsiao *University of Texas at San Antonio* *Class of 2017*

Sponsored by: Stephen K. Tyring, MD, PhD, MBA, Department of Dermatology

Supported by: The University of Texas MD Anderson Cancer Center and The University of Texas Health Science Center at Houston (UTHealth) Graduate School of Biomedical Sciences

Key Words: HPyV7, 4EBP-1, MAPK Pathway, PP2A, PPM1G, Akt/mTor pathway

Merkel cell polyomavirus (MCPyV) and human polyomavirus 7 (HPyV7) are implicated in the pathogenesis of Merkel cell carcinoma (MCC) and human epithelial thymomas respectively. Thymomas have been associated with different paraneoplastic skin diseases, and are a growing concern in the dermatological field. However, the molecular biology of these polyomavirus-associated thymomas is still not well understood.

All human polyomaviruses encode a small T antigen, which may affect the phosphorylation of proteins critical to signal transduction pathways. MCPyV sT has been shown to transform rodent cells. To investigate the oncogenic potential of HPyV7, we studied the effect its sT has on signal transduction pathways and compared it to that of the MCPyV sT. The current study focused on the Akt-mTor pathway which regulates cap-dependent translation and the mitogen-activated protein kinase (MAPK) pathway which regulates cell growth and mitosis. We used His-TRX pull down assay to find interaction between the HPyV7 sT and important protein phosphatase regulators in these pathways: Protein Phosphatase 2A (PP2A) of the MAPK, and Protein Phosphatase Mg2+/Mn2+ dependent 1 G (PPM1G) of the AKT/mTor. Our data showed that HPyV7 sT binds to both PP2A and PPM1G.

Western blotting with phospho-specific antibodies was then used to observe if the pathways regulated by the phosphatases displayed any abnormalities in cells with inducible overexpression of HPyV7 sT. Within the AKT-mTor pathway, we focused on eukaryotic translation initiation factor 4E-binding protein 1 (4E-BP1), a protein that is dephosphorylated by PPM1G, but when phosphorylated leads to enhanced cap-dependent translation. Our data shows 4E-BP1 is hyperphosphorylated in the presence of HPyV7 sT. In the MAPK pathway, a downstream factor called c-Jun shows hyperphosphorylation, but none of the canonical upstream factors such as MEK, ERK, and JNK were hyperphosphorylated.

We conclude that cells induced with HPyV7 sT show hyperphosphorylation in 4E-BP1 of the AKT-mTor pathway as well as in c-Jun of the MAPK pathway, similar to MCPyV sT. Considering that MCPyV is the only known oncovirus among the human polyomaviruses, our data provides evidence for HPyV7's role as a potential oncovirus.

ABSTRACT

Effects of Hematocrit (Hct) Levels on Clinical Outcome During the Cardiopulmonary Bypass (CPB) and Deep Hypothermic Circulatory Arrest (DHCA) in Ascending Aortic Surgery

Suhyun Jeong *The University of Texas at Austin* *Class of 2018*

Sponsored by: Shao Feng Zhou, MD, Department of Anesthesiology
Supported by: Shao Feng Zhou, MD, Department of Anesthesiology; The University of Texas at Houston Medical School – Office of the Dean
Key Words: Ischemia, Intraoperative, Hematocrit, Transfusions

Organ ischemia, due to blood loss, is often a precautionary concern during intraoperative cardiovascular surgery. Blood transfusions are carried out to combat anemia, but there is an emphasis on blood transfusion conservation because of poor clinical outcome and monetary cost. Previous studies indicate that patients can generally tolerate low hemoglobin (Hg) levels of 8-7 g/dl and for most aortic/aortic arch surgeries, transfusions occur intraoperatively. However, intraoperative hemodilution during CPB may lead to anemia and ischemia. In the case of CPB with DHCA, hematocrit concentrations were lowered to reduce blood viscosity and maintain proper oxygen delivery. Yet, specific concentrations are crucial. Hypothermia diminishes the need for oxygenation due to lowered tissue metabolic rates, but itself stops oxygen delivery. In this study, we analyzed the variable effects of temperature on hematocrit levels to determine which Hct concentration reduced the need for transfusions, while preventing organ ischemia and minimalizing the effects of anemia. From 2004 – 2015, thousands of patients have undergone aortic surgery supported by CPB with DHCA. Patient data was analyzed to study the correlation between hematocrit concentration, organ impairment, and morbidity using a generalized propensity score analysis. A linear regression analysis was implemented to distinguish factors associated with the hematocrit. Results showed a median nadir hematocrit of 30%. The nadir hematocrit was linked with negative renal function (P ¼ .012), increased myocardial injury (P ¼ .004), longer postoperative ventilator support (P<.001), longer hospital stay (P<.001), and higher mortality (P ¼ .042). Despite the risks involving transfusion, the optimal scenario appears to be a combination of transfusion and hematocrit that minimalizes the negative effects of both. Further investigations are ongoing to improve this balance for usage in cardiovascular surgery.

ABSTRACT

Quantitation of Cell-Density Effects on Twitching Motility

Kimberley Kissoon *Del Mar College* *Class of 2016*

Sponsored by: Heidi B. Kaplan, PhD, Department of Microbiology and Molecular Genetics
Supported by: The University of Texas MD Anderson Cancer Center and The University of Texas Health Science Center at Houston (UTHealth) Graduate School of Biomedical Sciences
Key Words: Social motility, twitching, cell – density dependent, *M. xanthus*, *P. aeruginosa*.

Twitching motility is type IV pili-mediated flagella-independent group movement on a solid surface by gram-negative bacteria, including *Pseudomonas aeruginosa* and *Myxococcus xanthus,* a pathogen and a non-pathogen respectively. Currently, the most accepted mechanism thought to drive this motility is the binding of type IV pili to a neighboring cell's surface, causing pilus retraction which pulls the cell forward towards the next cell. We support an alternative hypothesis, that the pili attach to exopolysaccharide (EPS) secreted onto the surface by the cell. This predicts that high density colonies expand more rapidly and at a constant rate, as more cells produce more EPS, allowing these cells to move earlier and ultimately farther. A mathematical model devised to represent this mechanism for twitching behavior was tested experimentally. Liquid cultures of *M. xanthus* DK1218, a strain exhibiting only twitching motility, were grown, diluted to different densities ($2x10^7$ – $4x10^9$), and 3 µl spots of each density were placed onto agar plates. The plates were incubated at 32˚C in a humid environment for up to 96 hrs. Each spot was imaged with a camera attached to a dissecting microscope, and the distance the edge of each colony moved was measured at least twice a day. Under standard conditions (1% casitone in 0.5% agar plates), as expected, the higher densities colonies expanded more rapidly and as a result traveled farther. However, at all densities the colonies slowed down over time, deviating from our prediction. To eliminate the slowing down, two types of conditions were tested: variations in the agar content of the plates (0.3%, 0.4%); variations in nutrient composition (0.5%, 1.5%, 2% casitone, and 1% casitone with 0.2% yeast extract). Only the high nutrient plates (0.2% casitone, 1% casitone with 0.2% yeast extract) resulted in constant expansion. Future experiments will confirm these results, allow for more in depth statistical analysis, and expand testing our studies with *P. aeruginosa* and the *M. xanthus* rippling motility by twitching only cells.

ABSTRACT

Activity of Virulence Regulator Chimeras in *Bacillus anthracis*

Henry Landis *Amherst College* *Class of 2017*

Sponsored by: Theresa M. Koehler, PhD, Department of Microbiology and Molecular Genetics
Supported by: The University of Texas MD Anderson Cancer Center and The University of Texas Health Science Center at Houston (UTHealth) Graduate School of Biomedical Sciences
Key Words: Domains, specificity, chimeric proteins, activity

AtxA is characterized as the master virulence regulator in *Bacillus anthracis.* A positive transcriptional regulator, it is responsible for the production of the three components of the anthrax toxin on the pXO1 plasmid, as well as the biosynthetic capsule on the pXO2 plasmid. Recently, a crystal structure of AtxA has been derived, revealing five distinct protein domains, including DNA-binding domains (DBD) as well as phosphotransferase system (PTS) regulatory domains (PRD). AtxA controls the transcription of, among other genes, AcpA and AcpB, which are located on pXO2. AcpA and AcpB are paralogs of AtxA, and as such are predicted to have DBD's and PRD's. The regulons of each gene are overlapping yet distinct. To discern potential roles of the distinct protein domains of AtxA, AcpA, and AcpB in target specificity, we will create chimeric regulators and test the proteins for gene regulation *in vivo*. I created three chimeric DNA constructs using overlap PCR. The chimeric genes were cloned in a vector for expression in *B. anthracis*. Work to assess stability and function of the chimeric proteins is in progress.

ABSTRACT

5′-AMP Regulates Erythrocytes Oxygen Affinity

Han Shawn Ling *The University of Texas at Austin* *Class of 2017*

Sponsored by: Cheng Chi Lee PhD, Zhaoyang Zhao PhD, Department of Biochemistry and Molecular Biology

Supported by: 5R01GM104510-03; The University of Texas at Houston Medical School – Office of the Dean

Key Words: p50, adenine nucleotides, mouse model, organic phosphate

A transient state of hypometabolism can be induced in mammals via the administration of 5′-adenosine monophosphate (5′-AMP)[1]. Our earlier studies have implicated the uptake of 5′-AMP by erythrocytes to be a critical initiation step for inducing this hypometabolic state[2]. We have proposed that the uptake of 5′-AMP altered erythrocyte intracellular adenine nucleotides equilibrium that in turn lead to decreased hemoglobin (Hb) affinity for oxygen. It is well established that some organic phosphates, including adenine nucleotides, bind to Hb, change its ternary structure, and alter its affinity for oxygen. Initial studies have shown that the p50 value of erythrocytes increased linearly with increasing concentration of 5′-AMP even at 15 mM extracellular AMP level, which was surprising. This observation raised the possibility that other factors were likely involved. Here, we further investigated how exogenous 5′-AMP alter erythrocyte 50% saturation pressure for oxygen (p50), using a Hemox Analyzer instrument. It is well known that erythrocytes p50 can be altered by change in pH, a phenomenon known as the "Bohr effect". To examine whether the "Bohr effect" contribute to the AMP regulation of p50 we previously observed, we measured the pH of the Hemox buffer solutions with various concentration of 5′-AMP. We observed that the pH values of commercial Hemox buffer were altered significantly by the additions of 5′-AMP, starting around 2 mM. To separate the "Bohr effect" from the effect of 5′-AMP on erythrocytes p50, we undertook a reformulation of the Hemox solution with different buffer formula using Tris-HCl, HEPES, or MOPS. Now, we have arrived on a Hemox buffer with 100 mM Tris-HCl, whose pH value remain stable upon addition of 5′-AMP up to 10 mM. Then, the p50 values of the erythrocytes were measured with increasing concentration of 5′-AMP. We observed that the p50 values increase linearly up to 4 mM of exogenous 5′-AMP, whereby it reaches a saturation value. The saturable character of the 5′-AMP regulation of the p50 suggests for the first time that upon entering the erythrocytes, 5′-AMP regulate Hb oxygen affinity by binding to specific binding sites on Hb.

References:

1. Zhang, J., Kaasik, K., Blackburn, M.R., and Lee, C.C. Constant darkness is a circadian metabolic signal in mammals. *Nature.* 439, 340-343 (2006).
2. Zhang J., Fang Z., Jud C., Vansteensel M.J., Kaasik K., Lee C.C., Albrecht U., Tamanini F., Meijer J.H., Oostra B.A., and Nelson D.L. Fragile X Related Proteins Regulate Mammalian Circadian Behavioral Rhythms. *Am J Hum Genet.* 83: 43-52. (2008)

ABSTRACT

ENU-Derived Deletion in Mouse Mutant Line 308

Fatma Muge Ozguc *University of California, Berkeley* *Class of 2017*

Sponsored by: Seung-Hee Yoo, PhD, Department of Biochemistry and Molecular Biology

Supported by: Seung-Hee Yoo, PhD, Zheng Chen, PhD, Department of Biochemistry and Molecular Biology; The University of Texas at Houston Medical School – Office of the Dean

Key Words: circadian period, ENU mutagenesis, Cry2

N-ethyl-*N*-nitrosourea (ENU) is a potent mutagen that can induce point mutations, and is commonly used in mouse forward genetics. After an ENU mutagenesis screen of 300 G1 mouse progenies, mutant line 308 has been shown to display a 1-hour longer circadian free-running period in constant darkness. The mutation in 308 has been mapped to chromosome 2. In this project, we aimed to identify the exact location of the mutation within chromosome 2. Since Cry2, a core clock gene, is known to be located in chromosome 2, a first-line study is to ascertain whether Cry2 is mutated. We designed a series of primers to amplify 11 exons from the Cry2 gene. PCR analysis failed to obtain specific amplifications for the desired amplicons only from the mutant line 308. In contrast, PCR reactions using wild-type mouse genomic DNA under the same conditions resulted in the desired amplicons. Western blotting analysis of CRY2 protein in 308 liver tissues also revealed a lack of CRY2 protein in contrast to the wild-type liver tissues. These results suggested a large deletion in the Cry2 genomic region instead of a point mutation as expected from ENU mutagenesis. To further map the deletion boundaries, we performed PCR for the neighboring genes of Cry2, which revealed that genes Mapk8ip1 and D930015M05Rik also showed no amplifications. This study therefore identified a surprising ENU-derived genomic deletion spanning at least three genes and suggests that the long-period phenotype in line 308 is likely to result from Cry2 deletion.

ABSTRACT

Repurposing Established Antibiotics for the Treatment of Multidrug-Resistant Pathogens

Mario Patlan *University of Texas at Brownsville* *Class of 2017*

Sponsored by: Herbert L. DuPont, MD, Charles Darkoh, PhD, School of Public Health

Supported by: The University of Texas MD Anderson Cancer Center and The University of Texas Health Science Center at Houston (UTHealth) Graduate School of Biomedical Sciences

Key Words: *Clostridium difficile*, Methicillin-Resistant *Staphylococcus aureus*, Ciprofloxacin, Indole, Multidrug Resistance

Multidrug resistance, traditionally defined as the ability of a microorganism to resist the effect of one or more distinct classes of antimicrobials, is an emerging public health concern due to widespread use of antibiotics in human and animal therapy. The goal of this study is to develop a novel treatment for multidrug-resistant bacteria by repurposing established antibiotics with agents that alter bacterial multidrug-resistance mechanisms. Ciprofloxacin, a second generation fluoroquinolone, was chosen as the model antibiotic given its widespread use and the abundance of clinically available ciprofloxacin-resistant bacterial strains. Indole has been established in our laboratory to interact with bacterial cell walls and create redox imbalances. Thus, we hypothesized that combining physiologic concentration of indole with sub-inhibitory concentrations of antibiotics should improve their antimicrobial effects. To test this hypothesis, multidrug-resistant *Clostridium difficile* and Methicillin-Resistant *Staphylococcus aureus* (MRSA) strains were incubated overnight with different concentrations of ciprofloxacin and indole. The growth of the bacterial strains was then monitored by optical density measurement at 600 nm. The results indicated that 4 mM indole decreases the minimum inhibitory concentration of ciprofloxacin against hypervirulent *C. difficile* strain CD196 from 32 µg/mL to 4 µg/mL and MRSA strain 3040A from 256 µg/mL to 64 µg/mL. These data demonstrate that combining ciprofloxacin and indole has a synergistic effect on bacterial growth and thus, decreases the minimum inhibitory concentration of ciprofloxacin.

ABSTRACT

Comparison of Tissue-Interface Pressure in Healthy Subjects Lying on Two Trauma Splinting Devices: The Vacuum Mattress and Long Spine Board

Mark N. Pernik *Austin College* *Class of 2018*

Sponsored by: Mark L. Prasarn, MD, Department of Orthopaedic Surgery
Supported by: Mark L. Prasarn, MD, Department of Orthopaedic Surgery; The University of Texas at Houston Medical School – Office of the Dean
Key Words: Vacuum, splint, spineboard, pressure, ulcer

Introduction:
Most emergency transport protocols in the United States currently call for the use of a rigid spine board (SB) to help immobilize the patient during transport and transfers. However, there are concerns that their use is associated with a risk of pressure ulcer development, and some have even proposed there may be little benefit to the unstable spine injured patient. An alternative device – the vacuum mattress splint (VMS) – has been shown by previous investigations to be a viable alternative to the SB. We hypothesize that the VMS will exert less pressure to the occiput, scapulae, sacrum, and heels when compared to the SB.

Methods:
In this prospective study, we enrolled healthy subjects to lie on the SB and VMS in random order while pressure measurements were recorded using a pressure measurement system. Sensors were placed underneath the occiput, scapulae, sacrum, and heels of each subject lying on each device. Three parameters were used to analyze differences between the two devices: 1) mean pressure of all active cells, 2) number of cells exceeding 9.3 kpa, and 3) maximal pressure (P_{max}).

Results:
In all regions, there was a significant reduction in the mean pressure of all active cells in the VMS. In the number of cells exceeding 9.3 kPa, we saw a significant reduction in the sacrum and scapulae in the VMS, fewer cells when examining the occiput but no statistical significance, and significantly more cells above this value in the heels of subjects on the VMS. P_{max} was significantly reduced in all regions, and was less than half when examining the sacrum (104.3 vs. 41.8 kPa, $p<.001$).

Conclusions:
This study could not exclude the possibility of pressure ulcer development in the VMS although there was a significant reduction in the mean pressure of all cells using this device. This indicates the VMS would likely reduce the incidence and severity of pressure ulcer development as compared to the rigid spine board. We advocate for the use of the VMS, but protocol must be implemented to ensure removal of the devices as soon as medically indicated.

ABSTRACT

The Expression of PBP5 across the Clades of *Enterococcus faecium*

Meredith Rae *Washington University in St. Louis* *Class of 2016*

Sponsored by: Barbara E. Murray, MD, Department of Internal Medicine
Supported by: The University of Texas MD Anderson Cancer Center and The University of Texas Health Science Center at Houston (UTHealth) Graduate School of Biomedical Sciences
Key Words: *Enterococcus faecium*, penicillin binding protein 5, ampicillin resistance

Enterococcus faecium is a leading cause of hospital-acquired infection and can be divided into three clades: clade B, containing human commensal isolates; subclade A1, the subclade responsible for human infection; and subclade A2, containing animal-associated strains as well as sporadic human infection isolates. Penicillin Binding Protein 5 (PBP5) plays a large role in intrinsic ampicillin resistance in *E. faecium*; resistance has been associated with higher expression of the gene as well as amino acid changes in the transpeptidase domain that result in decreased interaction with β-lactams. *pbp5* in *E. faecium* can be characterized into two forms: *pbp5-S* in ampicillin-susceptible community associated-strains (MIC ≤ 2 μg/mL), and *pbp5-R* in ampicillin-resistant hospital strains (MIC ≥ 16 μg/mL). Our first aim was to determine the relative levels of expression of PBP5 across the clades of *E. faecium*. We additionally sought to determine the presence of PBP5 expression in a community strain of *E. faecium*, Com15, carrying *pbp5-S,* and its two mutants complemented with *pbp5-R* from the C68 strain, a hospital-associated strain. We performed western blotting with an antibody produced against rPBP5 from the C68 strain to determine the relative levels of PBP5 expression. We detected higher levels of expression of PBP5 in the Clade A1 strains as compared to the Clade B strains. Furthermore, we confirmed the expression of similar low levels of PBP5 in Com15 and its two *pbp5-R* complements, whereas C68 showed significantly higher expression. We have shown previously that the *pbp5-R* complements in Com15 exhibit identical MICs to the Com15 carrying *pbp5-S*. Therefore, we conclude that in the Com15 carrying *pbp5-R*, low MIC is related to the low level of expression of PBP5 regardless of the *pbp5-R* or *S* form. The procedure should be repeated to ensure reproducibility, and positive controls of rPBP5 produced from Com15 and C68 should be included to confirm equal affinity of the antibody for the different PBP5 variants. In addition, future steps include the production of a *Δpbp5* mutant of the TX82 strain from Clade A1 as well as a mutant TX82 strain carrying *pbp5-S.* Once a procedure for reliably comparing the levels of PBP5 expression across the strains is determined, the levels of expression of the mutant strains in TX82 and Com15 as well as the wild type strains spanning the three clades can be compared to their respective MICs to test for a correlation between the two.

ABSTRACT

Association of DNA Methylation Age Acceleration with White Matter Hyperintensities

Abhay Raina *The University of Texas at Houston Medical School* *Class of 2019*

Sponsored by: Myriam Fornage, PhD, FAHA, Center for Human Genetics, Institute of Molecular Medicine

Supported by: The University of Texas at Houston Medical School – Office of the Dean

Key Words: Epigenetics, methylation, white matter hyperintensities

Background: DNA methylation is a widely studied mechanism of the control of gene expression. It has been shown that DNA methylation patterns can be used to predict a patient's age across a variety of different sample types and patient populations. The difference between the patient's chronological age and the predicted age based on the methylation data is known as "age acceleration." However, it is unclear whether age acceleration is independently associated with different neurological disease traits. Specifically, white matter hyperintensities are brain lesions visible on an MRI that are a significant predictor of neurological diseases such as stroke and dementia as well as overall mortality.

Methods: Methylation probe data and white matter hyperintensity severity scores were obtained through the Atherosclerosis Risk in Communities Study. Two different published sets of methylation probe predictors were used in order to estimate the DNA methylation age. Linear models were used in order to determine the effect of age acceleration on the white matter hyperintensities severity. These models included adjustment for risk factors including age, gender, proportion of different white blood cell types, smoking status, drinking status, BMI, blood pressure, hypertension medication use and diabetes incidence.

Results: The data indicated that the predicted methylation age was more highly correlated with white matter hyperintensities ($\rho = 0.31$) than the chronological age ($\rho = 0.29$). The risk-factor adjusted linear models indicated that age acceleration is a highly significant predictor of white matter hyperintensities ($p < 0.001$, $\beta = 0.03$). Other significant predictors include chronological age ($p < 1e\text{-}11$, $\beta = 0.07$), systolic blood pressure ($p < 0.001$, $\beta = 0.01$), smoking status ($p < 0.01$, $\beta = 0.30$), proportion of lymphocytes ($p < 0.01$, $\beta = -0.04$), proportion of monocytes ($p < 0.01$, $\beta = 0.03$) and proportion of neutrophils ($p < 0.05$, $\beta = -0.03$).

Conclusions: The risk-factor adjusted models indicate that the age acceleration was significantly associated with the severity of the white matter hyperintensities. However, chronological age had a much higher regression coefficient ($\beta = 0.07$) than age acceleration ($\beta = 0.03$), limiting the predictive value of the analysis. More research is needed to evaluate the association of age acceleration with other neurological diseases.

ABSTRACT

Approach for using Electronic Health Record (EHR) Data to Examine the Association between Periodontitis and Obesity

Angel Rivera *University of St. Thomas* *Class of 2016*

Sponsored by: Muhammad F. Walji, PhD, Department of Diagnostic and Biomedical Sciences, UT School of Dentistry

Supported by: Muhammad F. Walji, PhD, Department of Diagnostic and Biomedical Sciences, UT School of Dentistry; UT School of Dentistry at Houston Research Office

Key Words: Electronic health records, periodontal disease, obesity, data integration

Introduction: Electronic Health Records (EHRs) contain large amounts of patient data, which can be used for research to improve the health of individuals and the population. However, the availability, quality, heterogeneity, and incompleteness of the data can create barriers for conducting studies. The purpose of this research was to develop a method to use existing EHR data from both dental and medical clinics to examine the association between periodontitis and obesity. In addition, the secondary goal was to identify and address the challenges with using EHR data for secondary research. The dental EHR data were obtained from the BigMouth Dental Data Repository, which contained data from 6 dental schools, and the medical EHR data were obtained from the UT Physicians Outpatient Clinics.

Methods: The following 5-step process was used. Step 1 was to identify the necessary variables based on the diseases being studied. The required EHR data such as height, weight, periodontitis diagnosis, demographics, etc. and its format were determined based on a literature review and phenotyping. Phenotyping is the identification of conditions of interest by using specific variables found in the EHR data. Step 2 was to determine the availability of the necessary variables in the databases and how to handle missing data. Step 3 was to assess the characteristics (i.e. structured vs unstructured, measured vs self-reported) of the available data in order to evaluate the quality of the data and to determine the necessary data transformations. Step 4 was to identify how to integrate the data from the different sites to form a homogeneous dataset. Step 5 was to develop a strategy for the data extraction, cleaning, and analysis.

Results: Based on the 5-step process a total of 22 variables were included. The assessment of obesity was determined by Body Mass Index (BMI) and diagnostic codes (ICD) and the assessment of periodontitis was determined by full mouth exams and diagnostic codes (DDS). Patient diabetes status was identified using an existing phenotype, which included lab values, medications, and ICD codes. In many cases the data for a single variable, such as smoking frequency, in one source were coded differently from the data in another source. For these cases a common threshold was developed in order to integrate data in a meaningful way. If a certain variable had missing data then a replacement variable had to be used (i.e. missing income data was replaced with education-level data in order to represent socioeconomic status). Some of the

dental EHR data were self-reported so we compensated by using patient data collected from UT Physicians (i.e. height, weight, and diabetes status). A codebook was developed to communicate the requirements for data extraction.

Discussion/Conclusions: Although many challenges exist for using EHR data, the 5-step process demonstrates how to effectively use these data for dental research. The next step is to conduct statistical analysis in order to determine an association between obesity and periodontal disease.

ABSTRACT

Neonatal LPS-exposure, NMDAR Inhibition and HPA Axis Dysfunction in a Schizophrenia Rat Model

Efrain Rodriguez *The University of Texas – Pan American* *Class of 2015*

Sponsored by: Joao L. de Quevedo, MD, PhD, Department of Psychiatry and Behavioral Sciences

Supported by: Joao L. de Quevedo, MD, PhD, Department of Psychiatry and Behavioral Sciences; The University of Texas Medical School at Houston – Office of the Dean

Key Words: Ketamine, schizophrenia, HPA, LPS, NMDAR

Background: It is challenging to develop rodent preclinical models of complex psychiatric diseases. Recent studies suggest the involvement of neonatal immune system activation, Hypothalamic-Pituitary-Adrenal (HPA) axis dysfunction, and N-methyl-D-aspartate receptor (NMDAR) inhibition in the pathogenesis of schizophrenia. LPS, a component of gram negative bacteria cell walls, can induce activation of the neonatal immune system and ketamine, a NMDAR uncompetitive antagonist, can induce schizophrenia-like behaviors. In this study, we assessed whether administration of LPS and ketamine to rats causes HPA axis dysfunction and subsequent development of schizophrenia-like symptoms.

Methods: Neonatal male rats, age 3-4 days, were divided into 2 groups. LPS (50 μg/kg) or saline placebo solution were administered by intraperitoneal injection. During adulthood, age 53-59 days, rats from the placebo and LPS groups received a seven day treatment with either saline placebo solution or ketamine (5, 15, or 25 mg/kg) by intraperitoneal injection. After the 7 days of saline or ketamine treatment, rat locomotor activity was recorded followed by euthanasia and collection of cerebrospinal fluid, blood, and brain tissues. An ELISA corticosterone assay was performed on blood serum.

Results: Within the neonatal-placebo group, rats that received 25 mg/kg ketamine had increased locomotor activity and increased serum corticosterone compared to other neonatal-placebo group rats. Within the neonatal-LPS group, rats that received 25 mg/kg ketamine had increased locomotor activity compared to the other neonatal-LPS rats and serum corticosterone was similar among all neonatal-LPS rats.

Conclusion: Increased locomotor activity resembles the positive symptoms of schizophrenia (hyperactivity), and increased corticosterone concentration suggests HPA axis dysfunction. Within the neonatal-placebo group, NMDAR inhibition may have caused HPA axis dysfunction, and which supports the glutamate and HPA axis hyperactivity hypotheses of schizophrenia pathogenesis. Within the LPS group we had an unexpected result because serum corticosterone was similar among all rats.

ABSTRACT

Large Scale Ligand Screening of Allosteric Sites on KRAS

John Rogers *Class of 2019*

Sponsored by: Alemayehu A. Gorfe, PhD, Department of Integrative Biology and Pharmacology
Supported by: The University of Texas at Houston Medical School – Office of the Dean
Key Words: KRAS, cancer, drug-screening, Autodock

Introduction:
KRAS is a RAS protein involved in cell growth, division and apoptosis and a number of other cell functions. It is activated via a GTP binding mechanism and is found mutated in about 85% of RAS related cancers, most predominantly in pancreas and soft tissue cancers. Dr. Gorfe and other scientists have recently discovered four potential allosteric ligand-binding pockets on KRAS. This abstract presents the results of performing large scale drug-screening (aprox. two million ligands) on one of these pockets (p1) as well as a discussion on the testing of another allosteric site (p3).
Methods:
Autodock 4.2 was used to perform the ligand docking and DOVIS was used to run these Autodock tests in parallel to make the process more computationally efficient. The protein structures to dock the ligands on were obtained from molecular dynamics simulations conducted by another member of the group. Protein-ligand complexes were visualized using VMD software to confirm that Autodock chose a favorable conformation.
Results and Discussion:
The large-scale drug screening against p1 revealed several core structures that are necessary for increasing binding affinity. A large hydrophobic ring (benzene, cyclohexane, etc.) is necessary to sit in the pocket and a close nucleophilic side chain, most commonly indole rings or similar side chains are necessary to bind with a glutamic acid residue near the mouth of the pocket. Approximately two million ligands have been docked to p1 and the top 1,000 ligands will be reevaluated with a separate program, Autodock VINA, to get a consensus binding affinity measurement. The key residues found to be in close proximity to docked ligands in this pocket were GLU 37, THR 74, SER 39, and other residues found deep in the hydrophobic pocket.
Another approach was taken to studying the ligand interactions with the C-terminus pocket p3. Hocker et al. predicted that this pocket would be the primary binding site for a certain set of molecules and provided a list of potential ligands. These ligands in addition to several ligands in Sun et. al. and Shima et. al. were selected by chemical similarity from the Zinc Drugnow database and docked into p3. We discovered that the highly variable region's (HVR) orientation could have a large impact on the binding affinity of these ligands. P3 rests next to this anchor and linker region of the protein and when the HVR bends towards p3, a large pocket opens up to accommodate larger ligands. With this new information, we will screen additional ligands to determine key chemical features that are important to the binding affinity of potential ligands to p3.

ABSTRACT

Long Noncoding RNA Expression in the Mouse Model of Colitis

Trevor Schnupp *Texas A&M University* *Class of 2017*

Sponsored by: Jeremy S. Schaefer, PhD, Department of Diagnostic and Biomedical Sciences, UT School of Dentistry

Supported by: Career Development Award No. 3627 from the Crohn's and Colitis Foundation of America to Jeremy S. Schaefer, PhD

Key Words: Long Noncoding RNA, Colitis, Inflammation

Background: Non-coding RNAs (ncRNAs) are biologically active RNA molecules that are not translated into proteins to exert their effects. NcRNAs regulate gene expression to control a variety of biological processes including cell growth and differentiation. However, recent studies have implicated altered expression of the microRNA (miRNA) and long non-coding RNA (lncRNA) subcategories in disease. Studies of patients with Crohn's disease and ulcerative colitis, the principle members of a group of inflammatory conditions affecting the gastrointestinal tract surnamed inflammatory bowel disease (IBD), demonstrated that the expression of several miRNAs may be involved in disease pathobiology. Studies with the interleukin-10 knockout mouse (IL-10-/-), an animal model of intestinal inflammation, showed a similar result, specific miRNAs were elevated with pathology. However, little is known about the role of lncRNAs in these disorders. While the small 19-21 nucleotide miRNAs primarily regulate gene expression post-transcriptionally, the longer (greater than 200 nucleotides in length) lncRNAs exert their regulatory effects at the chromatin and transcriptional level.

Methods: A qPCR-based microarray was used in an initial screen of lncRNA expression in pooled colon RNA from IL-10 -/- mice with mild (pathology = 1) or severe pathology (pathology ≥ 3); pooled colon RNA from BALB/c was used as the control (pathology = 0). This initial screen identified several candidate lncRNAs with dysregulated expression. LncRNA expression was subsequently validated via replicate qPCR.

Results: The relative expression of Malat1, Hoxa11as, and RPS 15 was elevated in samples with mild pathology compared to the BALB/c controls. In IL-10-/- mice with severe pathology, Malat1, Hoxa11as, and RPS 15 expression was significantly decreased. The expression of H19 antisense was elevated in both mild and severe pathology.

Conclusion: These results suggest that an association exists between these lncRNAs and the progression of disease in the IL-10-/- mouse model of colitis. Further research is necessary to better define the exact nature of this relationship and the mechanism of action.

ABSTRACT

Investigating the Residues Important for the Co-aggregation of *Actinomyces oris* and *Streptococcus oralis*

Cara Schwab *Hendrix College* *Class of 2017*

Sponsored by: Hung Ton-That, PhD, Department of Microbiology and Molecular Genetics
Supported by: The University of Texas MD Anderson Cancer Center and The University of Texas Health Science Center at Houston (UTHealth) Graduate School of Biomedical Sciences
Key Words: Biofilm formation, teeth, protein, co-aggregation

Accumulation of biofilms on the tooth surface can lead to more serious conditions such as dental caries and periodontitis. In order to develop better preventatives for these illnesses, we need to understand more about how the oral biofilm forms. Biofilms formation occurs in a layered fashion, beginning with primary colonizers that bind the surface of the tooth and recruit other bacteria. *Actinomyces oris* is a primary colonizer, which utilizes pili for colonization. Type 1 pili bind the tooth surface, whereas type 2 pili are required for interbacterial interactions. Type 2 pili are comprised of a major backbone pilin, FimA, and one minor tip protein, either FimB or CafA. Previous research showed that the type 2 tip protein CafA binds to the receptor polysaccharide, *S. oralis*, and red blood cells which we measure using a co-aggregation assay. My goal for this summer was to pinpoint the segment of CafA responsible for this co-aggregation. Using ligation independent cloning into a plasmid tailored for protein purification, I made four different truncation constructs of *cafA* conserving regions that were previously shown to be necessary for protein stability. The recombinant proteins were incubated with *S. oralis* to identify which CafA fragment would bind the *S. oralis* receptor and inhibit co-aggregation with wild-type A. oris. If the truncated protein was essential for receptor binding, no co-aggregation would occur. If truncation was not essential for receptor binding, co-aggregation would occur. Although many of the constructs were difficult to purify, I discovered that amino acids 621-733 in CafA are not responsible for co-aggregation with *S. oralis*.

ABSTRACT

Role of *ACTA2* and *TGFB2* in Aortic Arch Development in Zebrafish

Brittney Sheena *Tulane University* *Class of 2018*

Sponsored by: Dianna M. Milewicz, MD, PhD, Department of Internal Medicine
Supported by: Dianna M. Milewicz, MD, PhD, Department of Internal Medicine
Key Words: familial thoracic aortic aneurysms and dissections, aortic arches, morpholino oligonucleotide, *ACTA2*, *TGFB2*

Background: Thoracic aortic aneurysms and dissections (TAAD) are the 15th leading cause of death in the United States. *ACTA2 and TGFB2* genetic mutations have been reported in families with TAAD. Mutations in *ACTA2* result in reduced smooth muscle cell contractility, weakening the aorta, while *TGFB2* mutations affect the transducing signals in the TGF-β signaling pathway. The embryology of ***the aortic arch*** *(AA)* ***system in zebrafish is very similar to*** that of birds and mammals. Although the complicated remodeling of the aortic arches that occurs in air-breathing vertebrates does not occur in zebrafish, the genetic and embryonic accessibility of the zebrafish make it a great model to identify genetic factors that help to set up and stabilize the initial aortic arch pattern.

Methodology: Transgenic *Tg* (*Flk1: EGFP*) zebrafish, which express green fluorescent protein in endothelial cells, were used to monitor and visualize AA development. The Control MO or ACTA2 MO or TGFB2 MO was injected into the yolk of 1- to 2-cell stage embryos at a dosage of 0.5 ng per embryo. The three groups of zebrafish were imaged using a Leica digital fluorescence microscope at 3 dpf, 4 dpf, and 5 dpf. Images focused on the AA and were taken under magnifications of 40x and 161x. Using ImageJ, the widths of AA4, AA5, and AA6 were measured from the 161x magnification images from 5 dpf.

Results and Conclusions: *ACTA2 and TGFB2* genes were independently determined to be involved in the development of zebrafish aortic arches. The average width of AA4 of the Control MO groups was 0.104 inches, while the average AA4 width of ACTA2 MO zebrafish and TGFB2 MO zebrafish were 0.129 and 0.131, respectively. The average control width of AA5 was 0.101, while with average width of ACTA2 MO zebrafish was 0.126 and TGFB2 MO was 0.129. The average width of AA6 of the control zebrafish was 0.107 in, while the average AA6 width of ACTA2 MO zebrafish and TGF-β2 MO zebrafish were 0.138 and 0.137, respectively. The increased AA widths in the ACTA2 MO and TGFB2 MO zebrafish were indicative of the genes' role in early aortic arch development. This system could be used to screen novel FTAAD genes for a role in aortic development.

ABSTRACT

Retinal Morphology of *Clock* Mutant Mice

Luke Tseng *Duke University* *Class of 2017*

Sponsored by: Christophe P. Ribelayga, PhD, Department of Ophthalmology and Visual Science

Supported by: NIH grant EY018640 to Christophe P. Ribelayga, PhD; The University of Texas at Houston Medical School – Office of the Dean

Key Words: Retina, retinal morphology, circadian rhythms, *Clock* mutation

Background: Circadian clocks intrinsic to the retina orchestrate retinal physiology and function on a daily basis. Central to the molecular clock mechanism in mammals is the transcription factor formed by the proteins CLOCK and BMAL1 that, upon dimerization, drives rhythms of gene expression and thereby of physiology. Previous studies have reported functional and morphological disorganization in the retina of *Bmal1* KO mice. Although it has been shown that a mutant *Clock* allele results in a dysfunctional CLOCK protein, whether the *Clock* mutation affects retinal function and/or morphology remains to be determined. Here we investigated the morphology of the retina of *Clock* mutant mice using confocal immunofluorescence microscopy.
Methods: Fixed retinas from +/+ (WT), *Clock*/+ (HET), and *Clock*/*Clock* (CLK) mice aged 2-6 months were processed using immunohistochemistry. Frozen retinal sections were labeled with antibodies against a variety of cell markers and mounted in DAPI. Morphological features and their respective antibodies were as follows: cones (α-cArr), starburst amacrine cells (α-ChAT), melanopsin cells (α-melanopsin), dopaminergic amacrine cells (α-TH), rod spherules (α-PSD95), ribbon synapses (α-CtBP2), bipolar cells (α-CHX10), rod bipolar cells (α-PKC), and horizontal cells (α-CALB). In addition, pieces of retinal whole-mounts from 6 WT, 6 HET, and 4 CLK mice were labeled with α-cArr, α-ChAT, α-melanopsin, and α-TH, to investigate the spatial distribution of the respective cell types. Images of the immunolabeled retinal tissue were taken using fluorescence or confocal microscopy. In addition to qualitative inspection of morphology, quantification of retinal layer thicknesses, cone pedicle height, and cell spatial density were done using the Zen Blue software (Zeiss).
Results: We found that the whole retina, inner nuclear layer and inner plexiform layer were slightly thinner (~ -10%) in HET retinas, compared to WT or CLK retinas. All immunolabeled cell types were present in all the genotypes and no apparent deformities for any cell type were found. No significant differences in spatial density were found for cones, dopaminergic amacrine cells, starburst cells or melanopsin cells between genotypes.
Conclusion: Experimental data showed no gross morphological defects in the retinas of *Clock* mutant mice. A plausible explanation for these results is that contrary to BMAL1 that is an essential and non-redundant clock component, CLOCK has partially redundant functions with another protein, NPAS2. It may thus be that the lack of defects we observed reflects the function of NPAS2. Further studies will use a *Clock;NPAS2*$^{-/-}$ mouse to investigate this hypothesis.

ABSTRACT

ITD Structured Literature Review

Sarah Tucker *Baylor University* *Class of 2016*

Sponsored by: Richard N. Bradley, MD, Department of Emergency Medicine
Supported by: Richard N. Bradley, MD, Department of Emergency Medicine; The University of Texas at Houston Medical School – Office of the Dean
Key Words: Impedance threshold device

The impedance threshold device was designed to create a greater negative intrathoracic pressure during the decompression phase of CPR, drawing more blood to the chest to be pushed out to the body in the succeeding compression. Many trials have tested the effectiveness of the ITD; while some studies show ITD use improves outcomes, others show the ITD to have no positive effect. The current study is a structured literature review that examines all relevant existing literature to answer the following question: does ITD use significantly improve outcomes in cardiac arrest situations? Using a specific search strategy we found 111 articles. We then screened abstracts, reviewed their full texts, and selected 32 relevant articles based on specific inclusion and exclusion criteria. Furthermore, we have begun the process of evaluating each article for bias (though this step is not yet complete). We pooled data from seven studies and found that in comparing standard CPR with and without an ITD, the relative risk of ROSC is 1.15 [0.85, 1.53] (95% CI). Interestingly, in comparing standard CPR with and without the ITD, the relative risk of favorable neurologic outcome (MRS ≤ 3) is 0.97 [0.82, 1.15]; in contrast, in comparing standard CPR to ACD CPR with an ITD, the relative risk of favorable neurological outcome is 1.44 [1.16, 1.80]. These results show the ITD generally only has a slightly positive impact on cardiac arrest outcomes. Further work remains to be done in evaluating the articles for bias and examining other outcomes.

ABSTRACT

Association of β-catenin-mediated Wnt Pathway Genes with Non-syndromic Cleft Lip with or without Cleft Palate

Kimberly Westerman *Rice University* *Class of 2016*

Sponsored by: Brett. T. Chiquet, DDS, PhD, Department of Pediatric Dentistry, UTHealth School of Dentistry

Supported by: Brett. T. Chiquet, DDS, PhD, Department of Pediatric Dentistry, UTHealth School of Dentistry; UTHealth School of Dentistry Research Office

Key Words: NSCLP, Wnt pathway, single nucleotide polymorphism, genotyping

Introduction: Non-syndromic cleft lip with or without cleft palate (NSCLP) is a common birth defect that occurs in 1 in 700 newborns, affecting 4,000 newborns per year in the U.S. NSCLP is caused by genetic and environmental factors. Previous studies have shown genes in the β-catenin-mediated Wnt pathway are expressed in craniofacial tissues and play a role in craniofacial development in animal models; some of these genes have also been shown to be associated with NSCLP. This study aims to expand on those results by analyzing the β-cantenin-mediated Wnt pathway genes in a NSCLP dataset.

Methods: Sixty single nucleotide polymorphisms (SNPs) from 16 genes were genotyped in 243 multiplex families (151 Caucasian, 92 Hispanic) and 564 simplex parent-child trios (348 Caucasian, 216 Hispanic) to assess their roles in NSCLP. The genes tested with the number of SNPs analyzed in parenthesis are as follows: *LRP5* (4), *LRP6* (3), *FZD6* (6), *WNT3* (3), *WNT3A* (6), *WNT5A* (1), *WNT8A* (1), *WNT9B* (1), *WNT11* (3), *DVL2* (3), *AXIN1* (7), *AXIN2* (6), *APC* (6), *GSK-3B* (6), *CTNNB1* (2), *DKK1* (2). The SNPs were genotyped using TaqMan® SNP Genotyping Assays and the Viia7 Real-Time PCR System for fluorescence detection. The SNPs were analyzed using FBAT, FBAT-e, and HBAT. To correct for multiple testing, a modified p-value of 0.003125 (0.05/16 genes) was used.

Results: Four single SNPs in genes *FZD6*, *WNT3A*, *WNT5A*, *WNT11*, and 46 2+ SNP haplotypes in *AXIN1*, *AXIN2, FZD6, LRP5, WNT3A,* and *WNT11* were associated with NSCLP. Putative promotor or enhancer SNPs were identified in two of the four significant single SNPs and 65% of the significant haplotypes. *WNT11* SNP rs1533767 had the strongest association in Caucasians (p=0.000006).

Conclusion: Genes *FZD6, LRP5, WNT3A, WNT5A, WNT11, AXIN1*, and *AXIN2* may contribute to the genetic cause of NSCLP in Caucasians and Hispanics. Our results suggest that promotor variants could play an important role in clefting etiology. Future studies will focus on testing for gene-gene interactions and to determine if the promotor variants alter the promotor function.

ABSTRACT

Tracking Sensorimotor and Cognitive Improvements After Mild Traumatic Brain Injury

Michelle J. Won *Rice University* *Class of 2017*

Sponsored by: Anne B. Sereno, PhD, Department of Neurobiology and Anatomy
Supported by: Anne B. Sereno, PhD, Department of Neurobiology and Anatomy; The University of Texas at Houston Medical School – Office of the Dean
Key Words: Mild Traumatic Brain Injury (mTBI), iPad, ImPACT, King-Devick

Mild traumatic brain injury (mTBI) annually affects 1.7 million people and can lead to prolonged post concussive symptoms such as headaches, forgetfulness, and impairment of everyday functions. An accurate objective measurement of symptomology is necessary to track recovery and perhaps predict residual symptomology. Our study used a novel iPad app to measure sensorimotor ability (ProPoint task) and cognitive control (AntiPoint task) in an mTBI population (n=10; mean age=18.7) coming into a concussion clinic. We sought to test whether performance on these measures related to time since injury (mean day since injury(DSI)=50.3), with performance improving over time. We also tested Control subjects (n=9; mean age=17.6; mean DSI=52.8), including both orthopedic injured (n=4) and uninjured (n=5) participants. In addition to the tablet tasks, all participants were tested on two standard concussive measures: the King-Devick task (a sports sideline assessment of concussion) and the Immediate Post-Concussion Assessment and Cognitive Testing (ImPACT) Symptom Scale.

All groups were matched in age, gender, and days since injury. We found that the mTBI group was significantly slower than Controls on both ProPoint and AntiPoint tasks, and both ProPoint and AntiPoint response times (RTs) decreased as days since injury increased. Additionally, there was a significant interaction between DSI and Group (mTBI and Control groups) with the reduction of AntiPoint RT across DSI significantly greater in the mTBI group compared to the Control group. In contrast, we found no significant differences between Groups on ImPACT Symptom Scores or King-Devick scores and no significant changes in performance on these measures with respect to days since injury. Additionally, there was no Group by DSI interaction for these other concussive measures; that is, no group differences with respect to DSI changes. A similar pattern of findings remained even when dropping the uninjured controls (i.e., including only orthopedic controls, n=4), although the interaction between Group and DSI for AntiPoint RT was no longer significant (p=0.12). These findings suggest that these novel iPad tasks are significantly more sensitive to changes in sensorimotor and cognitive changes across time than the current standard concussive measures. Such measures may prove an accurate objective measurement of neurocognitive function and provide a tool to objectively track cognitive deficits and perhaps predict residual symptomology. Future work may use a within subject design to explore whether performance on these tasks in an individual can predict residual symptomology.

ABSTRACT

Intestinal Transit and Contractility of the Small Intestine in Edema Induced Rats

Grace Yang *Rice University* *Class of 2016*

Sponsored by: Karen Uray, PhD, Department of Pediatric Surgery
Supported by: Karen Uray, PhD, Department of Pediatric Surgery
Key Words: Edema, Intestine, Contractility, Transit, Ileus, Elastic Modulus

Background Intestinal edema is an excess accumulation of fluid in the interstitial spaces of the intestinal wall which results in a condition called ileus, a decrease in intestinal motility. We sought to explore the link between decreased muscle contractility and varying degrees of intestinal edema, and the extent to which edema contributes to decreased intestinal transit.
Methods Varying levels of edema were introduced into rats by partially occluding the superior mesenteric vein and infusing resuscitation fluid. Rats were randomly divided into four groups that were injected with 20, 40, 80 or 120 ml/kg of saline solution to induce different levels of edema. Six hours after induction of edema, rats were sacrificed and the distal small intestine was collected for measurement of contractility. Longitudinal contractile activity of the intestine was measured by hanging a length of the small intestine in the organ bath where the contractile force of the intestine was monitored by an external force displacement transducer connected to a PowerLab. Parameters such as integral, integral relative to minimum, average cyclic height (amplitude), average cyclic minimum (tone) and average cyclic frequency were calculated and normalized to the tissue cross sectional area. Intestinal transit was measured by injecting a nonabsorbable dextran labeled with fluorescent isothiocyanate (FITC) dye into the proximal duodenum 30 minutes before sacrifice. After sacrifice, the entire small intestine was removed and divided into 10 equal segments, and the FITC-Dextran concentrations in each segment were determined by spectrophotometry. The geometric center for each rat was then determined based on the distribution of the FITC-Dextran. The elastic modulus of the intestine was also calculated. The set up was similar to that used for contractility measurements. However, after - equilibration, intestines were stretched in increments of 1 mm with recordings of the new length and its corresponding force measured by the tensiometer. The elastic modulus was then calculated by dividing engineering stress by engineering strain.
Results Integral relative to minimum and amplitude generally followed the same trend as that of intestinal transit- decreasing as the level of edema increased. Tone, on the other hand, increased with increasing levels of edema. The elastic modulus decreased as the levels of edema increased, meaning that the more edematous an intestine became, the less resistant the intestine was to deformation.
Conclusion Edema induced decreased contraction amplitude and decreased elastic modulus but increased tone. Integral relative to minimum and amplitude correlated well with intestinal transit.

ABSTRACT

Review of Ferumoxytol as Contrast Agent for fMRI

Caroliina Yin *New Jersey Institute of Technology* *Class of 2017*

Sponsored by: Alan Prossin, MD, Department of Psychiatry and Behavioral Sciences
Supported by: Alan Prossin, MD, Department of Psychiatry and Behavioral Sciences; The University of Texas at Houston Medical School – Office of the Dean
Key Words: BOLD, fMRI, ferumoxytol, CBV, iron oxide, contrast agent

INTRO - Development and application of blood oxygen level dependent MRI (BOLD MRI) research paradigms has made substantial contribution to modern neuroscience. However, the incremental gains to knowledge of basic neuroscience processes are beginning to lag, possibly due to the lack of specificity associated with BOLD fMRI data. Enhancing contrast in fMRI research via pre-treatment with ferumoxytol shows significant promise in enhancing specificity associated with findings from fMRI research *(Mandeville 1999*; *Kim 2013*;*Mandeville 2012*). Ferumoxytol, an utltrasmall paramagnetic iron oxide nanoparticle, is an FDA-approved medication prescribed for treatment of specific iron deficiency anemia in humans. Ferumoxytol may also have promise as an fMRI contrast. It has long half-life, enabling a steady concentration during experimental imaging (*Kim 2013*) as compared to the short half-life of other commonly used contrasts (*Mandeville 2012*). However, it remains unclear whether benefits of ferumoxytol contrast enhanced MRI are reliable and worthy of investigating their ability to enhance specificity of BOLD fMRI neuroscience research.
METHODS - We reviewed existing literature to determine whether evidence shows pre-treatment with ferumoxytol enhances the fMRI BOLD response and if so, by what mechanisms. Using PUBMED, we confined search criteria to the following mesh terms in body text: ferumoxytol AND "fmri".
RESEARCH STUDIES - This search yielded 11 publications: 6 directly applicable to our question of which only 3 represented novel research findings and 3 discussed possible mechanisms for ferumoxytol's effects on fMRI. Two of the manuscripts presented novel results from separate human studies, identifying advantages with iron contrast fMRI as opposed to standard BOLD fMRI. One human study of 4 volunteers finger tapping in response to audio cues found that ferumoxytol pre-treatment improved contrast to noise ratio (CNR) by a factor of 2.0-2.9 *(Qiu et al. 2012)*. Evidence suggests these benefits derive indirectly from CNR improvements that are greater in amplitude than concurrent decrease in signal to contrast ratio (Mandeville 2012). In a resting state fMRI study, ferumoxytol administration was associated with higher resolution images capable of differentiating resting state networks from nearby blood vessels (*D'Arceuil et al. 2013)*. Similar improvements were found in an fMRI study of six rats. In this study, ferumoxytol enhanced visualization of olfactory bulb activation at 9.4T *(Poplawsky and Kim 2014)*. Additionally, ferumoxytol administration increases fMRI sensitivity to brain microvasculature *(Qiu et al. 2012)*. However, these benefits diminish at stronger

magnetic fields (*Kim et al. 2013),* suggesting that potential gains from ferumoxytol are viable even for MRI scanners with lower field capacities.

OTHER FINDINGS AND FUTURE DIRECTION - Our review of the limited extant literature found ferumoxytol pre-treatment to amplify fMRI detection power. However, exactly how these achievements are obtained remains unclear. The few publications resulting from our search highlight the novelty of iron enhanced fMRI research, but their preliminary results suggest that ferumoxytol has diverse applications beyond treatment for iron deficiency anemia. Compared to BOLD fMRI, ferumoxytol-enhanced fMRI has shown higher sensitivity and spatial specificity (*Qiu et al. 2012*), which can help expand knowledge about pharmacological impacts on neural function, enhancing specificity of conventional BOLD fMRI, and further study mechanisms underlying the BOLD response.

ABSTRACT

Characterization of Mice Lines Conditionally Deficient for connexin36 in Rod or in Cone Photoreceptors

Sean Youn *Rice University* *Class of 2018*

Sponsored by: Christophe P. Ribelayga, PhD, Department of Ophthalmology and Visual Science

Supported by: NIH grant EY018640 to Christophe P. Ribelayga, PhD; The University of Texas at Houston Medical School – Office of the Dean

Key Words: gap junctions, retina, photoreceptors, connexin36

Background: Photoreceptors are electrically coupled through gap junctions that are formed of connexins. The presence of connexin36 (Cx36) between cones and between rods and cones has been clearly established, but whether rods express Cx36 has remained elusive. Here we strove to gain evidence that Cx36 is the rod connexin using rod- or cone-specific Cx36 knock out (KO) mice and confocal immunofluorescence microscopy detection of Cx36. We hypothesized that the absence of Cx36 in one of the two coupled photoreceptor types would result in no gap junction formation--as this is generally observed for most connexins-- and thus that the absence of Cx36 in either rods or cones should eliminate rod-cone gap junctions.

Methods: Wild type, cone-specific *Cx36*$^{-/-}$ (*HRGP-cre;Cx36*$^{f/f}$), and rod-specific *Cx36*$^{-/-}$ (*Rho-i75cre;Cx36*$^{f/f}$) mice were euthanized by cervical dislocation. The eyes were promptly harvested, fixed in paraformaldehyde, cryoprotected and cryostat sectioned into 12-µm slices. Sections were subject to antigen retrieval and blocked in normal donkey serum, stained with primary antibodies against Cx36 and cone arrestin, and then with donkey-anti-mouse and donkey-anti-rabbit secondary antibodies conjugated to Dylight549 and Alexa488 fluorophores, respectively. Sections were then stained with DAPI and observed under a confocal microscope (Zeiss 780).

Results: In the outer plexiform layer (OPL) of the wild type retina, Cx36 plaques were found at the telodendria points of contact between cone pedicles (consistent with cone-cone coupling), as well as on the roof of the cone pedicles and along the telodendrias (consistent with rod-cone coupling). In addition, sparse plaques of small size were found throughout the outer nuclear layer (ONL) not visibly associated with cone axons (consistent with rod-rod coupling). In the rod-specific KO, there was a ~68% decrease in the number of Cx36 plaques in the ONL + OPL, but Cx36 plaques were still visible at cone-cone contact points. In the cone-specific KO, there were no plaques on top of cone pedicles or associated with the telodendrias or telodendria contact points. There were few remaining plaques in the OPL + ONL, presumably associated with rod-rod coupling. Noteworthy was that the expression of Cx36 plaques located below the cone pedicles (in the dendrites of bipolar cells) and in the inner plexiform layer was not significantly changed in either of the Cx36 knockouts compared to the wild type.

Conclusion: The observation that Cx36 plaques are visible only at cone-cone contact points in the rod-specific KO indicates that most gap junctions associated with cone pedicles are rod-cone and that Cx36 is expressed in the rods. The difficulty of finding Cx36 plaques between photoreceptors in the cone-specific KO is consistent with the small size of the gap junctions between rods and the limitation imposed by the point spread function of the confocal microscope. Future experiments will include markers of the rod membrane (e.g. PSD95) to confirm the association of these plaques with the rods.

ABSTRACT

The Effects of the Glycocalyx and Shear Stress on Metastatic Potential

Allen Zhou *University at Buffalo, SUNY* *Class of 2016*

Sponsored by: Pamela Wenzel, PhD, Department of Pediatric Surgery
Supported by: Pamela Wenzel, PhD, Department of Pediatric Surgery; The University of Texas at Houston Medical School – Office of the Dean
Key Words: Glycocalyx, YAP/TAZ, Cell Motility, Shear Stress, Oncogenes

Background
YAP and TAZ are two oncogenic proteins that respond to biomechanical cues, including extracellular matrix stiffness (ECM), cell density, and cell elasticity. The Hippo pathway negatively regulates YAP by phosphorylating serine residue 127 of the YAP protein. In the absence of Hippo activity, YAP and TAZ translocate into the nucleus and transcriptionally upregulate genes that drive proliferation, survival, and invasive behavior. Many studies implicate mechanical cues in YAP/TAZ regulation, but little if any published work examines the role of the glycocalyx in determination of YAP/TAZ activity. The glycocalyx is a glycoprotein present on the cell surface that senses mechanical force and modifies cell-cell/cell-ECM adhesion, migration, and proliferation. The glycocalyx is exquisitely sensitive to frictional force caused by fluid flow, or shear stress, in the vasculature and lymphatics. The nature of my research is to evaluate the role of the glycocalyx and shear stress in regulation of cancer cell motility and YAP/TAZ target gene expression.
Experiments
To disrupt glycocalyx function, we enzymatically removed the heparin component of the glycocalyx on breast cancer (MDA-MB231) and prostate cancer (PC3) cells with heparinase III. Migration speed was compared by analyzing motility throughout six hours of static culture with time-lapse imaging. YAP/TAZ activation was quantified by immunoblotting for phosphorylated and total YAP, TAZ, and beta-actin. Downstream targets of YAP/TAZ and metastasis-related genes, MMP9, AMOTL2, and CTGF, were examined by quantitative RT-PCR. We then compared the effects of glycocalyx removal in the presence of 0.05 dyne/cm^2 wall shear stress (WSS) using microfluidic channels to simulate lymphatic flow. Each experiment included cells with and without heparinase treatment under static and WSS conditions.
Results
In both breast and prostate cancer cell lines, heparinase treatment significantly increased cell motility under static conditions ($p<0.001$). Activation of YAP and TAZ and expression of downstream target genes, CTGF, AMOTL2, and MMP9, were not significantly changed by glycocalyx removal. When cells were exposed to WSS without heparinase treatment, cell motility was significantly induced, consistent with previous unpublished work in the Wenzel lab. Motility triggered by heparinase treatment under static conditions was not further increased by WSS, implicating the glycocalyx in sensing and responding to mechanical forces in a YAP/TAZ independent fashion, perhaps signaling through a redundant mechanism that

drives motility in response to fluid flow.

Conclusions

Our data suggest that the removal of the glycocalyx can accelerate migration of cancer cells under static conditions by decreasing cellular adhesion, but cells fail to respond to mechanical forces when WSS is present. In the current study, YAP and TAZ were not involved downstream of glycocalyx signaling. Possible mediators of glycocalyx function will be investigated in future studies.

UTHealth™ | Medical School

The University of Texas
Health Science Center at Houston

International Medical Students

ABSTRACT

Characterization of Centrin5 in Trypanosoma brucei

Yongyan Chen *Shanghai Jiao Tong University School of Medicine* *Class of 2016*

Sponsored by: Ziyin Li, PhD, Department of Microbiology and Molecular Genetics
Keywords: Trypanosoma brucei, RNAi, Centrin5, epitope tagging

Background: Centrins are evolutionarily conserved calcium-binding proteins, which are ubiquitously found in eukaryotes and participate in a number of cellular processes, including centriole and basal body duplication. In Trypanosoma brucei, an early branching parasitic protozoan and the causative agent of human sleeping sickness, five centrins have been identified, among which TbCentrin1 (akaTbCen3), TbCentrin2, and TbCentrin4 (aka TbCen1) are localized to the flagellar basal body and regulates basal body duplication and segregation, and one of them, TbCentrin2, has an additional role in Golgi biogenesis. TbCentrin3 regulates cell motility by maintaining the stability of an inner arm dynein in the flagellum. However, little is known about the subcellular localization and function of the TbCentrin5 (Tb927.11.13900). Therefore, the aim of this study is to find out whether TbCentrin5 plays any essential role in regulating T. brucei.

Method: The whole experiment was divided into following mainly three parts:

Trypanosome cell culture and RNAi construction

Procyclic 29–13 cell line was cultivated and RNAi of TbCentrin5 was carried out using the stem-loop RNAi construct. To induce RNAi, the clonal cell line was incubated with 1.0 μg ml^{-1} tetracycline, and cell

growth was monitored by counting the cell number with a hemacytometer. The cell growth curve would be made to detect any difference between the controlled cell lines and the induced one.

In situ epitope tagging of TbCentrin5

A DNA fragment corresponding to the C-terminal coding region of TbCentrin5 was amplified by PCR and cloned into the pC-3HA-PAC vector and transfected into two cell lines, one is 29-13 cell line and another one was harboring the pSL-TbCentrin5 RNAi construct.

Immunofluorescence microscopy

29-13 cell line which already had the TbCentrin5 tagged with triple-HA were incubated with the anti-HA antibodies, then the slides were mounted in the mounting medium containing DAPI, using the immunofluorescence microscopy to determine the localization of centrin5 in T.brucei.

Result: The cell growth curve showed the density of Tbcentrin5 RNAi cells wasn't evidently different from the non-induced control cells and there wasn't any unusual phenotype like spinning and tumbling or losing motility under a light microscopy. Under a immunofluorescence microscopy, TbCentrin5 looked like localizing in the whole cytoplasm, but the signal was very faint.

Conclusion: Through this study, TbCentrin5 may not be proved having any essential function in regulating Trypanosoma brucei.

ABSTRACT

Intra-Lesion Heterogeneity in Multiple Sclerosis

Atsushi Hayashi *Tokushima University* *Class of 2018*

Sponsored by: Refaat E. Gabr, PhD, Department of Diagnostic and Interventional Imaging
Keywords: Multiple Sclerosis, MRI, Lesion Heterogeneity

Background: Multiple sclerosis (MS) is a chronic inflammatory disease of the central nervous system (CNS). MS is characterized by demyelinating white matter lesions (WML). Those lesions can be detected using magnetic resonance imaging (MRI). WML appear as hypo-intensity on T1-weighted MRI (T1 black holes), hyper-intensity on T2-weighted MRI, enhancement on contrast-enhanced scans, etc. These variations may reflect heterogeneity in WMLs.
Objective: To investigate characteristics of MS lesions and intra-lesion heterogeneity.
Methods: We conducted a literature review of lesion heterogeneity in MS [1-4]. Besides, we implemented one MRI technique using algebraic techniques (ADIMA), using dual-echo MRI data using MATLAB (a high-level scientific language to explore and visualize data). ADIMA [1] uses normalized images of the PD-weighted (PDw) image and T2-weighted (T2w) scan (pixel values in the range 0–1). Next, a pseudo-T1 (pT1) image is calculated from PDw and T2w (pT1=PDw-T2w). Finally, the absolute intensity difference between the PDw and pT1 is calculated to obtain the ADIMA image.
Results: There are two basic ADIMA types of lesions: ADIMA-b which is the bright regions within WML, and ADIMA-d, the subset of dark regions within WML. ADIMA-b has high T1 and T2 values, and low magnetization-transfer ratio (MTR), and is only partly contained within T1-WML [1]. ADIMA-d has slightly low T1 and T2, and slightly high MTR, and similar underlying characteristics to T2-WML. The combined ADIMA-b with ADIMA-d has a mean volume much greater than WML detected on T2w. Fig. 1 shows example processed MRI showing ADIMA-b (arrow lesion core) and ADIMA-d (arrow dark rim) regions processed using MATLAB.
Discussion: MRI dual-echo data analysis with algebraic methods enabled the classification of conventional WML into new groups that have different characteristics. This is a promising approach for designing new MRI pulse sequence to study MS lesion heterogeneity. Lesion heterogeneity can help confirm the diagnosis of MS, assess the response to treatment, and determine the disease pattern of MS.

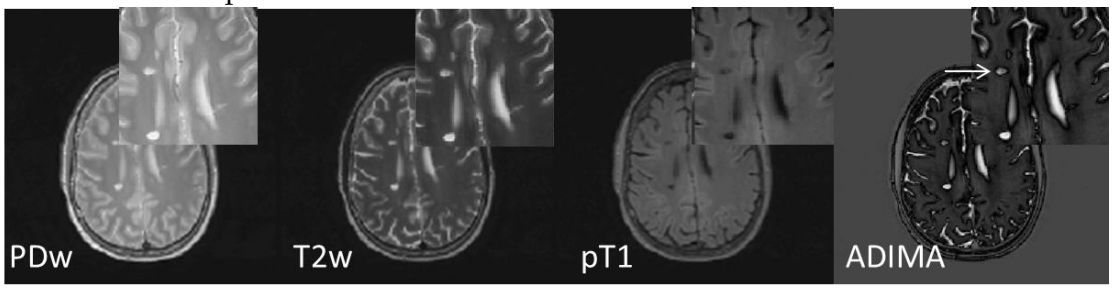

References: [1] Yiannakas, Marios C., et al. "ADvanced IMage Algebra (ADIMA): a novel method for depicting multiple sclerosis lesion heterogeneity, as demonstrated by quantitative MRI." Multiple Sclerosis Journal (2012): 1352458512462074. [2] Lucchinetti, Claudia, et al. "Heterogeneity of multiple sclerosis lesions: implications for the pathogenesis of demyelination." Annals of neurology 47.6 (2000): 707-717. [3] Llufriu, Sara, et al. "T2 hypointense rims and ring-enhancing lesions in MS." Multiple Sclerosis 16.11 (2010): 1317-1325. [4] Haacke, E. Mark, et al. "Characterizing iron deposition in multiple sclerosis lesions using susceptibility weighted imaging." Journal of Magnetic Resonance Imaging 29.3 (2009): 537-544.

ABSTRACT

Saki Higashi *University of Tokushima* *Class of 2016*

Sponsored by: Larry Kramer, MD, Department of Diagnostic and Interventional Imaging
Keywords: Trypanosoma brucei, RNAi, Centrin5, epitope tagging

Introduction: Visual impairment (VIIP) in astronauts is a recently described phenomenon, hypothesized to be due to microgravity-induced intracranial hypertension that occurs during extended missions on the International Space Station (ISS). Environmental factors such as carbon dioxide (CO2) which is present at abnormally high levels has also been hypothesized to be contributory due to its vasodilatory effect known to increase intracranial pressure. The purpose of this study was to determine the quantitative changes in cerebral blood flow (CBF), internal jugular venous flow (IJVF) and cerebrospinal fluid flow (CSFF) using a terrestrial-based analog model of the space environment in an effort to better understand changes in intracranial fluid hydrodynamics that could contribute to VIIP.
Methods: 6 subjects were tested in two groups of 3 subjects each. Each group underwent baseline testing and then randomly assigned to a condition (0.5% CO2 or ambient air) defined as Condition 1(C1) and condition 2(C2). C1 and C2 were combined with negative 12 degree head down tilt (HDT) for 24 hours defined as session 1(S1). HDT was used to represent the analog of cephalad fluid shift observed in microgravity. At the end of the condition the subjects underwent an additional 2 hours of 3% CO2 defined as session 2(S2) to mimic acute exposure to high levels of CO2. A crossover design was used after each group so each subject experienced condition 1 or 2 with a one week washout period between conditions. A CINE phase-contrast flow sequence was acquired perpendicular to the internal carotid artery and the mid cerebral aqueduct using a 3T magnet at baseline and then following each condition and session. Total CBF, IJVF and CSFF were calculated on a dedicated workstation using flow analysis software. C1 and C2 remain blinded to the research team.
Results: There was a significant decrease in CBF volume in C1S1 compared to baseline (P= 0.02) and a significant increase in CBF volume in C1S2 compared to C1S1 (p=0.05). CBF volume in C1S2 compared to baseline was not significantly different (P=0.08). There was no significant change in CBF volume between baseline and C2S1 or between baseline and C2S2. There was no significant change in IJVF and CSFF between baseline and any condition or session.
Discussion/Conclusion: Our results show a significant decrease in CBF volume due to HDT indicating increased outflow resistance that is reversed by 2 hours of inhaled 3% CO2. Increased outflow resistance is hypothesized due to cephalad fluid shift with HDT and microgravity. We hypothesize that abnormally high levels of CO2 measured on the ISS compensates for increased outflow resistance secondary to vasodilatation of the carotid artery with resultant increased CBF. Our terrestrial model of the ISS environment divided into individual components of HDT and CO2 thus helps explain the paradoxical preserved middle cerebral artery flow observed in astronauts in microgravity using transcranial Doppler. The combination of increased outflow resistance due to cephalad fluid shift counteracted by CO2

induced vasodilatation may accentuate transient intracranial pressure increases normally found during systolic CBF. The results of this study, therefore further supports the hypothesis of raised intracranial pressure as the etiology of visual impairment in astronauts.

ABSTRACT

Mechanism of Subcellular Trafficking of ABCG transporter White

Hongyue Jiang *Shanghai Jiao Tong University School of Medicine* *Class of 2017*

Sponsored by: Sheng Zhang, PhD, Center for Metabolic and Degenerative Diseases, the Brown Foundation Institute of Molecular Medicine, Department of Neurobiology and Anatomy

Keywords: ABCG1 transporter, White, subcellular trafficking, lysosome-related organelles

Introduction: ABCG1 is an ATP-binding cassette transporter important for cholesterol homeostasis and insulin secretion. One interesting layer of regulation of ABCG1 is at subcellular level, where it is predominantly localized on vesicular-like organelles inside the cytoplasm, although little is know about the origin of these ABCG1-positive organelles and how such specific subcellular targeting of ABCG1 is achieved. Our study aims to address these questions by analyzing *White*, a close homologue of human ABCG1 in model organism *Drosophila.*
White corresponds to the first, white eye-colored fly mutant isolated by Morgan a century ago that laid the basis of modern genetics. At subcellular level, White protein localizes specifically on a unique cytoplasmic organelle called pigment granule (PG), a type of lysosome-related organelles (LROs). White determines the pigmentation of adult tissues such as eyes and renal-like-malpigian tubules by forming heterodimer with Brown or Scarlet, two other ABCG family transporters, to transport red or brown pigments, respectively, into PGs. Importantly for our study, more than 85 eye color mutants exist in *Drosophila* and many of them, such as mutants in the conserved adaptor protein-3 (AP-3) complex and vacuole protein sorting complex class C (VPS-C), affect White function by disrupting the proper subcellular localization and/or trafficking of White to PGs. Accordingly, we aim to carry out systematic imaging analyses of this collection of eye color mutants to determine the sequential of trafficking events and the governing principles of White targeting to PGs. The results will shed light on the mechanism controlling the specific subcellular trafficking and distribution of ABCG1 in human cells.
Methods: Dissect malpigian tubules from the wildtype control and difference groups of eye color mutants, including transporters (*bw1*, *st1*, "*bw1;st1*" double), AP-3 complex (*or1, rb1, g1, g2, cm1*), VPS-C complex (*car1*, *dor1*), BLOC-2 (*p1*, *pp*), as well as Rab38 (*ltd1*) and Rab38GEF (*ca1*) alleles, followed by multiple-immunofluorescent labeling for White, F-Actin, DNA (DAPI) and lectins (PNA). High-resolution imaging analyses using compound fluorescent microscope, to determine the subcellular distribution and morphologies of White-positive structures.
Results: White is specifically localized on (1) LRO vesicles of both large and small sizes in wildtype; (2) mainly on vesicles of large sizes in *bw1* mutant; (3) only on vesicles of much smaller sizes in *st1* mutant; (4) diffusively distributed and its level significantly reduced in "*bw1;st1*" double mutant; (5) no or few visible granules in AP-3 mutants; (6) large web-like structures of abnormal morphology in VPS-C mutants; (7) compact, high-density vesicles of small uniform sizes in BLOC-2 mutants; (8) abnormal endosomal structures in *ltd* mutants.
Conclusions: (1) The maturation and exit of White (and likely ABCG1) from the ER requires its

obligate dimer formation with Brown or Scarlet; (2) Co-transporters Brown and Scarlet determine two distinct populations of PGs of different unique sizes; (3) PG-targeting of White is mediated through multiple intermediate sorting steps involving the TGN and endosomes that are sequentially mediated by sorting and transport machineries including AP-3, VPS-C, BLOC-2, Rab38 and others that will be further investigated in future.

ABSTRACT

Intracellular Location of PSNRPS4 in *Pezicula* sp. NRRL12192

Guilin Li *Shanghai Jiao Tong University School of Medicine* *Class of 2020*

Sponsored by: Gerald F. Bills, PhD, Institute of Molecular Medicine

Keywords: Nonribosomal Peptide Synthase, *Pezicula* sp. NRRL12192, GFP, Sporiofungin

Background: Sporiofungin, produced by the fungus *Pezicula* sp. NRRL12192, is a member of echinocandin class of fungal lipopeptides that provide the parent molecules of three different antifungal drugs. Echinocandins prevent fungal growth by inhibiting fungal cell wall biosynthesis. The nonribosomal peptide synthetase (NRPS)-polyketide synthase (PKS) gene cluster responsible for sporiofungin biosynthesis has not been elucidated to date. Genomic sequencing of *Pezicula* sp. NRRL12192 identified the NRPS-PKS gene cluster responsible for sporiofungin biosynthesis. Disruption mutant of the NRPS gene *psnrps4* in this gene cluster abolished sporiofungin production, suggesting that *psnrps4* is involved in the sporiofungin biosynthesis. However, the intracellular location of the echinocandin NRPS protein is unknown in echinocandin-producing fungi.
Significance: Knowing the location of PSNRPS4 in *Pezicula* sp. NRRL12192 is necessary to understand the natural function of the echinocandins and whether they are synthesized in intracellular organelles and whether they interact with producing strain's cell wall.
Hypothesis: PSNRPS4 is located in an intracellular organelle, e.g. the Golgi apparatus or endoplasmic reticulum. We can visualize its location by fusing a green fluorescent protein (GFP) gene to the NRPS gene. When they are co-expressed in the fungal cell, their cytological location can be visualized by fluorescence microscopy.
Experimental Design:
(1) To fuse a gfp with *psnrps4*, 3' region of *psnrps4* before the stop codon, the downstream of *psnrps4*, the *gfp* reporter gene were amplified and inserted into pAg1-Nat1 to give the vector pAg1-Nat1-psnrps4-gfp.
(2) *Pezicula* sp. NRRL12192 was transformed with the vector by *Agrobacterium tumefaciens*-mediated transformation. After isolation of single spores from the transformants, the positive transformants of Δ*psnrps4-gfp* will be determined by PCR.
(3) Organelles will be counterstained with different dyes.
(4) The transformants and parent strains of *Pezicula* sp. will be observed by fluorescence microscopy to identify the localization of PSNRPS4 based on the GFP signal.
Results: This project is still in progress. Vector pAg1-Nat1-psnrps4-gfp has been constructed, and transferred into *Pezicula* sp. NRRL12192. One positive transformant was obtained.
Conclusions: No conclusion can be drawn at this point. Further investigation into that transformant is required in order to verify our hypothesis.

ABSTRACT

Visualizing Structural and Motility features of *Helicobacter pylori with Cryo-Electron Tomography*

Wei-Ting Lin *Fu Jen Catholic University* *Class of 2019*

Sponsored by: Jun, Liu, PhD, Department of Pathology and Laboratory Medicine
Keywords: Helicobacter pylori, cryo-ET, flagella, sheath, tip, motor, motility, chemotaxis, prokaryotic cytoskeleton

With up to 50% of population infected, *Helicobacter pylori* is an important pathogen that lead to gastric duodenal diseases and even cancer. Prevailed by Dr. Barry Marshall, who won the Nobel prize in 2005 for showing *H. pylori* is the cause of most peptic ulcers. *H. pylori* is a type of bacillus bacteria with unipolar 4~6 flagella. The bacteria move in an extremely high speed even in viscous solution. To understand the relationship between its motility and colonization as well as pathogenesis, we use cryo-electron microcopy (cryo-EM) to study the bacterium and its flagella.

Cryo-EM is emerging as a novel and powerful imaging technique that can visualize intact microbes at native state. The bacterial culture was placed on EM grid by freezing rapidly with liquid ethane and stored in liquid nitrogen. After inserted into the microscope, high-energy electrons penetrate the specimen, and form 2D high-resolution images, which were recorded on a new generation direct electron detector. The electron microscope was able to automatically collect images from different angles, enabling us to have a 3D view of an intact bacterial cell.

We analyzed more than 300 bacteria by cryo-EM and discovered several features probably related to the unique motility of *H. pylori*. First, some of *H. pylori* are coccoid forms instead of helical and bacillary from in normal. This special shape possibly symbolizes the bacteria have changed colonization, causing more severe symptoms such as cancers. Second, we also found some bundle-like cytoskeleton structures inside the cells. Third, flagellar filaments of *H. pylori* are enveloped by membrane sheath, which might help the bacteria to avoid innate immune recognitions. Interestingly, part of membrane sheath is swollen as a bulb, especially on the filament tip. These membrane bulbs may increase surface area that enhances efficiency of the motility. Last but not the least, we found about 170 motors embedded in cell envelopes and determined *in situ* motor structure by sophisticated image analysis. This structure revealed the most detailed view of the nanomachine that is used to generate torques to propel the germ. With these amazing features, *H. pylori* is capable to generate high mobility and lead to various syndromes to our GI system.

Though *H. pylori* can be treated with antibiotics, alternative therapies are still necessary, considering the number of germs with drug resistance increases considerably. Our studies on *H. pylori* and its unipolar flagella provide new insights into cellular structure, motility and colonization. More medications can be developed to attenuate their mobility and eradicate them from human bodies.

ABSTRACT

Cardiac-specific Over-activation of the Mechanistic Target of Rapamycin Complex 1 results in Metabolic, Structural and Functional Remodeling in the Heart

Saki Saijo *Tokushima University* *Class of 2018*

Sponsored by: Heinrich Taegtmeyer, MD, DPhil, Department of Internal Medicine-Cardiology

Keywords: heart failure, hypertrophy, mTORC1, TSC2, G6P, remodeling

Before the heart fails, it remodels metabolically and structurally in an attempt to maintain contractile function. Metabolically, the heart increases its reliance on carbohydrates for energy provision. Structurally, the heart hypertrophies to sustain increased hemodynamic stress. There is evidence suggesting the activation of the mechanistic Target Of Rapamycin complex 1 (mTORC1) pathway is closely tied to glucose uptake by the heart to drive structural and functional remodeling before the stressed heart fails. We have previously shown that when the heart is subjected to acute stress, the glycolytic intermediate glucose 6-phosphate (G6P) accumulates and results in mTORC1 activation, ER stress and contractile dysfunction. Also, studies in kidney have shown that mTORC1 reciprocatively upregulates glucose transporter 1 (Glut1) expression and glucose uptake. Therefore, we decided to test the hypothesis that chronic mTORC1 overactivation results in G6P accumulation, and precedes functional and structural remodeling in the heart. To test this hypothesis, we used mice with inducible, cardiac-specific deficiency of the protein tuberin (TSC2), a member of the tuberous sclerosis complex, the principal inhibitor of mTORC1. Immunoblotting was performed on protein markers to confirm activation of mTORC1 downstream targets and of the unfolded protein response. Intracellular G6P concentration was measured using an NADH coupled enzymatic assay. Serial echocardiograms were performed on mice to evaluate structural and functional changes. The results indicate that chronic mTORC1 activation in the heart results in G6P accumulation – metabolic remodeling- that precedes structural and functional remodeling. We conclude that mTORC1 activation is key in the pathogenesis of cardiac hypertrophy and failure.

ABSTRACT

Systematic Analysis of Interplay between F-box Proteins and Cullin-1 and Implications of F-box Protein Structure in SCF Complex Formation

Le Sun *Shanghai Jiao Tong University School of Medicine* *Class of 2017*

Sponsored by: Jianping Jin, PhD, Department of Biochemistry and Molecular Biology

Keywords: F-box proteins, the SCF ubiquitin ligases, protein interactions, Cullin1

Background:
Ubiquitin-dependent protein degradation plays pivotal roles in cell survival and other biological activities. Protein ubiquitination is fulfilled by E1 activating enzymes, E2 conjugating enzymes and E3 ubiquitin ligases. F-box proteins belong to a family of substrate specificity factors in the SCF (Skp1-Cullin1-F-box protein) ubiquitin ligases. To date, ~69 F-box proteins have been discovered in human genome. However, many of them have not been linked to any biological functions. Some F-box proteins form authentic SCF ubiquitin ligases. However, others might not form typical SCF complexes, due to failed interactions between Cullin1 and F-box proteins, like Fbxo45. Thus far, it is still unclear how many F-box proteins could form typical SCF ubiquitin ligases. Our study aims to systematically analyze the formation of the SCF ubiquitin ligases by all of the human F-box proteins and to probe into how F-box protein sequences affect the formation of the SCF complex. This study will clarify the organization of the SCF ubiquitin ligases and define extra sequence features for the formation of the SCF ubiquitin ligases.
Materials and methods:
Human F-box genes were subcloned into a Gateway entry plasmid and then shuttled into expression vectors with a N-terminal HA tag. F-box mutations were created using a PCR-based in vitro mutagenesis method. Their sequences were validated by DNA sequencing.
HA-tagged F-box proteins were expressed in HEK293T cells by transient transfection approach using polyethylenimine (PEI). Cells were collected at 48 hours post-transfection and lysed for immunoprecipitation (IP) using anti-HA agarose resins. The interactions between F-box proteins and Cullin1 were detected using western blots.
Results:
Thus far, we have cloned 4 new F-box genes, Fbxl7, Fbxo34, Fbxo46 and Fbxo39. We found all of them interact with Cullin1, suggesting these F-box proteins could form typical SCF ubiquitin ligases. We have also created five mutants of Fbxl2 and will determine their contribution to the formation of the SCF using IP-western method.
Discussion:
Our study will provide a systematic view about how the interaction between F-box protein and Cullin1 affects the formation of the SCF ubiquitin ligases.

ABSTRACT

p38 MAPK Mediates Cancer-induced Autophagy Activation and Myotube Atrophy

Yiman Wang *Shanghai Jiaotong University School of Medicine* *Class of 2017*

Sponsored by: Yi-Ping Li, PhD, Department of Integrative Biology and Pharmacology

Keywords: Autophagy, LC3, p38 MAPK, SB202190, myotube

Background: Autophagy is one of the mechanisms through which cellular proteins are degraded. It is formed by isolation of part of the cytoplasm by membrane to form autophagosomes that fuses with the lysosome for degradation. LC3 is one of the marker proteins for autophagosome formation, during which LC3-I is modified into LC3-II. Hence, increase in LC3-II suggests increase of autophagy in cells. The p38 mitogen-activated protein kinases (MAPK) family is an inflammation-activated signaling pathway that can activate autophagy. Because autophagy is an important contributor to cancer cachexia, we examined whether p38MAPK mediates cancer-induced autophagy activation and muscle atrophy.

Hypothesis: p38 MAPK mediates cancer-induced autophagy activation and myotube atrophy.

Method: Murine C2C12 myoblasts were cultured in growth medium (DMEM supplemented with 10% fetal bovine serum) at 37°C under 5% CO_2. At 85~90% confluence, myoblast differentiation was induced by incubation for 96 h in differentiation medium (DMEM supplemented with 4% heat-inactivated horse serum) to form myotubes. Conditioned medium from 48-hour cultures of Lewis lung carcinoma (LLC) were centrifuged (1000 x g, 5 min) and the supernatant (LCM) was added to myotube cultures (25% final volume in fresh medium) with or without SB202190, an inhibitor of p38MAPK, for 8 h or 72 h. Western blotting was carried out to measure LC3 levels at 8 h. Immunofluorescence was used to calculate and compare the size of C2C12 myotubes at 72 h.

Results: LCM induces LC3-II increase, which is blocked by SB202190. LCM-induced myotube atrophy is dependent on p38 MAPK.

Conclusion: LCM stimulates autophagy activity and causes myotube atrophy. Inhibition of p38 MAPK prevents these effects, suggesting that p38 MAPK is an important mediator for cancer-induced muscle wasting through the activation of autophagy. Therefore, p38 MAPK could be a target for managing cancer cachexia.

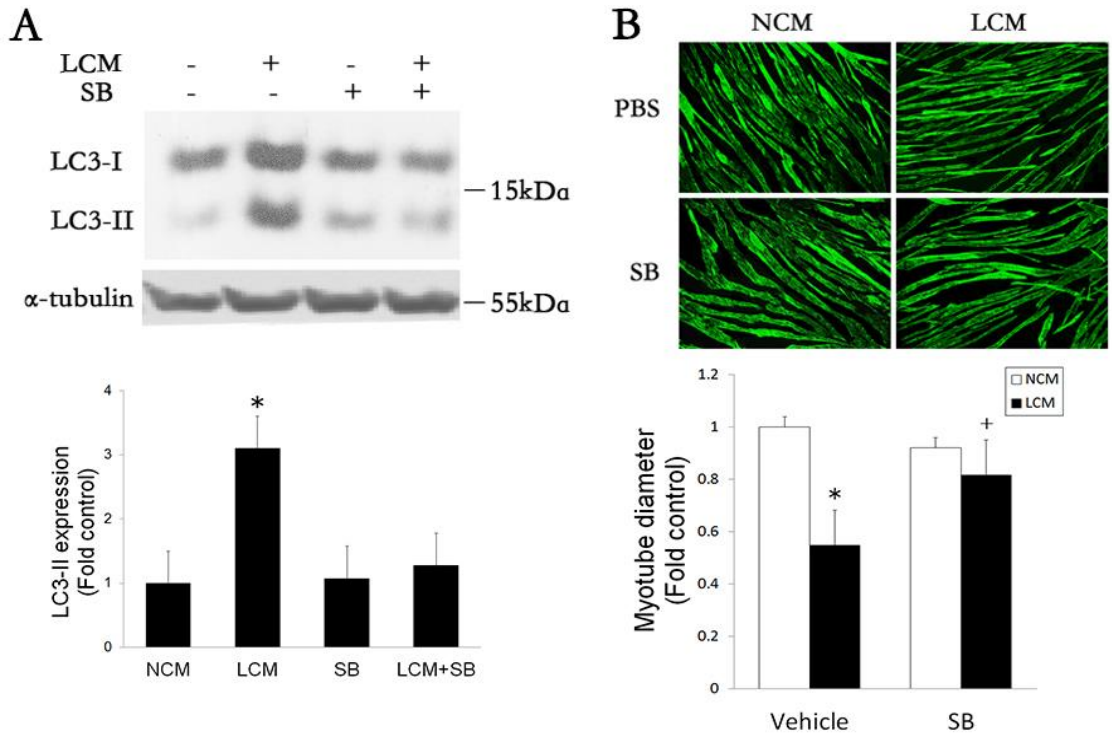

Figure. Inhibition of p38 MAPK prevents LC3-II increase and myotube atrophy. NCM denotes non-Lewis lung carcinoma cell-conditioned medium. **A** *denotes a difference ($P<0.05$) based on ANOVA. **B** *denotes a difference ($P<0.05$) from PBS control (PBS/vehicle) and + denotes a difference from LCM control (LCM/vehicle) determined by ANOVA.

ABSTRACT

Exploring the Feedback Loop between Lipin 1 Level and SREBP 1/SREBP 2 Level

Yizhao Xie *Shanghai Jiao Tong University School of Medicine* *Class of 2017*

Sponsored by: Guangwei Du, PhD, Department of Integrative Biology and Pharmacology

Keywords: Lipin, SREBP, Lipid Metabolism, Positive Feedback

Background: Lipin is unique such that it is able to modulate lipid metabolism with its dual functionality. On the ER, Lipin carries out its activity as a phosphatidic acid phosphatases converting phosphatidic acid (PA) to diacylglycerol (DAG), a direct pre-cursor for triacylglycerol (TAG) and phospholipid biosynthesis. Lipin can also enter the nucleus to act as a transcription co-activator to help turn on genes involved in fatty acid oxidation. Similarly, sterol regulatory element binding proteins (SREBPs) is a regulator of lipids in the cells. In its inactive form, SREBP is located on the ER, however, when the cells are low in lipids, SREBP will be transported to the Golgi to undergo proteolytic cleavage resulting in the release of the N-terminus. The cleaved form will then enter the nucleus and turn on lipogenic genes involved in cholesterol, fatty acid, and triglyceride synthesis. As both Lipin and SREBP play an important role in regulating lipid metabolism, we are interested to see if functional connection exists between these two proteins.

Methods: A variety of cancer cells were used. Lentiviral constructs expressing Flag-SREBP1 and Flag-SREBP2 were produced through sub-cloning. These clones were then stably over-expressed into HCC 1806, T98G, and U2OS cells.

Data and Analysis: When cells were over-expressed with SREBP, Lipin1 levels were upregulated compared to wildtype. This shows that Lipin1 levels could be positively affected by SREBP levels. When Lipin 1 was knocked down by shRNA, SREBP underwent proteolytic cleavage from its inactive full length to its active N-terminus form, resulting in an accumulation of the N-terminus compared to shRNA control. This suggests that PA accumulation from Lipin1 knockdown could be regulating SREBP processing. Additionally, Lipin1 knockdown also led to the proteolytic cleavage of the constitutively expressed exogenous FLAG-SREBPs, supporting that SREBP processing occurred at the post-translational level. Immunofluorescence staining showed SREBP accumulation in the nucleus when Lipin was knockdown, while cells treated with shRNA control showed ER localization. This is consistent to the trend we observed on western blot, hinting that there could be a positive feedback loop such that PA
accumulation due to Lipin1 knockdown could cause SREBP to sense lower levels of TAG and phospholipids being produced, resulting in the processing of SREBP to allow for the cells to act accordingly to the change. Further studies can be carried out focusing on the mechanism as well as the potential applications of this feedback loop.

ABSTRACT

Identification of Cellular Sources of Elevated Gremlin 1 in Chronic Pancreatitis

Yunze Xu *Shanghai Jiaotong University School of Medicine* *Class of 2019*

Sponsored by: Yanna Cao, MD, Tien C. Ko, MD, Department of Surgery

Keywords: Chronic pancreatitis; Gremlin; Bone morphogenetic protein; α-SMA

Background/Significance. Chronic pancreatitis (CP) is a highly debilitating disease characterized by progressive pancreatic inflammation and fibrosis that ultimately leads to exocrine and endocrine dysfunction. Gremlin 1 is an endogenous antagonist of bone morphogenetic proteins (BMPs). Recently, our group has reported that BMP signaling pathway has an anti-fibrogenic role in the pancreas *in vivo* under CP induction. Gremlin 1 is upregulated in human CP and a mouse CP model *in vivo*. Deficiency of Gremlin 1 in mice attenuates pancreatic fibrosis under CP induction *in vivo*. These results demonstrate that Gremlin 1 is a key pro-fibrogenic factor in CP. However, cellular sources of Gremlin 1 in CP remain largely unresolved. Understanding what cell types express elevated Gremlin 1 during CP is essential for generating specific Gremlin 1 knockout and further investigating role of Gremlin 1 in CP.
Methods. To identify cellular source of Gremlin 1 expression in CP in this study, we performed an immunofluorescence co-staining survey of Gremlin 1 in several pancreatic cell types in a CP mouse model. Swiss Webster mice (female, 6-8 weeks) were under CP induction by repetitive intraperitoneal injections of cerulein (50 μg/kg, five hourly injections/day, 3 days/week) for up to 4 weeks. Pancreatic tissue paraffin sections collected from these mice were stained using Gremlin 1 antibody paired with several antibodies against: α-Smooth muscle actin (SMA) as a marker of active pancreatic stellate cells, E-cadherin as a marker of epithelial cells, and cluster of differentiation (CD)31 as a marker of endothelial cells.
Results/Data. We found that highly expressed Gremlin 1 was co-localized with α-SMA as well as with CD31. No apparent co-localization between Gremlin 1 and E-cadherin was observed.
Conclusions. In conclusion, our data showed that over-expression of Gremlin 1 in CP was produced in activated pancreatic stellate cells and endothelial cells. Thus our study provides justification of specific Gremlin 1 knockout in pancreatic stellate cells and endothelial cells for further investigation of Gremlin 1's role in CP.

ABSTRACT

The Effect of Human Lactoferrin on BCG Infected Peripheral Blood Cells

Ai Yamazaki ***Tokushima University*** ***Class of 2018***

Sponsored by: Jeffrey K. Actor, PhD, Department of Pathology and Laboratory Medicine*
Keywords: Tuberculosis, Lactoferrin , BCG, macrophage, IL-6, TNF-α, IL-12p40, CD40

Back ground: Tuberculosis (TB) caused by infection with *Mycobacterium tuberculosis* (MTB) causes nearly 1.7 million deaths every year. Much attention has been given to improving the BCG vaccine. This study examines lactoferrin (LF) to promote effective immune function in macrophages in a BCG *in vitro* infection model.

Methods: Human blood peripheral white blood cell macrophages from two volunteers were isolated by gradient centrifugation. $2x10^6$cells were cultured for 2 weeks in RPMI media supplemented with 400pg/ml human GM-CSF. Cells were infected with 1-3 $x10^6$ Bacillus Calmette-Guerin (BCG) in the presence or absence of bovine Lactoferrin (bLF) or recombinant human lactoferrin (rhLF) at 10 or 100 ug/ml. Control cells were cultured alone or with LF. Supernatants collected after 7 days were evaluated for production of pro-inflammatory cytokines IL-6, IL-10, IL-12p40and TNF-α by enzyme linked immunosorbent assay. Recovered treated cells were also examined by flow cytometry using fluorescence to evaluate changes in antigen presentation surface molecules. Tagged reagents used included antibodies: HLA-FITC, CD40-PE, CD86-PerCPcy5, CD80-PEcy7, CD1b-APC, HLA-DR-Alexa700 and CD1c-Pacific blue.

Results: Lactoferrin augmented immune responses in BCG infected macrophages. Infection with BCG alone leads to depressed production of IL-6, IL-10, IL-12p40 and TNF-α. Addition of LF significantly increased production of all these cytokines. In contrast, LF reduced production of IL-10 from infected cells. LF worked most effectively when used at 10ug/ml. One volunteer's cells responded more favorably to the bLF, while the other individual showed significant changes using rhLF. Almost no IL-6, TNF-α or IL-12p40 was produced from non-infected control cells, or cells treated with only bLF or rhLF. Of interest, only surface expression of CD40 was increased the presence of the LFs, raising the suppressed response expected from BCG infection. There was no change in expression of Class I, Class II, CD1b, CD1c,CD86, or CD80.

Conclusion: Pro-inflammatory cytokines are crucial components of acute reactivity to MTB. Both bLF and hLF caused significant increase in TNF-α, IL-6, and IL-12p40. These changes, in the presence of increased CD40 surface expression, may be beneficial to assist T activation events and subsequent B cell development. Thus, LF may be a useful adjuvant to augment the BCG vaccine and support development of protective anti-TB responses.

*special thanks to Shen-An Hwang, PhD, Department of Pathology and Laboratory Medicine.

ABSTRACT

Muscle Derived Small-size Stem Cells Contribute to Tissue Regeneration through Blood Transportation

Zhicong Zhao *Shanghai Jiao Tong University School of Medicine* *Class of 2017*

Sponsored by: Yong Li, MD, PhD, Department of Pediatric Surgery
Keywords: Muscle derived small-size stem cells, Blood transport, Tissue regeneration

Background: Regenerative medicine is a novel medicine that holds permission to fully heal the damaged tissues or organs. Stem cells are the base cell source for regenerative medicine, because they are able to the ability to differentiate into many different types of cells. One kind of stem cells has been attended, they are very small in sized (~5micro), has stem cell behaviors, and presents in a small population (0.6%) among several of tissues. Our laboratory has discovered one kind of small-size stem cells within the murine skeletal muscles, which can be isolated based on their surface markers: SCA-1+/CXCR4+/MSX-1+/CD45-. Those muscle derived small size stem cells (Mu3SCs) have aggressive migration and myogenic differentiation abilities, indicating their potential capability to improve muscle regeneration and prevent muscle-wasting processes.

Hypothesis: Mu3SCs can be transported from muscle to blood and circulated into various tissues, thus involved the tissue regeneration or repair as needed. Mu3SCs have the ability to differentiate into specific cell types when they are stable in the resident tissues, physiological exercise can enhance this procedure.

Methods: Firstly, we obtained the Mu3SCs from murine muscle by using FACS sorting based on its small size and surface expression markers: SCA-1+/CXCR4+/MSX-1+/CD45-. Then the Mu3SCs were pre-labeled with GFP and enlarged populations. We performed a systemic delivery of the Mu3SCs-GFP+ into NSG mice, an immunodeficiency mouse model through the tail vein. The GFP+ cells were idenfitied in the blood at day 3, 7, 10 and 21 days after injection into NSG mice. At the same time, mice were sacrificed at 7, 21 and 28 days after cell delivery, and their brain, heart, lung, kidney, spleen, gastrocnemius and tibialis anterior muscles were harvested for histological analysis. All the tissues were frozen sectioned into 12 μm slices. Sections were then stained with DAPI. Finally, we investigated to estimate the GFP fluorescent signal within those tissues to evaluate the Mu3SCs' migration and survival abilities after blood delivery.

Results: We detected the Mu3SCs ($GFP^+/DAPI^+$) within the circulating blood of target NSG mice while the amount of GFP+ numbers is declining with timing. We also detected the GFP+ cells within brain, heart, lung, kidney, spleen, gastrocnemius and tibialis anterior muscles of the NSG mice, indicating the migration abilities of Mu3SCs.

Discussion: Although we discovered that Mu3SCs could transport through blood circulation and survive in various tissues, the inherent tumorigenesis still remains unknown. Besides, in order to further test the function and ability of survived Mu3SCs in different tissues, their specific markers need to be determined with collocalizing GFP signal. The final goal of this project is to prove-of-concept that exercise can promote and release more stem cells from muscles into blood that can explain the benefits of physiological exercise to human.

Conclusion: Mu3SCs can be transported from blood into different tissues or organs and resident into the host tissues for a while. Thus, Mu3SCs have the potential to differentiate specific type of cells to involve host tissue regeneration and repair.